AD

AMRA CR 63-04/4

INVESTIGATION OF SOLIDIFICATION OF HIGH-STRENGTH STEEL CASTINGS

INTERIM REPORT

by
D. R. Poirier and M. C. Flemings
Department of Metallurgy
Massachusetts Institute of Technology

for Contract Period
dates
October 1, 1964 — September 30, 1965

MASSACHUSETTS INSTITUTE OF TECHNOLOGY
Cambridge, Massachusetts 02139

Contract No. DA-19-020-AMC-5443(X)

U.S. Army Materials Research Agency
Watertown, Massachusetts 02172

AMRA CR 63-04/4

AMRA CR 63-04/4

INVESTIGATION OF SOLIDIFICATION OF HIGH-STRENGTH STEEL CASTINGS

INTERIM REPORT

by

D. R. Poirier, M. C. Flemings
Department of Metallurgy
Massachusetts Institute of Technology

for Contract Period
dates
October 1, 1964 - September 30, 1965

MASSACHUSETTS INSTITUTE OF TECHNOLOGY
CAMBRIDGE, MASSACHUSETTS 02139

Contract No. DA-19-020-AMC-5443(X)

AMCMS Code No. 5025.11.842
Department of the Army Project No. 1A02440A110

U.S. ARMY MATERIALS RESEARCH AGENCY
WATERTOWN, MASSACHUSETTS 02172

ABSTRACT

An analytical and experimental study has been made of microsegregation in dendritic solidification of ternary iron-carbon-chromium alloys. The most realistic model considered assumes uniform concentrations of carbon and chromium in the interdendritic liquid, equilibrium at the solid liquid interface, no diffusion of chromium in the solid, and a uniform concentrations of carbon in the solid.

Alloys studied experimentally were all of 1.5 per cent chromium, with carbon contents ranging from .96 to 3.00 per cent carbon. Estimates of the extent of diffusion for carbon and chromium as well as microprobe analyses showed that carbon diffuses extensively in the solid during solidification and chromium diffuses only a limited amount.

Segregation ratios of common alloying elements in medium carbon, low alloy steel were compiled from the literature. Some of these data were combined with measurements from this investigation to illustrate the overall effect of carbon on the segregation ratio of chromium in iron-low chromium alloys.

An alternative measure of microsegregation to the "Segregation Ratio", S, was introduced. This measure, σ^m, was termed "Composition Deviation Index". Comparison of theory and experiment was made for the segregation ratio and the composition deviation index for iron-1.5 per cent chromium alloys with carbon. Experimental results for σ^m were determined for carbon contents between .96 and 1.75 per cent carbon and compared to theoretical calculations for carbon contents from .96 to 3.00 per cent. Theoretical values (based on no diffusion of chromium in the solid) of σ^m increased from .22 at .96 per cent carbon to .35 at 1.75 per cent carbon and then decreased to .16 at 3.00 per cent carbon. The experimental values were somewhat lower (15 to 30 per cent lower) due, it is believed, to limited diffusion of chromium in the solid.

Segregation ratios were experimentally and theoretically determined for alloys between .96 to 3.00 per cent carbon, and measurements of other investigators at lower carbon contents were used. The segregation ratio increased from unity at zero per cent carbon to about 4.5 - 5.0 at 1.5 per cent carbon and then decreased to 3 at 3.00 per cent carbon. Theoretically derived segregation ratios between .96 and 3.00 per cent carbon showed the same general dependence; however, the theoretical values were lower except at one per cent.

Fundamental to the study of solute redistribution during solidification is detailed knowledge of the solid-liquid equilibria. For this reason the determination of the austenite-liquidus of the iron-carbon-chromium system was made which included evaluating the activity of iron, carbon, and chromium in liquid iron and austenite as functions of temperature and composition.

TABLE OF CONTENTS

LIST OF FIGURES

LIST OF TABLES

ACKNOWLEDGEMENTS

Portions of this work, where referenced, are from an earlier study conducted under United States Air Force Sponsorship[16]. Computations were performed, primarily, at the M.I.T. Computation Center, using an IBM 7090 Computer. Assistance of Dr. H. D. Brody in programming is gratefully acknowledged.

INTRODUCTION

This report summarizes research conducted during the third year of a continuing research program on steel solidification. Work conducted during the first two years of the program has been reported[1,2].

The first period (December 9, 1962 to September 30, 1963) comprised a study of dendrite structure, microsegregation and homogenization of low alloy steel[1,3]. Dendrite morphology was found to be platelike; microsegregation was found to be significant and relatively insensitive to cooling rate. Substantial homogenization of alloy elements other than carbon was found to require much higher temperatures and longer times than those generally employed in practice. Ahearn and Quigley[4] then showed the substantial improvement in mechanical properties obtainable when more complete homogenization is obtained.

The second period[2] (October 1, 1963 to September 30, 1964) comprised a theoretical and experimental study of microsegregation in binary iron-base alloys, in which substantial diffusion occurs in the solid during solidification. Reasonable agreement between theory and experiment was obtained for an iron-nickel alloy. Work on this topic has continued and is to be the subject of a later report.

The aim of the research described herein is to apply the theoretical model for microsegregation to a ternary iron-base alloy, and to compare results of calculations with experiment. The ternary iron-carbon-chromium system was chosen for study; experiments and calculations were

conducted on alloys containing 1.5 per cent chromium, with carbon varied from 0 to 3 per cent. Calculations were done, for the most part, using an IBM 7090 computer.

Only a limited amount of data are available in the literature on microsegregation measurements in multi-component iron-base alloys, and nothing is available on quantitative comparison with theory. Investigations[1,5-12] have been made of segregation in ferrous-alloys, notably medium carbon (.21 - .62 per cent carbon), low alloy steels; results for these steels are presented in Table I. Results reported are for the common alloying elements (manganese, nickel, chromium, molybdenum, silicon, tungsten, and copper); impurity elements (sulfur, phosphorus, and arsenic) are excluded as well as less frequently encountered elements (tin, niobium). Average values of the segregation ratios are given in Figure 1 (along with the number of alloys in which the segregation ratio was determined and the range of composition for the applicable ratio). Figure 1 indicates that segregation ratio for manganese and nickel lie between 1 and 2 for all alloys examined. Segregation ratios for chromium and molybdenum are higher and show more scatter. The casting conditions of the various alloys investigated varied widely. Ingots ranged from 100 tons to laboratory size with structures that included columnar and equiaxed zones; some ingots solidified rapidly, other slowly.

Philibert et al[13] have indicated that carbon increases the extent of microsegregation of various elements in iron alloys. It was stated that the extent of carbon's effect depended on the absolute value of thermodynamic interaction parameter of the third element with carbon in

TABLE I

SUMMARY OF MICROSEGREGATION MEASUREMENTS IN MULTICOMPONENT CARBON STEELS

	Ingot Composition, Weight Per Cent							Segregation Ratio, S					
Reference	C	Mn	Si	Ni	Cr	Mo	Others	Mn	Ni	Cr	Mo	Others	Remarks
6	.24	.53	.30	2.5	.65	.27	-	-	1.2-1.3	2	7	-	Columnar and equiaxed zones
7	.44	.65	.35	-	-	-	.57(Cu)	1.6	-	-	-	1.4(Cu)	Columnar, bottom of ingot
6	.35	.50	-	2.5	.66	.29	-	-	1.3	1.9	7.3	-	100 ton ingot
8	.38	.60	.20	1.35	.99	.24	-	1.1	1.2-1.4	1.4-1.5	-	-	Columnar and equiaxed zones
5	.30	.37	.13	1.51	.97	.27	-	-	1.1-1.3	1.2-1.5	-	-	Edge and center of ingot, columnar and equiaxed
5	.35	.09	.08	1.48	1.02	.33	-	-	1.1-1.3	1.2-1.4	-	-	Edge and center of ingot, columnar
5	.36	.58	.48	1.49	1.05	.28	-	-	1.4	1.7	-	-	Edge and center of ingot, equiaxed
1	.40	.70	.30	1.80	.80	0.25	-	1.4-1.8	1.1-1.3	1.5-2.4	-	-	Columnar, 1.7 to 5.7 inches from chill
9	.21	-	-	4.03	1.45	-	.75(W)	-	1.2	1.4	-	1.6(W)	2.9 ton ingot
9	.21	.93	-	-	1.22	-	-	1.4	-	1.4	-	-	3.6 ton ingot
9	.23	-	.40	-	3.13	-	-	-	-	1.4	-	-	2.6 ton ingot
9	.42	-	-	-	1.55	-	-	-	-	1.9	-	-	2.9 ton ingot
9	.42	.68	-	-	1.0	-	-	1.6	-	1.9	-	-	3.6 ton ingot
9	.45	1.50	-	-	-	-	-	1.5	-	-	-	-	4.6 ton ingot
10	.31	.84	.35	2.79	0.79	.53	-	1.4-1.5	1.2-1.3	1.3-1.5	3.7-4.0	-	Columnar, 0 - 3-1/2 inches from chill
11	.36	1.30	-	-	-	.5	-	1.6	-	-	6.8	-	
11	.47	-	-	-	.50	-	-	-	-	4	-	-	2.2 pound ingot cooling rate 4°C/minute
11	.62	.51	-	-	-	-	-	1.6	-	-	-	-	
12	.40	1.85	1.29	1.75	.83	.28	-	1.4-1.6	1.4-1.6	1.4-1.5	-	1.5-1.7(Si)	8 inch diameter ingot
6	.46	-	-	1.48	-	-	-	-	1	-	-	-	

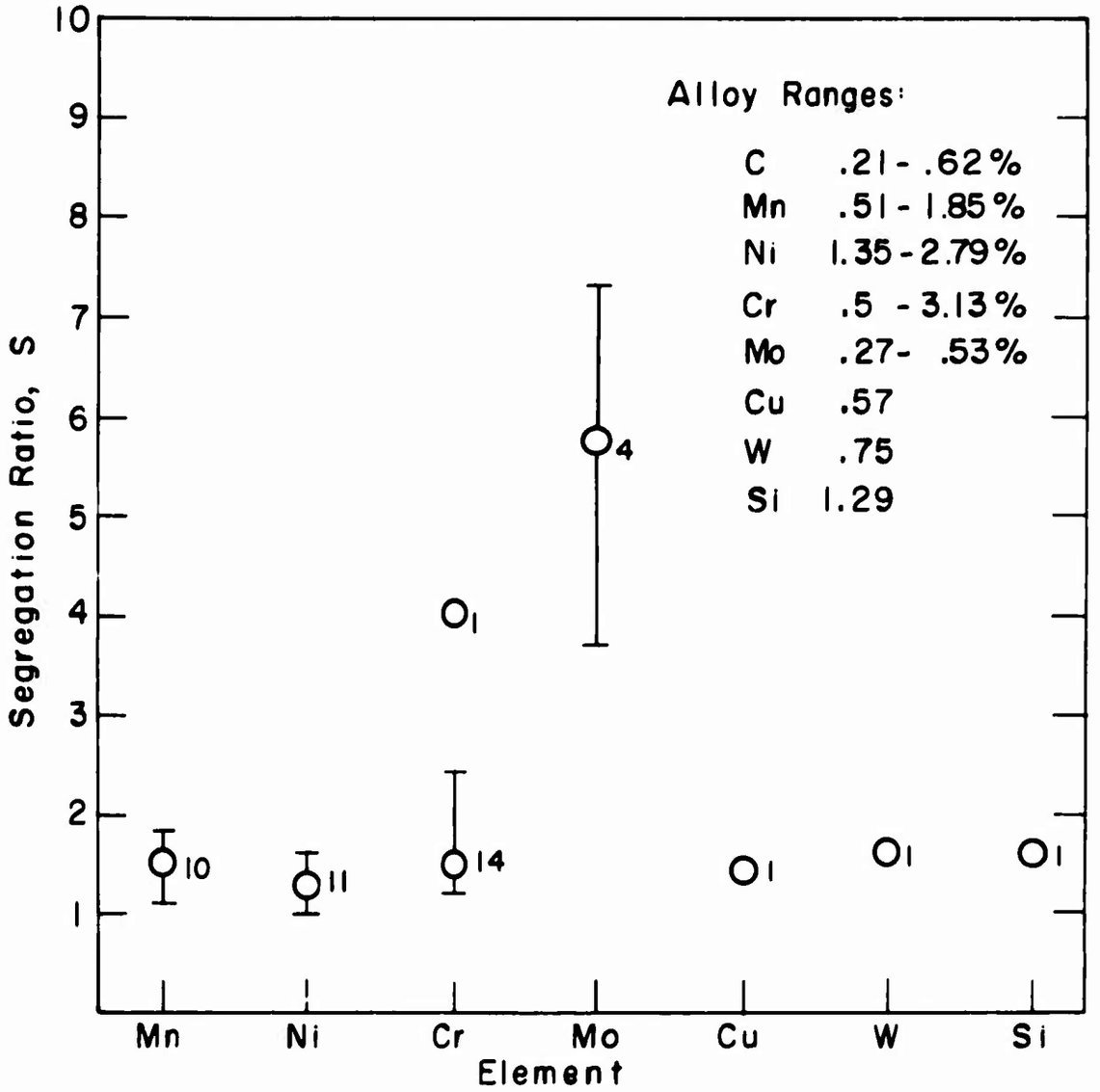

Figure 1: Segregation ratios for common alloying elements in medium carbon, low alloy steels.

Numbers beside the points represent the number of alloys involved for the respective elements. Data from Table I.

liquid iron. For example, carbon affects the segregation of arsenic more strongly than chromium and does not alter the segregation of nickel. This observation by Philibert et al[13], although perhaps valid, is not fundamental for understanding solute redistribution during solidification of iron-carbon-X alloys, as will be shown in later sections.

In addition to the data on low alloy steels discussed above, Melford[14] has obtained data on iron-carbon-chromium alloys which are summarized in Table II and discussed later in the text. Finally, some data have been reported for 52100 alloy (iron-1.5 per cent chromium-1.0 per cent carbon) in an earlier research study at M.I.T.[15]; these are also discussed later in the text.

TABLE II

Summary of Microsegegation Measurements on Iron-1.5 Cr Alloys Containing 0 to 2% Carbon (from Melford[14])

Per Cent Carbon	Segregation Ratio, S
0	1.4
0.3	1.7
0.7	2.9
0.8	3.0
1.1	4.8
1.5	5.5
1.8	3.5
2.0	3.6

PART I: MICROSEGREGATION CALCULATIONS

A. Analysis of Microsegregation in Multi-Component Alloys

Ingots and castings of alloys contain three regions during solidification; the extent of each of these depends on alloy analysis and thermal conditions. The regions are (1) completely solid, (2) partially solid and partially liquid, and (3) completely liquid. The redistribution of solute which is considered herein occurs within a small "volume element" situated in the liquid-solid zone as it passes from being completely liquid to completely solid.

The assumptions used for developing expressions of solute redistribution during the dendritic solidification of alloys have been discussed in detail[16,17], and are:

1. Negligible undercooling before formation of solid.
2. Negligible interface supercooling from kinetic or curvature effects.
3. Equilibrium partition ratio applies at the interface.
4. Negligible constitutional supercooling.
5. No thermal gradient in the liquid.
6. No macroscopic mass flow.
7. Solidification proceeds, at a given point in a casting or ingot, by continuous advance of a liquid-solid interface (e.g., continuous thickening of dendrite arms).

It follows from the foregoing assumptions that the liquid within each "volume element" is uniform in composition, and the equilibrium partition ratio applies at the liquid-solid interface. The equilibrium partition ratio may vary as solidification proceeds and the composition of the solid may or may not be uniform.

With the foregoing assumptions, it is possible to describe solute redistribution (and hence microsegregation) in multi-component alloys provided only that extent of diffusion in the solid is also described. In the following we consider two limiting cases: (1) complete diffusion in the solid, and (2) no diffusion in the solid. It will be shown later that the first limiting case is an excellent approximation of solute redistribution of carbon in iron-carbon-chromium alloys and the second is a reasonable approximation for redistribution of chromium in most such alloys.

1. Complete Diffusion in the Solid.

A material balance for component i is written:

$$C_{oi} = f_S C_{Si} + f_L C_{Li} \qquad (1)$$

where C_{oi} = overall weight fraction of component i

C_{Si}, C_{Li} = weight fraction of component i in solid and liquid respectively

f_S, f_L = weight fraction solid and liquid respectively

or $$C_{Si} = \frac{k_i C_{oi}}{1 - f_S(1 - k_i)} \quad (2)$$

where $$k_i = \frac{C_{Si}}{C_{Li}} = \text{equilibrium partition ratio} \quad (2a)$$

2. No Diffusion in the Solid.

In this case, the materials balance for component i is written:

$$f_L dC_{Li} = (C_{Li} - C^*_{Si}) df_S \quad (3)$$

where C^*_{Si} = interface composition of component i

or $$\frac{dC^*_{Si}}{C^*_{Si}} = (1 - k_i) \frac{df_S}{1 - f_S} \quad (4)$$

where, since equilibrium is maintained at the liquid-solid interface

$$k_i = \frac{C^*_{Si}}{C_{Li}} \quad (4a)$$

B. Determination of the Iron Rich Corner of the Ternary Phase Diagram Fe-C-Cr (with Tie Lines)

Equations (2) and (4) are the basic limiting cases describing solute redistribution in multi-component alloys. To apply these to a given alloy it is necessary to know the partition ratio, k_i, for each component i present (as a function of liquid composition during solidification). Hence, it is necessary to know, in general, the phase diagram for the portion of the system considered, including tie lines.

Unfortunately, for iron base alloys, ternary (or quaternary) phase diagrams are scarce; when they are available, tie lines are not generally given. In the iron-carbon-chromium system, to be considered herein, some data on ternary phase fields are available, but almost no information is available on tie lines.

Because reliable data on partition ratios, k_i, were not available for iron-carbon-chromium alloys, a substantial portion of this work has been devoted to establishing these through (1) correlation of existing data, (2) thermodynamic calculations, and (3) experiment. This work is summarized in the Appendices and only the result given here.

Figure 2 shows the liquidus surface of the iron-carbon-chromium system for 0 - 20 per cent chromiun and 0.5 - 4.5 per cent carbon. The isotherms in Figure 3 show the gamma solidus surface for the iron-carbon-chromium system (.1 - 2.3 per cent carbon, 0 - 17 per cent chromium). Superimposed on this diagram are the locii of liquid compositions (per cent chromium) that are in equilibrium, at the temperatures given, with solid austenite of composition given by the axes. This method of plotting the data permits the same data to be represented by the two figures as would be given by a series of fourteen diagrams if the equilibria were presented in the customary manner (i.e., isothermal sections showing the tie lines in the two phase regions).

As an example of the use of Figures 2 and 3, consider a liquid containing 5 per cent chromium. At 1225°C, the solid in equilibrium with this liquid contains (according to Figure 3) 4 per cent chromium and 1.61 per cent carbon. From Figure 2, the liquid is seen to contain

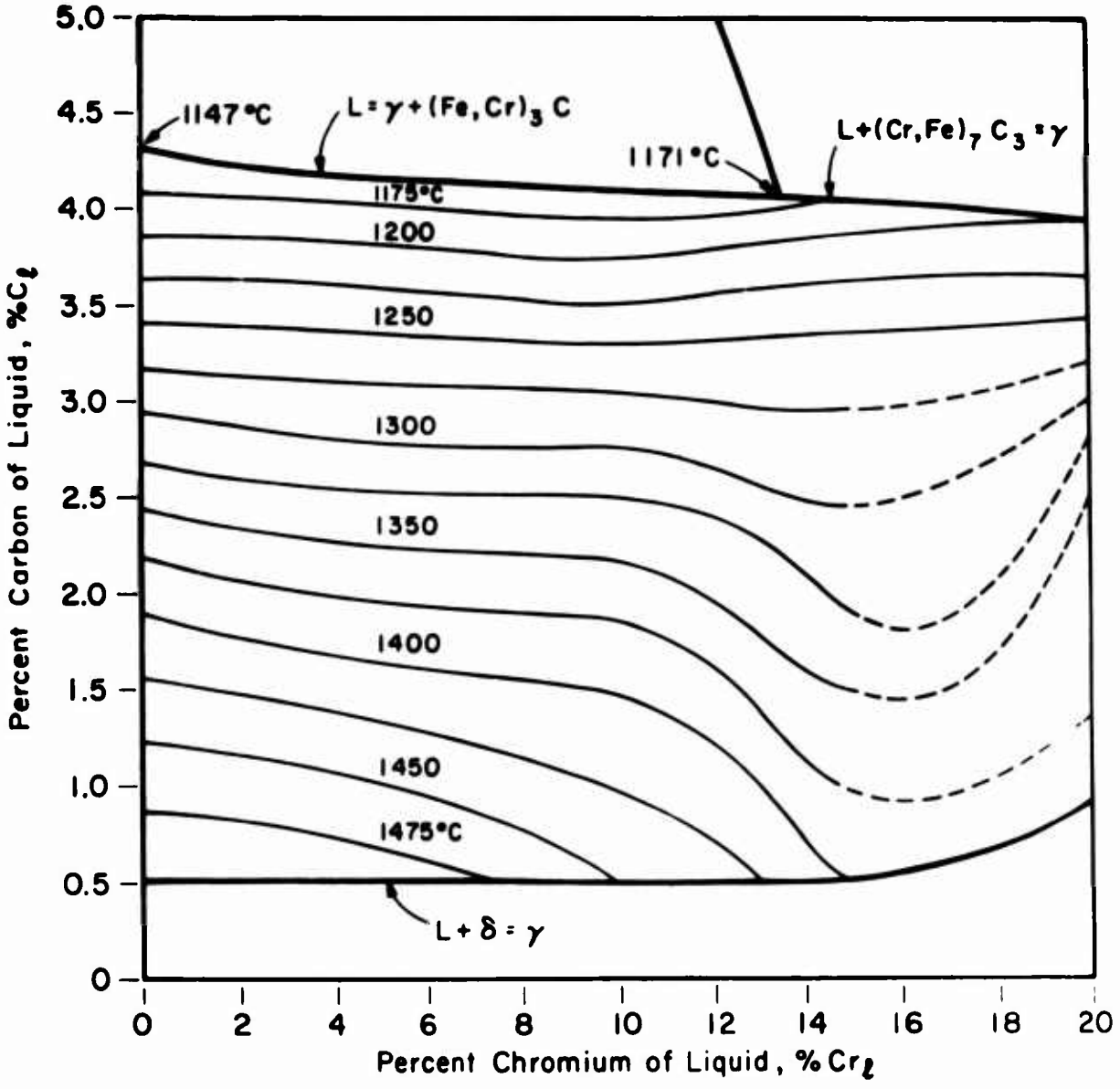

Figure 2: The iron-chromium-carbon gamma liquidus surface.

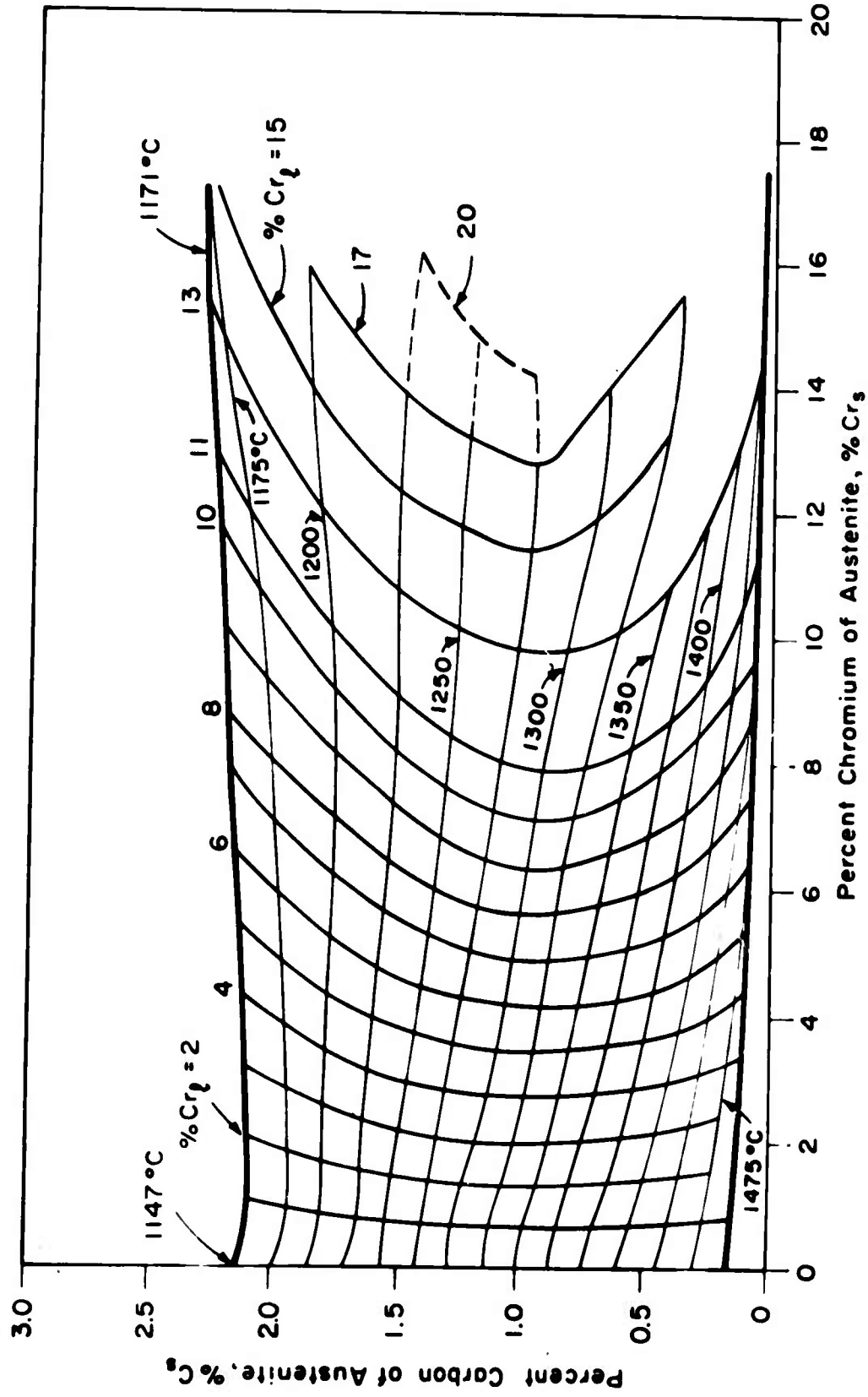

Figure 3: The iron-carbon-chromium gamma solidus surface.

The austenite in equilibrium with a particular liquid composition is found by the intersection of the liquid chromium concentration with the appropriate isotherm.

3.58 per cent carbon. Hence, the partition ratio for chromium, k_{Cr} at this liquid composition is 0.80 and the partition ratio of carbon, k_C, is 0.45.

Figures 4 and 5 show, respectively, the partition ratios of chromium and carbon for the iron-carbon-chromium alloys of interest. By knowing the temperature involved and the concentration of one component, in one phase, the partition ratio can be uniquely determined. The partition ratios are plotted in Figures 3 and 4 as a function of chromium concentration in the liquid with the temperature as a parametric variable.

For chromium, the partition ration at a given temperature increases with per cent chromium in the liquid. The lower partition ratios are at intermediate temperatures (1275 - 1325°C) which correspond to carbon contents of approximately 3 per cent. At higher or lower temperatures (lower or higher carbon contents, respectively), the partition ratio of chromium increases. This diagram clearly shows that the partition ratio of chromium varies considerably during the solidification process.

The partition ratio of carbon can be described as decreasing with chromium additions for all temperatures down to 1225°C. Below this temperature the ratio increases with increasing amounts of chromium. With no exception, the partition ratio of carbon increases with decreasing temperature.

C. Evaluation of Solute Redistribution of Ternary Iron-Carbon-Chromium Alloys

Using the partition ratios of Figures 4 and 5 it is now possible to calculate solute redistribution (and hence final microsegregation) for various iron-carbon-chromium alloys. This is done by simultaneous solution of equations (2) and/or (4) for the two solutes present, over

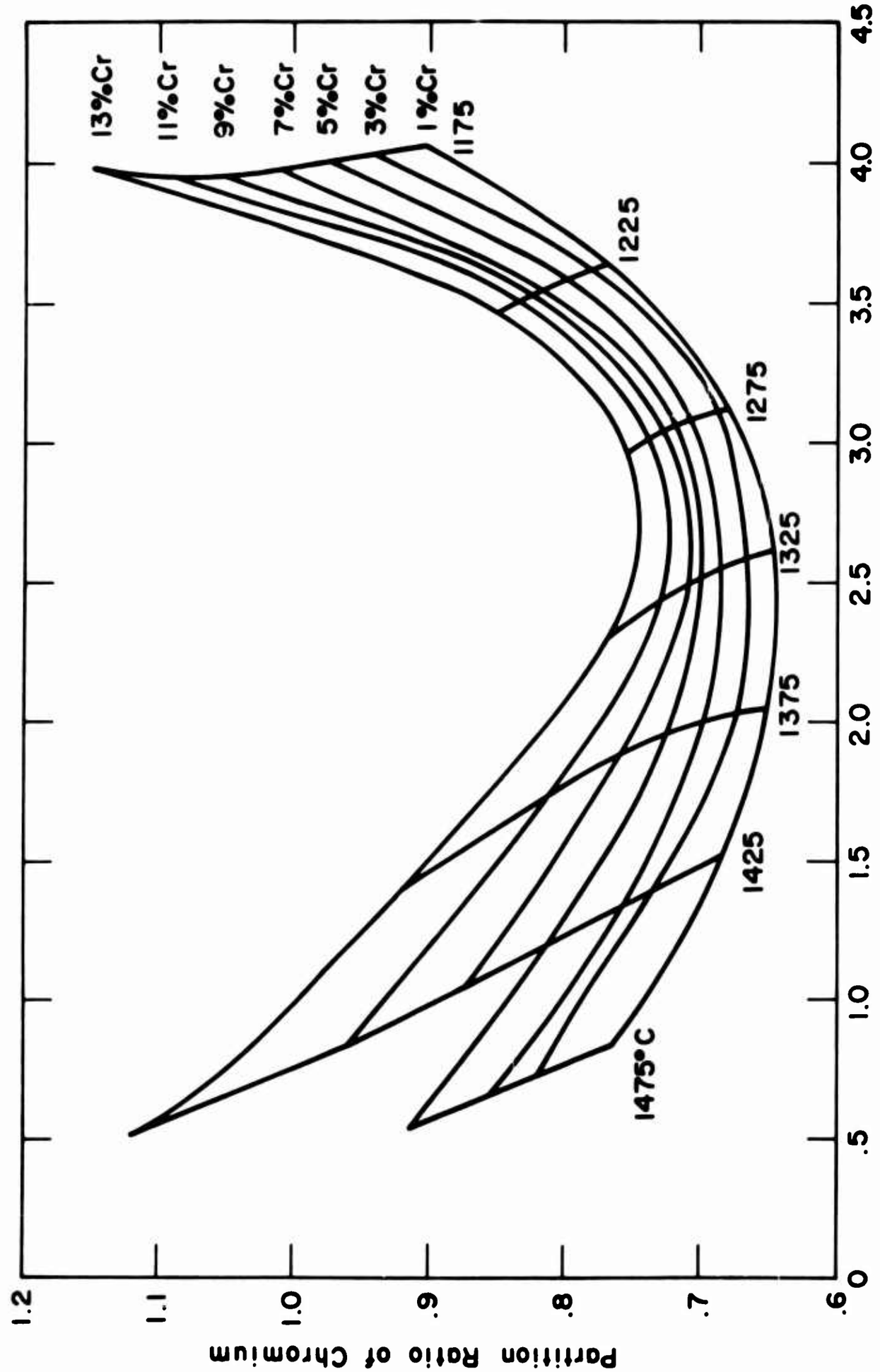

Figure 4: Partition ratio of chromium versus per cent carbon in the liquid.

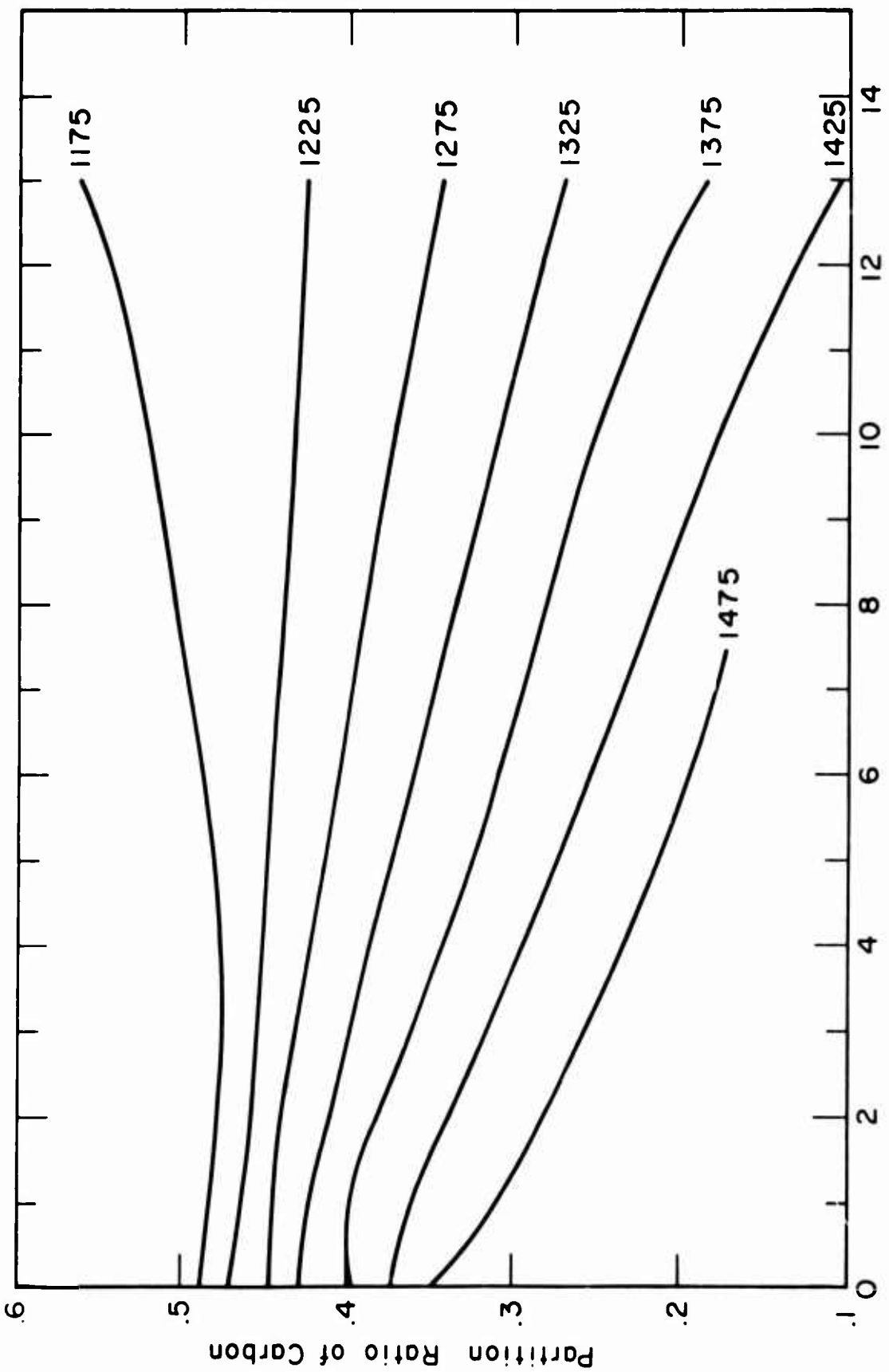

Figure 5: Partition ratio of carbon versus per cent chromium in the liquid.

small intervals of solidification*. We consider as example below AISI 52100 alloy (iron-1.15 per cent chromium-1.0 per cent carbon).

Assume first that both solutes in the 52100 alloy diffuse completely in the solid. Hence solute redistribution for both elements is described by equation (2). Results of simultaneous solution of equations (2), for carbon and chromium, are plotted in Figure 6 as interface composition, C_S^*, versus fraction solid f_S.

As second example, consider that the carbon diffuses completely in the solid and the chromium diffuses negligibly (and the activity coefficient of the carbon is independent of chromium concentration). Now the solute redistribution of carbon obeys equation (2) and that of chromium obeys equation (4). Results of calculation using these two equations, and the partition ratios of Figures 4 and 5, are given in Figure 7.

Finally, if neither carbon nor chromium diffuse in the solid, solute redistributions for both elements are given by equation (4), and are plotted in Figure 8.

Figures 6 and 8 are included for illustrative purposes only, since as will be shown later for the alloys considered herein, by far the most realistic assumptions are those embodied in Figure 7 (i.e., complete diffusion of carbon in the solid, no diffusion of chromium).

---

* These calculations are time consuming if done manually; for this work an IBM 7090 Computer, Computation Center, M.I.T., was employed.

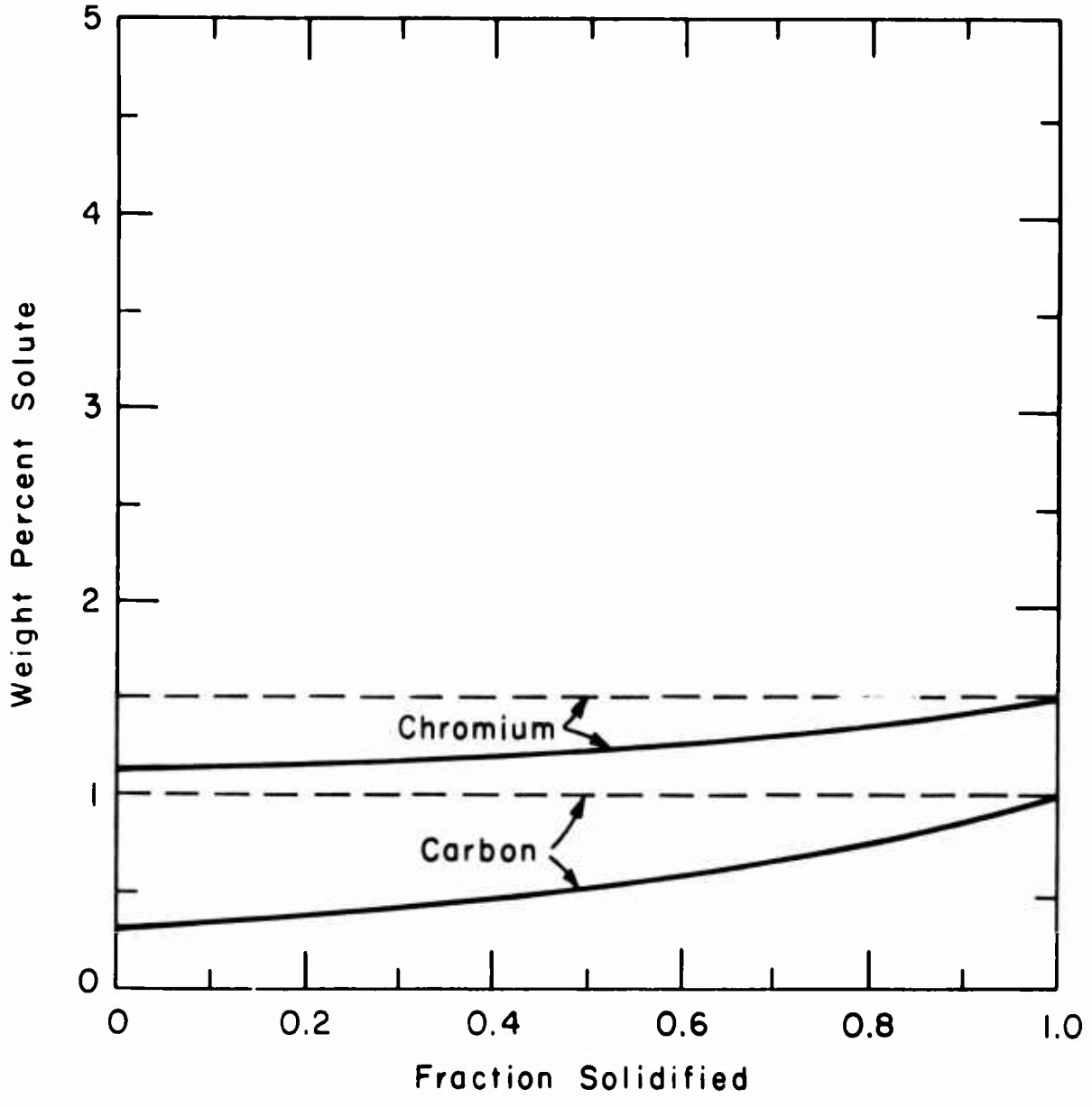

Figure 6: Solid composition, iron-1 per cent carbon-1.5 per cent chromium alloy, assuming complete diffusion of both solutes in the solid during solidification.

Solid lines represent interface compositions during solidification; dotted lines represented solute distribution after solidification.

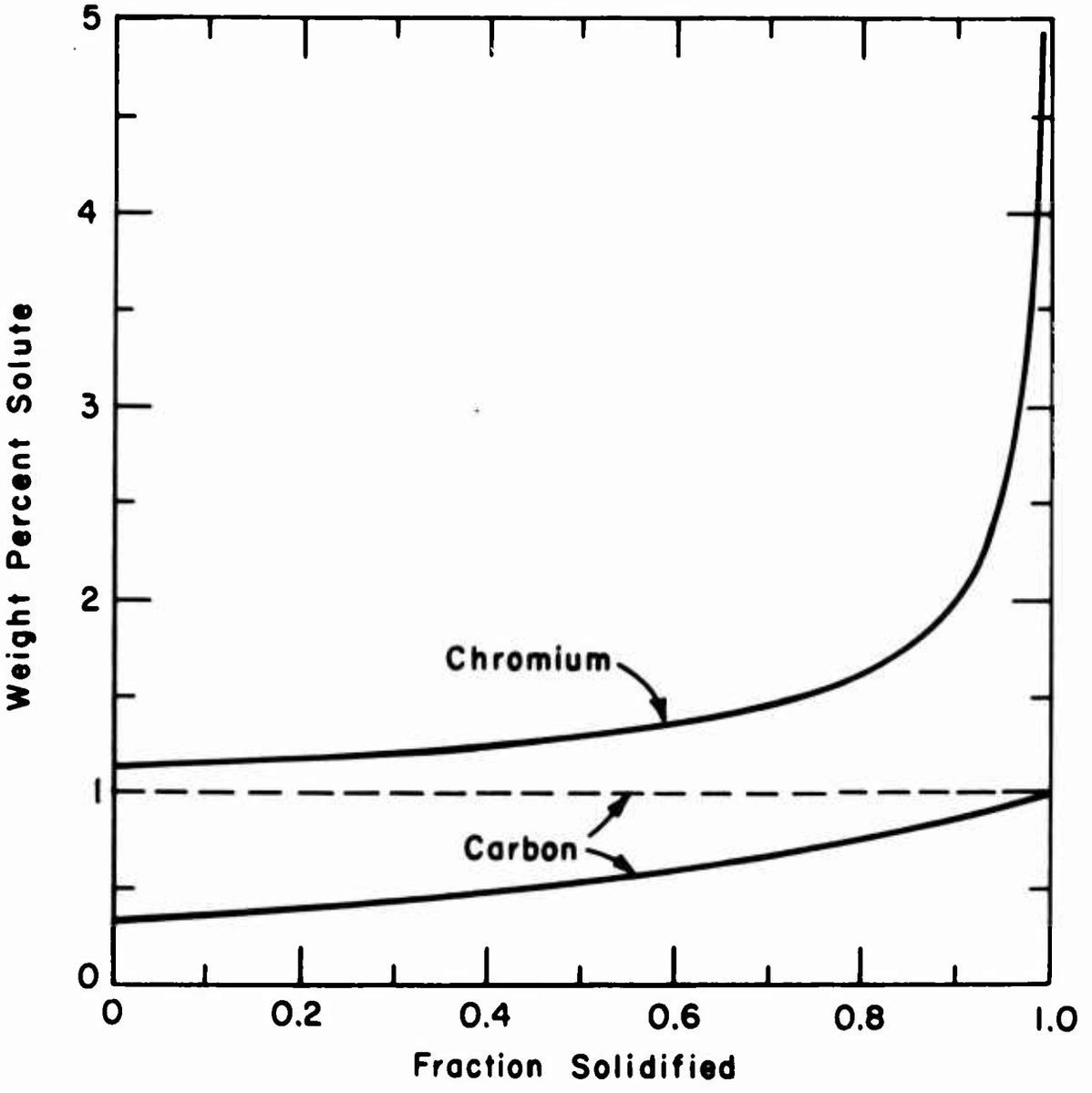

Figure 7: Solid composition iron-1 per cent carbon-1.5 per cent chromium alloy, assuming no diffusion in the solid of chromium, and complete diffusion of carbon.

The dotted line represents the final carbon distribution.

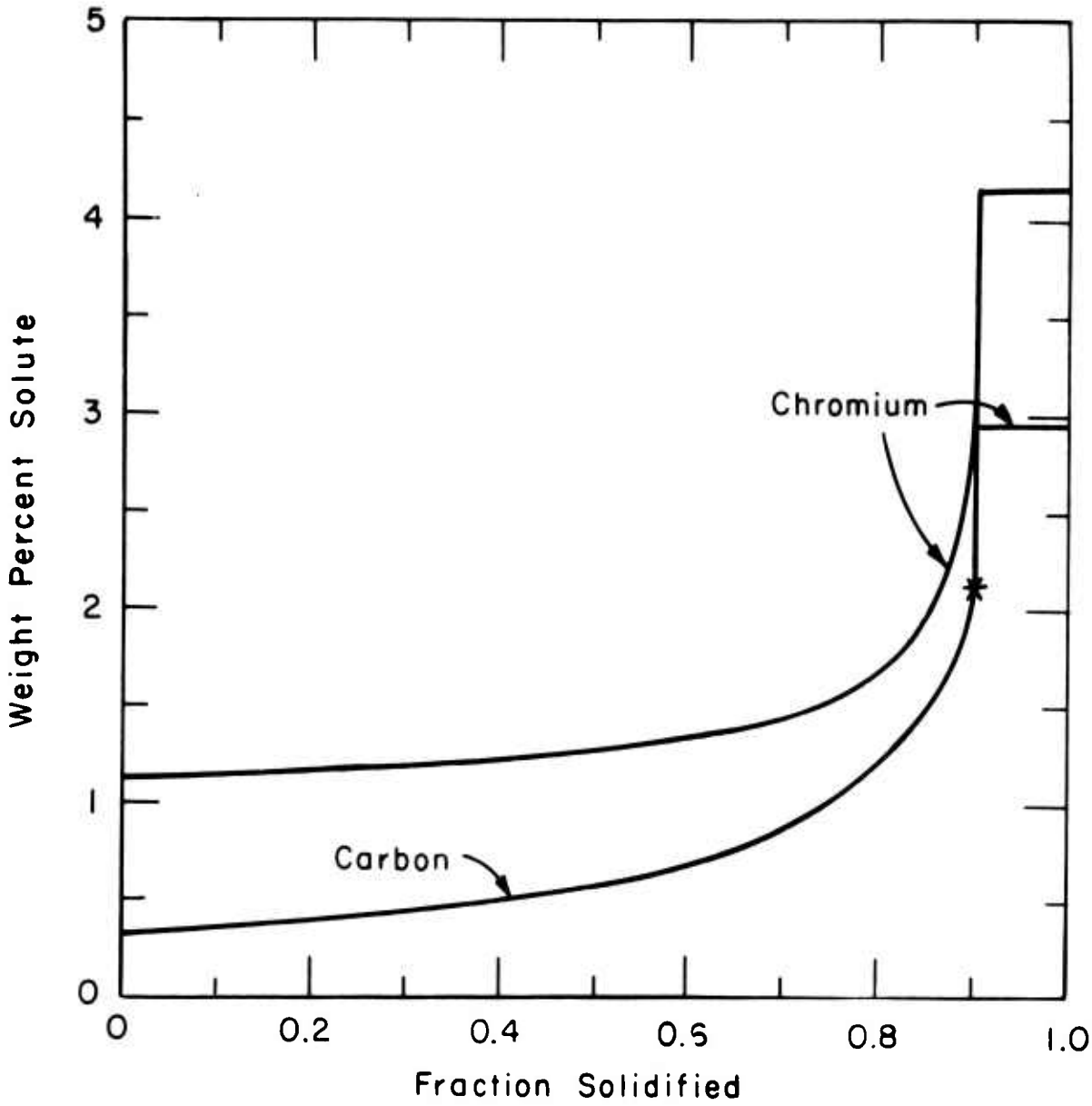

Figure 8: Solid composition iron-1 per cent carbon-1.5 per cent chromium alloy, assuming no diffusion of either solute in the solid.

Final solute distribution was calculated for a series of experimental alloys to be discussed later, all of which contained approximately 1.5 per cent chromium. Results of these calculations (made identical to those summarized in Figure 7) are given in Figure 9.

By combination of Figures 2, 3 and 9 (or by direct calculation), it is possible to plot fraction solid (at a given location) versus temperature at that location. This is done in Figure 10.

D. Measures of Microsegregation

The solute redistribution curves given earlier (C_S versus f_S) provide a complete description of "severity of microsegregation"[16] (although not its form or spacing, which depends on dendrite size and morphology). For comparison with experiment, however, it is desirable to assign a simple index to this "severity of segregation". Some useful indices are described below.

(a) Segregation Ratio.

An index of segregation that has been widely used to date[1-18] is the "Segregation Ratio", S, generally defined as:

$$S = \frac{(C_S)_{max}}{(C_S)_{min}} \qquad (5)$$

where S = segregation ratio

$(C_S)_{max}$ = maximum composition of solid (found in interdendritic regions for $k < 1$)

$(C_S)_{min}$ = minimum composition of solid (found in dendrite spine for $k < 1$)

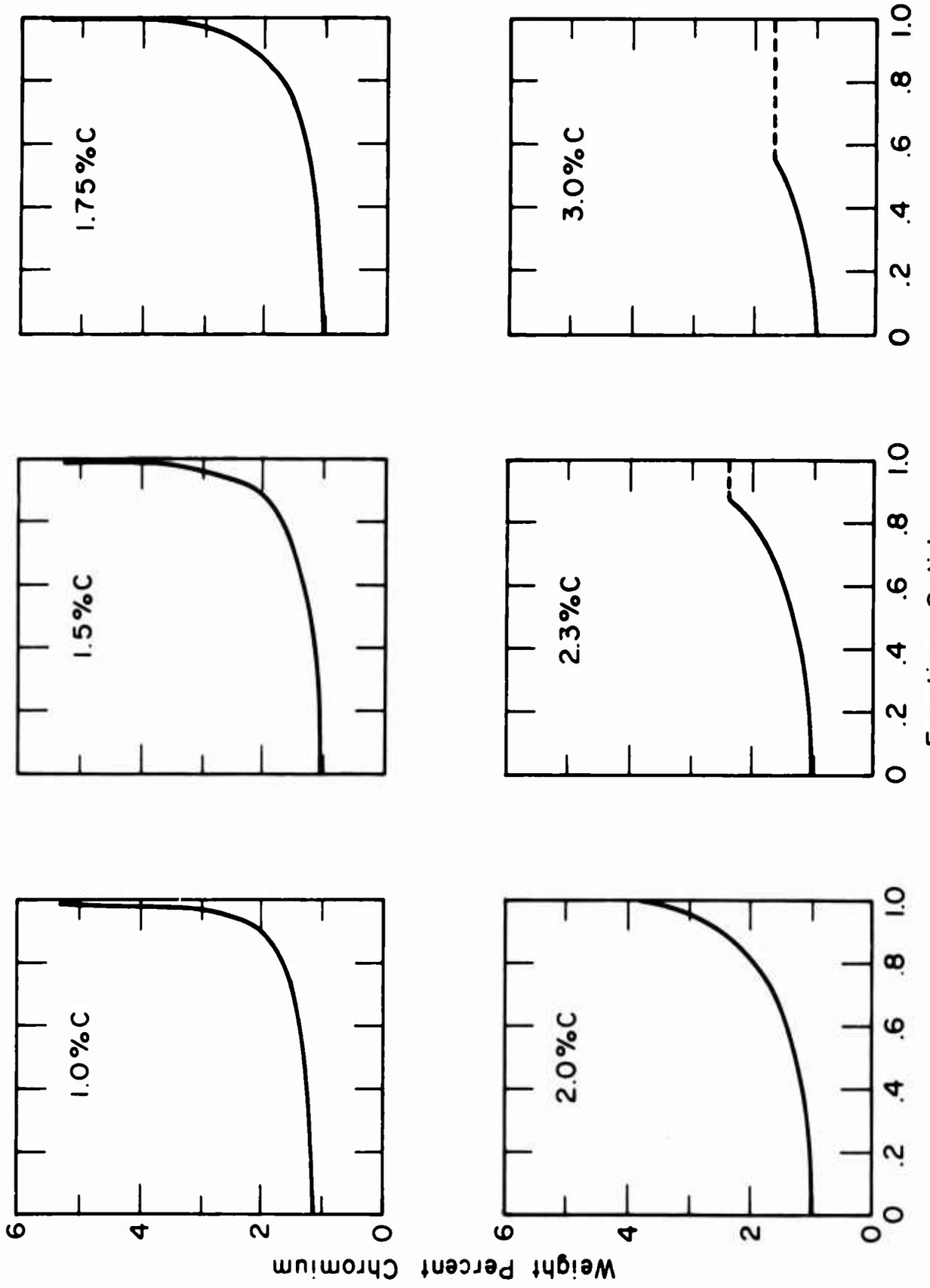

Figure 9: Calculated weight per cent chromium versus fraction solid for a series of Fe-C-Cr alloys, containing 1.5 per cent chromium, assuming no diffusion of chromium in the solid and complete diffusion of carbon.

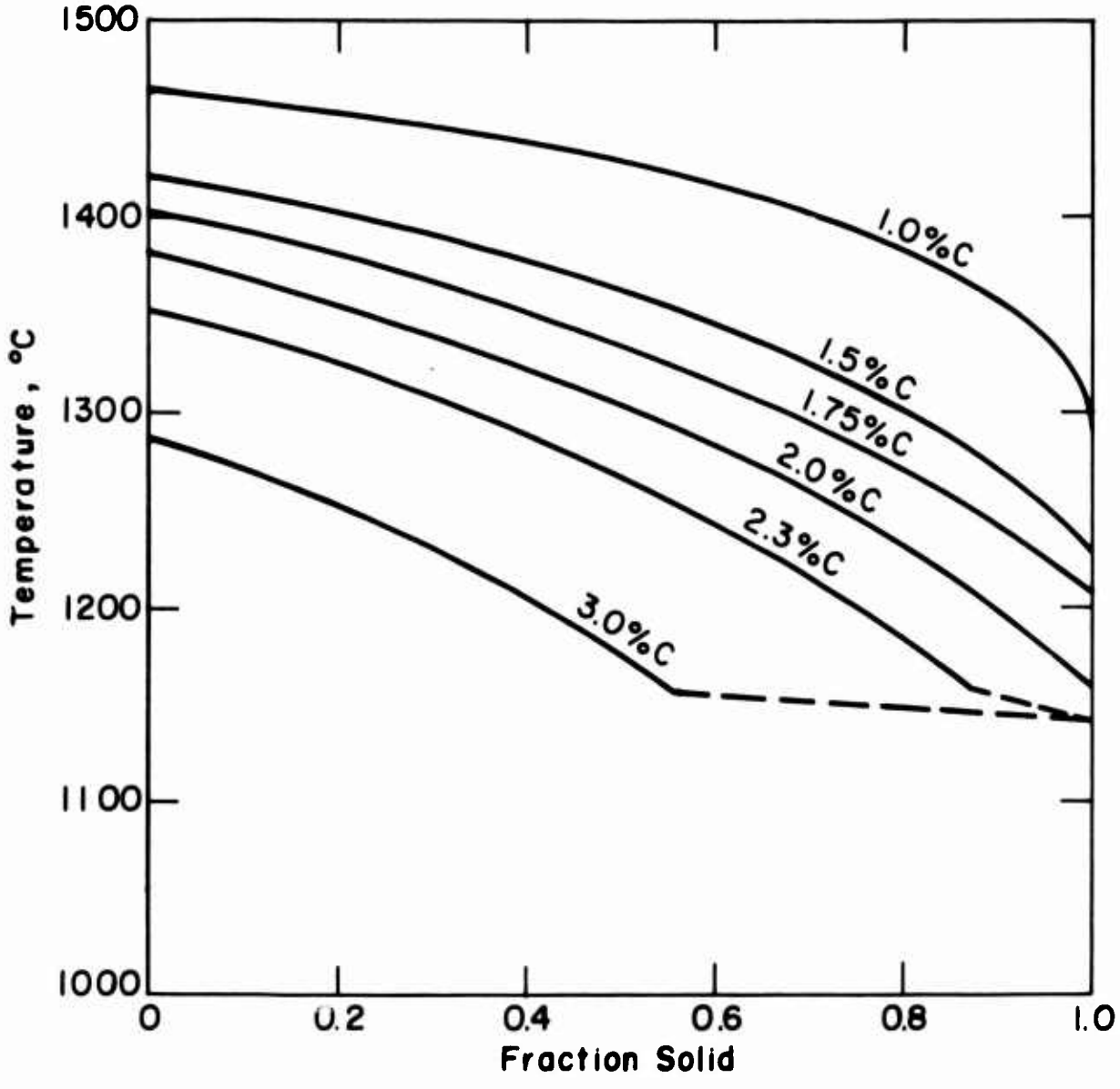

Figure 10: Fraction solid versus temperature for iron-carbon-chromium alloys calculated assuming no diffusion of chromium and complete diffusion of carbon in the solid.

Calculated for alloys of 1.5 per cent chromium, and of carbon contents from 1.0 to 3.0 per cent carbon.

This index has the advantages that (1) it is simply calculated, (2) it can be approximately determined experimentally quite simply. Disadvantages include the fact that it is tedious and sometimes impossible to obtain experimentally a segregation ratio with a high degree of accuracy, because concentrations may approach asymptotically very high values at the end of solidification (and hence over very small distances). These concentration changes may take place over distances of the same order as probe spot size, and in any case, the steep concentration gradients over small distances mean that small difference in amount of diffusion can profoundly affect measured segregation ratio. Other disadvantages include the fact that, in multiphase alloys, segregation ratio may not be a very sensitive index to changes in microsegregation.

Segregation ratios for the iron-carbon-chromium alloys shown in Figure 9 are plotted in Figure 11, as segregation ratios versus per cent carbon, for constant chromium. Because composition of alloys in Figure 9 asymptotically approach high values at the end of solidification $(C_S)_{max}$, of equation (5) has been arbitrarily taken as that composition of $f_S = 0.99$.

2. Amount of Second Phase.

A second measure of microsegregation which has been employed[16,17,19] is amount of second phase (e.g., fraction eutectic). Fraction eutectic, f_E, taken from curves such as those of Figure 9 are plotted versus per cent carbon in Figure 12, for chromium ≅ 1.5 per cent.

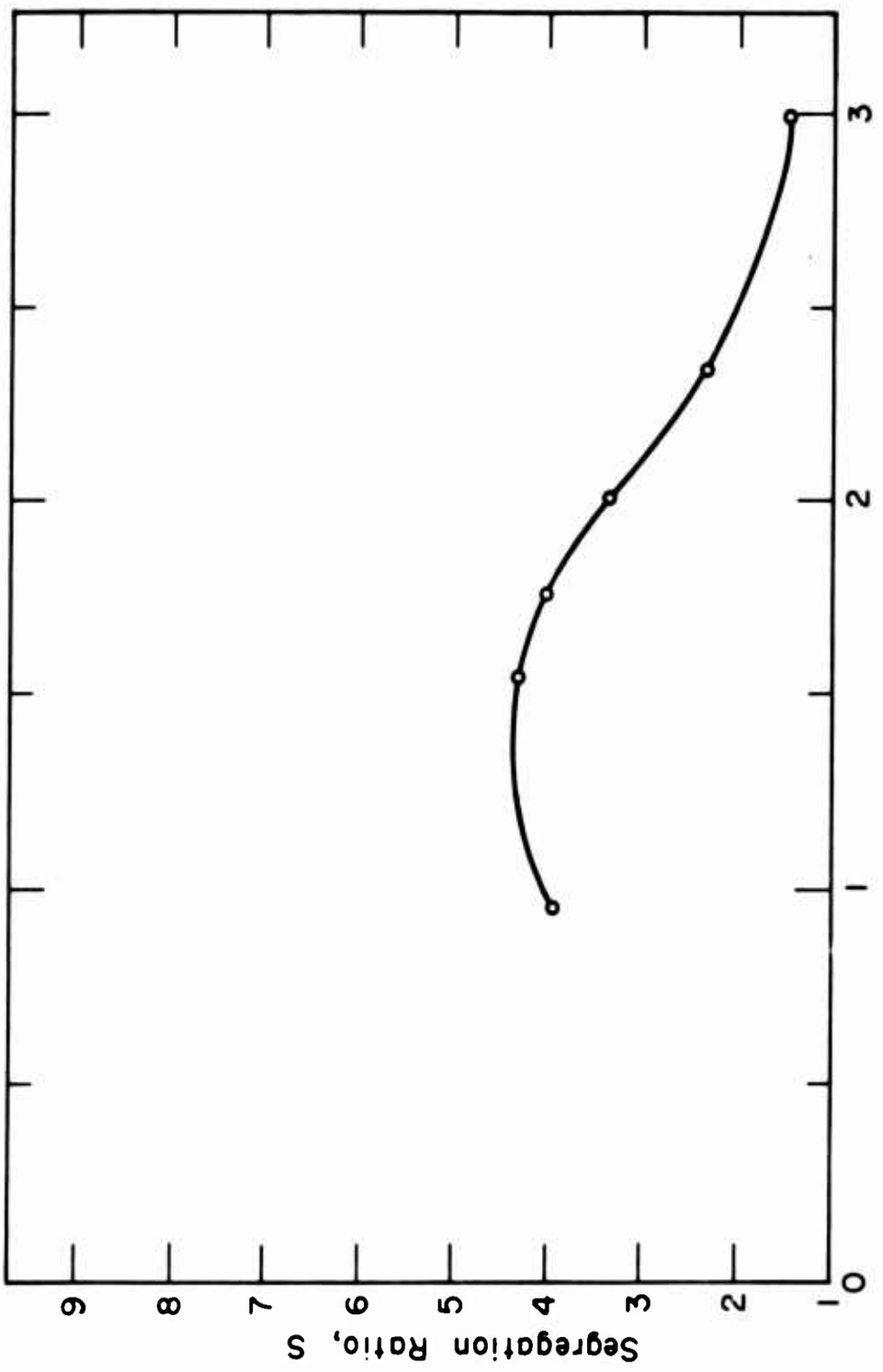

Figure 11: Calculated segregation ratio, iron-1.5 per cent chromium alloy containing 1 - 3 per cent carbon.

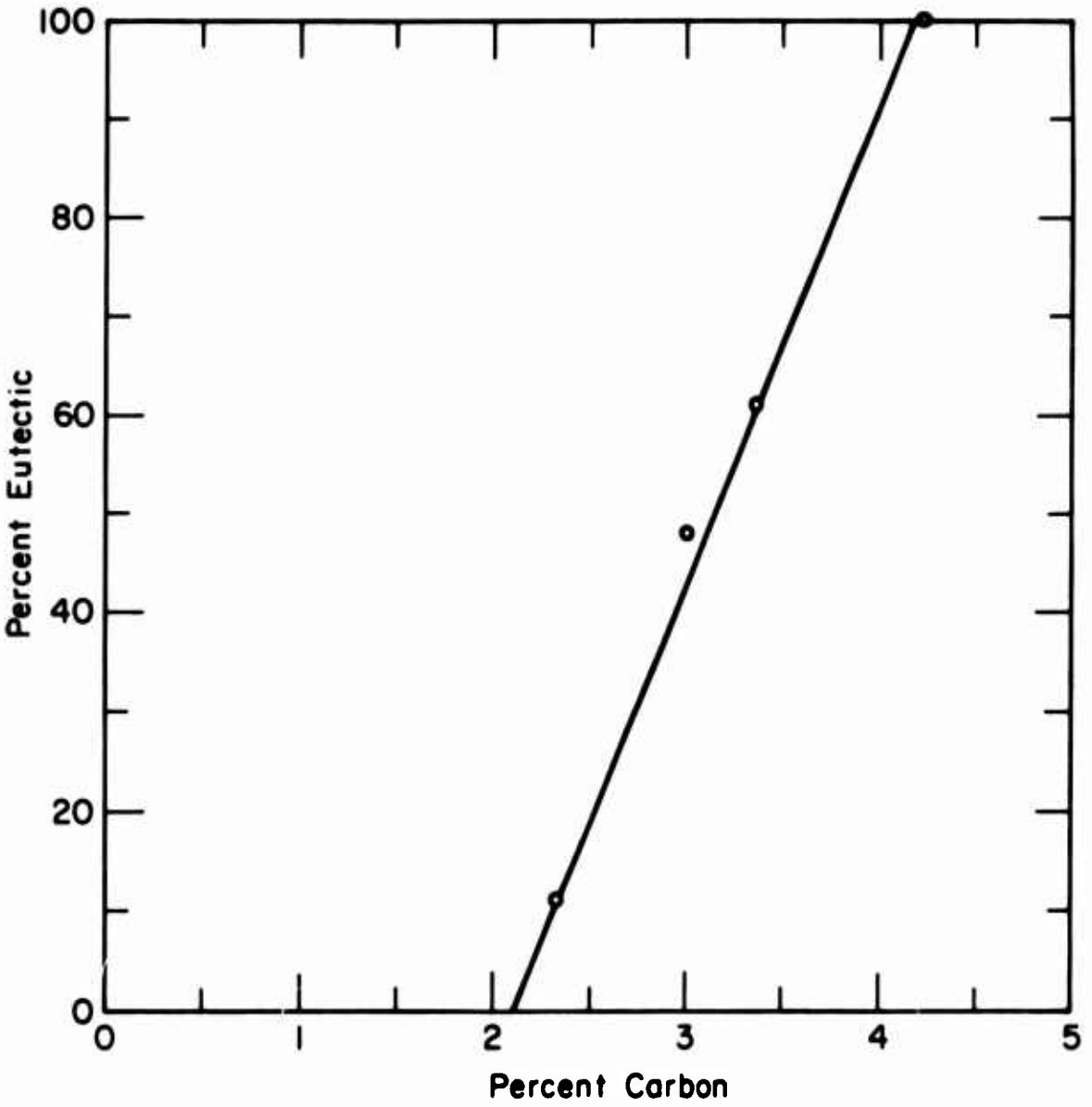

Figure 12: Calculated fraction eutectic (ledeburite) assuming no diffusion of chromium and complete diffusion of carbon during solidification for alloys with 1.5 per cent chromium.

3. Composition Deviation Index.

An alternative measure of microsegregation, incorporating some of the attributes of both the foregoing is composition deviation index σ^m, defined as:

$$\sigma^m = \frac{1}{C_{oi}} \int_0^1 |C_{Si} - C_{oi}| \, df'_S \qquad (6)$$

where C_{Si} = composition of isoconcentration surface enclosing volume fraction of solid f'_S. ($f'_S = f_S$ for no solid diffusion.)

This parameter has the following properties. If there is no segregation $\sigma^m = 0$; for maximum segregation the partition ratio equals zero and the alloy must solidify so that

$$C_{Si} = 0 \qquad 0 \leq f'_S < \left(1 - \frac{C_{oi}}{C_{Mi}}\right)$$

$$C_{Si} = C_{Mi} \qquad \left(1 - \frac{C_{oi}}{C_{Mi}}\right) < f'_S \leq 1$$

where C_{Mi} = maximum concentration, and

$$\sigma^m = 1 - \frac{C_{oi}}{C_{Mi}} \qquad (7)$$

For alloys that are homogenized at a temperature such that the equilibrium state is a single phase, σ^m approaches zero with time. For alloys whose equilibrium state is two phases,

$$\sigma^m \rightarrow \frac{2(C_{Oi} - C_{\alpha i})(C_{Oi} - C_{\beta i})}{C_{Oi}(C_{\alpha i} - C_{\beta i})} \qquad (8)$$

where $C_{\alpha i}$, $C_{\beta i}$ = concentration of i in the two equilibrium phases

To eliminate experimental difficulties in determining the exact concentration profile for the last stages of solidification, equation (6) is written:

$$\sigma^m = \frac{2}{C_{Oi}} \int_0^{\bar{f}'_S} |C_{Si} - C_{Oi}| \, df'_S \qquad (9)$$

where $\bar{f}'_S$ = volume fraction at C_{Si} equal to C_{Oi}

Advantages of σ^m as an index of segregation include (1) it allows comparison of microsegregation in single phase alloys with that in multiphase alloys, (2) it can be introduced directly into solutions of Fick's second law to describe homogenization kinetics.

From an experimental point of view, advantages include (1) determination of σ^m depends not on accurate location and measurement of maxima and minima, but on compositions at all values of f'_S, and (2) σ^m can readily be determined by simple experimental procedures to be described later.

Figure 13 shows σ^m plotted versus per cent carbon for iron-carbon-chromium alloys containing approximately 1.5 per cent chromium, calculated from curves in Figure 9.

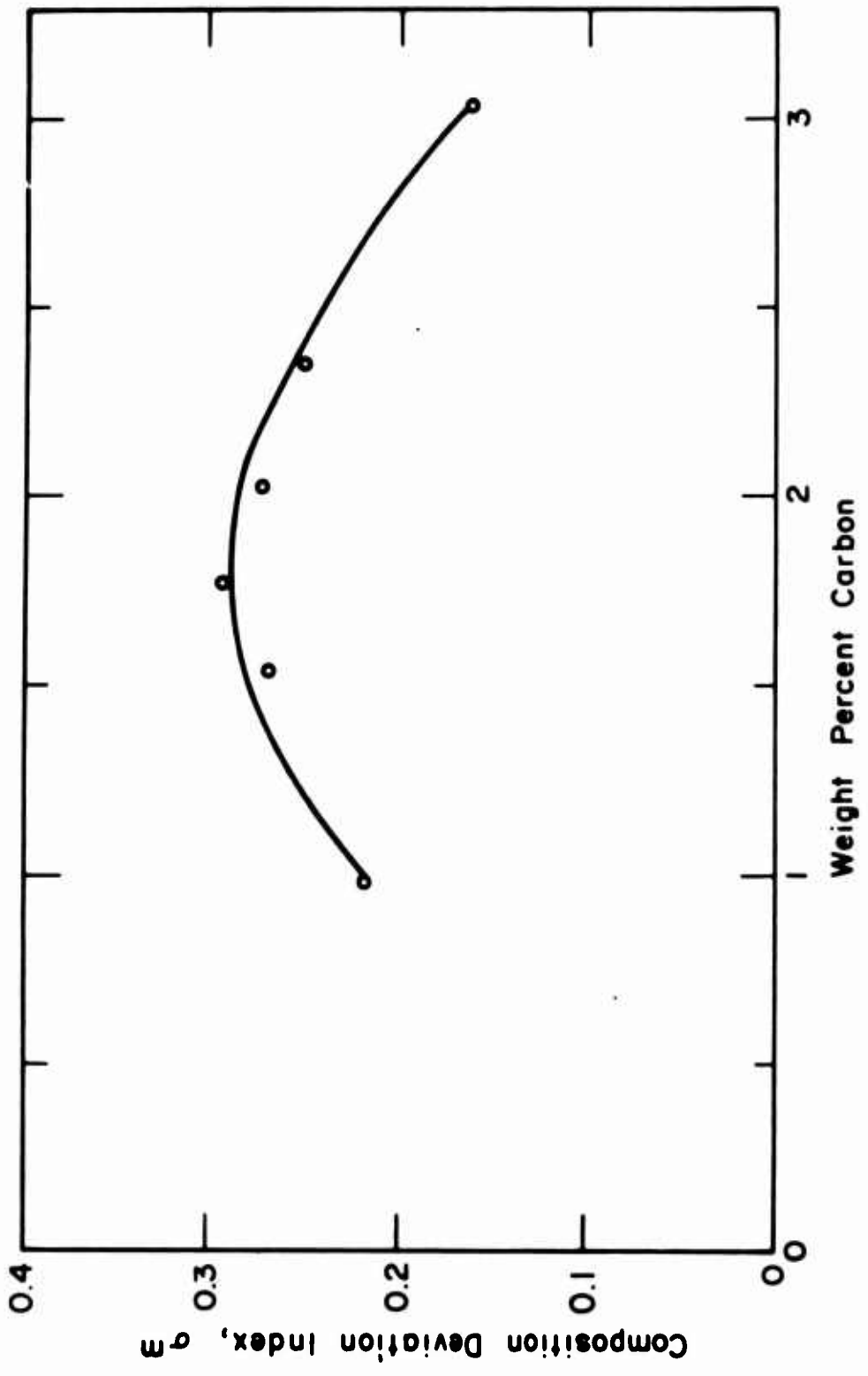

Figure 13: Calculated composition deviation index, σ_m, versus weight per cent carbon for iron-carbon-chromium alloys containing 1.5 per cent chromium.

PART II: MEASUREMENTS OF MICROSEGREGATION

A. Experimental Procedure

1. Castings Poured.

Six small ingots (80 - 100 grams) were melted and cast in a vacuum induction furnace. The alloys were melted in alumina crucibles and allowed to solidify in situ. All alloys were iron-carbon-chromium with approximately constant chromium content (1.5 per cent); carbon contents ranged from 0.96 to 3.00 per cent. Compositions, cooling rates during solidification, and dendrite arm spacings are given for each of the ingots in Table III. Structure of all castings was equiaxed.

To study effect of solidification rate on microsegregation, a unidirectionally solidified ingot was cast of one alloy (iron-1.5 per cent chromium-1.0 per cent carbon)*. Ingot weight was approximately 40 pounds. Thermocouples were inserted in the mold to measure cooling rates at different locations. Figure 14 shows the mold design**.

Metal melted for this ingot was electrolytic iron, chromium, and high purity cast iron. Melting was by induction, in a magnesia crucible under a blanket of argon gas. Deoxidation was carried out

---

* Measured composition (wet chemical analysis) was 1.02 per cent carbon, 1.63 per cent chromium, 0.47 per cent manganese, 0.60 per cent silicon.

** This ingot was used only to obtain thermal data to relate experiment to theory. Structure study and microsegregation measurements were on an ingot cast in identical manner, under auspices of an earlier research program[15].

TABLE III

Summary of Experiments on Small Ingots

Casting Designation	Melt Analyses % C	% Cr	Solidification Interval Cooling Rate, °C/Second	Dendrite Element Spacing μ
a	3.00	1.44	.91	55
b	2.32	1.48	1.03	72
c	2.01	1.49	.94	84
d	1.75	1.48	.89	70
e	1.54	1.45	.92	72
f	0.96	1.48	.87	87

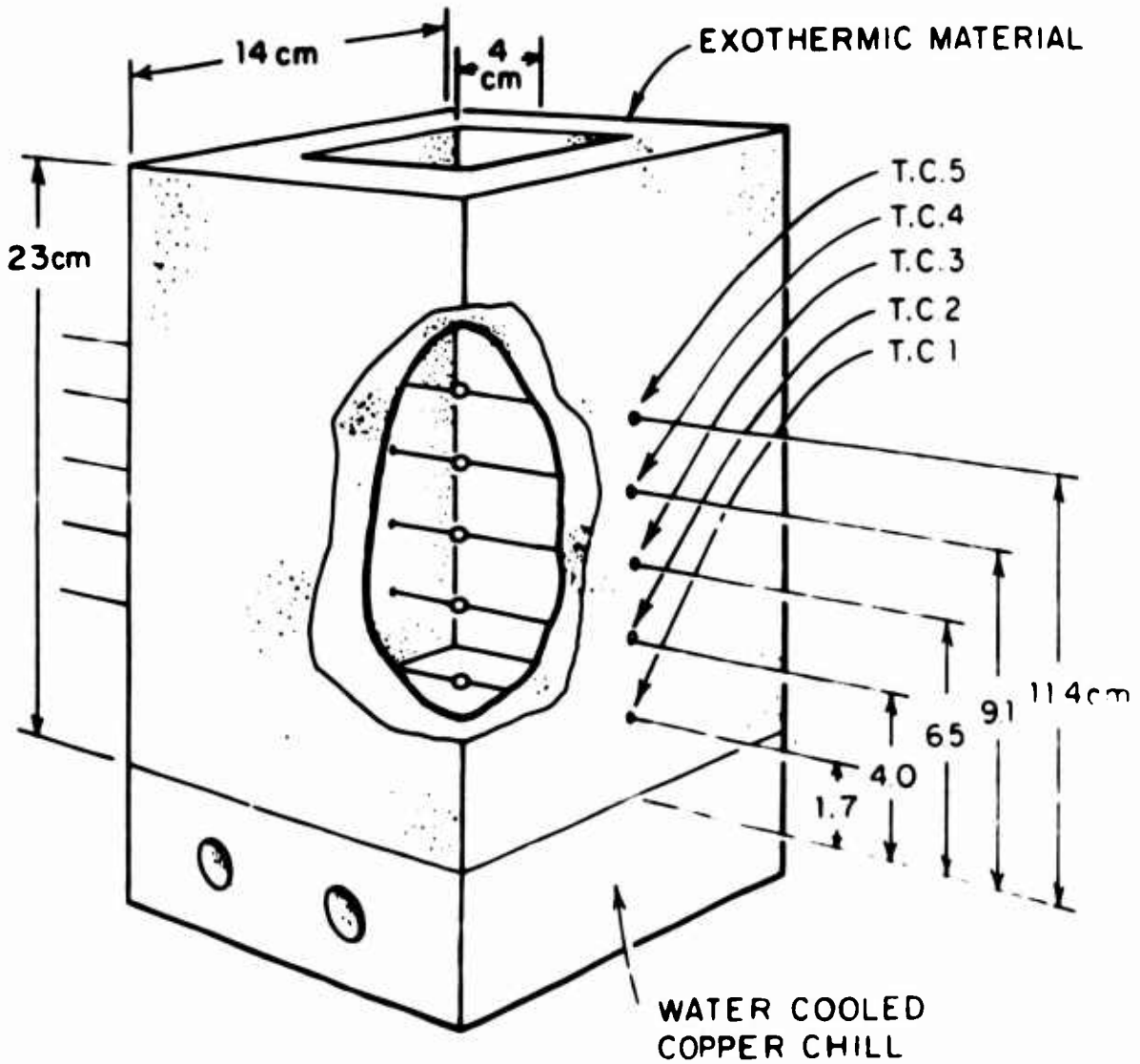

Figure 14: Mold for producing unidirectional ingot. Shown are locations of thermocouples used to obtain cooling curves.

with 0.1 per cent aluminum, and the ingot was poured at 1600°C. After cooling, the ingot was sectioned and examined; structure was fully columnar. The cooling curves for the ingot, obtained by a sixteen-point recorder for the thermocouples 4.0 to 11.4 cm. from the chill and by a continuous strip chart recorder for the thermocouple 1.7 cm. from the chill, are shown in Figure 15.

2. Microstructures.

Prior to microprobe study, specimens were removed for metallographic study from an identical unidirectional ingot to the one on which thermal analysis was conducted. In order to better delineate the structure, the specimens were heated for 15 minutes at 825 - 850°C in an argon atmosphere and water quenched. At the elevated temperature carbides coexist with austenite; quenching results in a martensitic matrix with a higher concentration of carbides in the interdendritic (chromium-rich) regions. Typical microstructures can be seen in Figure 16; dendrite arm spacings are plotted in Figure 17.

3. Microprobe Analysis.

In the alloys studied, the concentration gradients of chromium are small in the low solute regions, but often quite steep in the interdendritic regions. Thus the chromium minima could be found easily, by directing the microprobe scan across dendrite cores. To determine maxima the samples were manually scanned in the interdendritic areas, and the instaneous intensity was detected; point counts (30 second intergration times) were then made at close intervals (1 - 3μ) across the maximum.

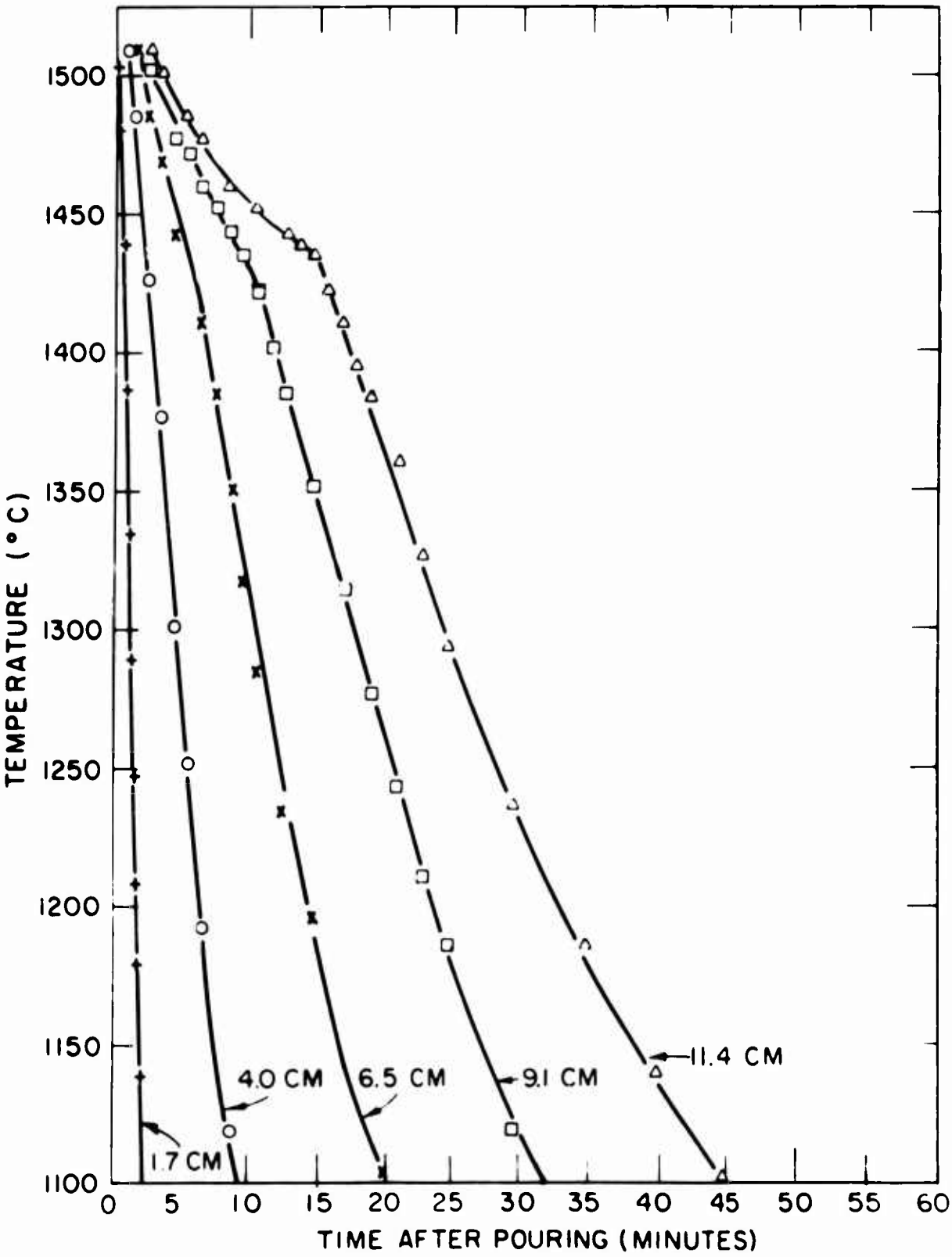

Figure 15: Cooling curves for the unidirectionally solidified 52100 ingot.

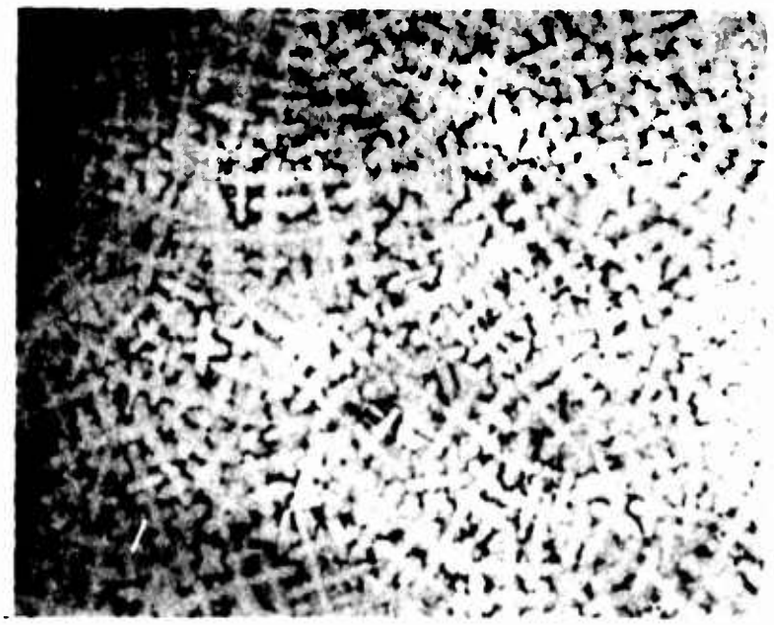

(a)

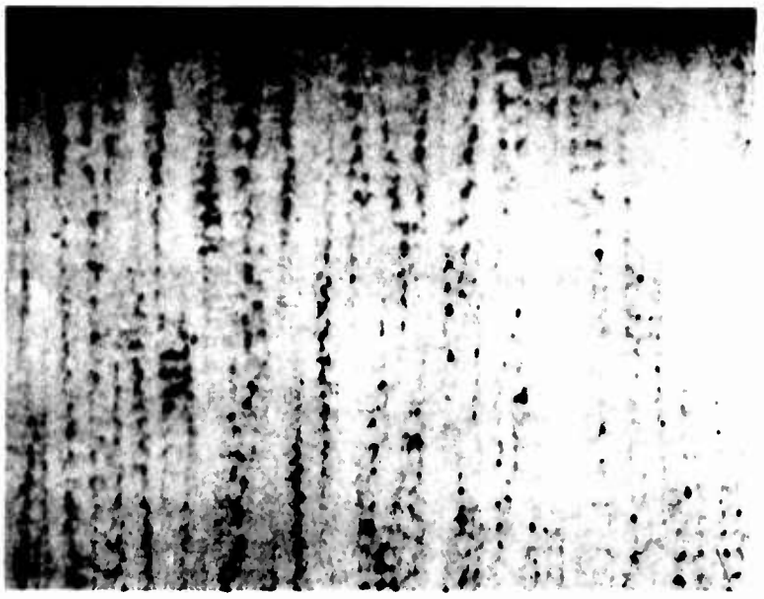

(b)

Figure 16: Dendritic structure of 52100 unidirectional ingot two inches from the chill[15].

(a) perpendicular to heat flow, 12X.
(b) parallel to heat flow, 12X.

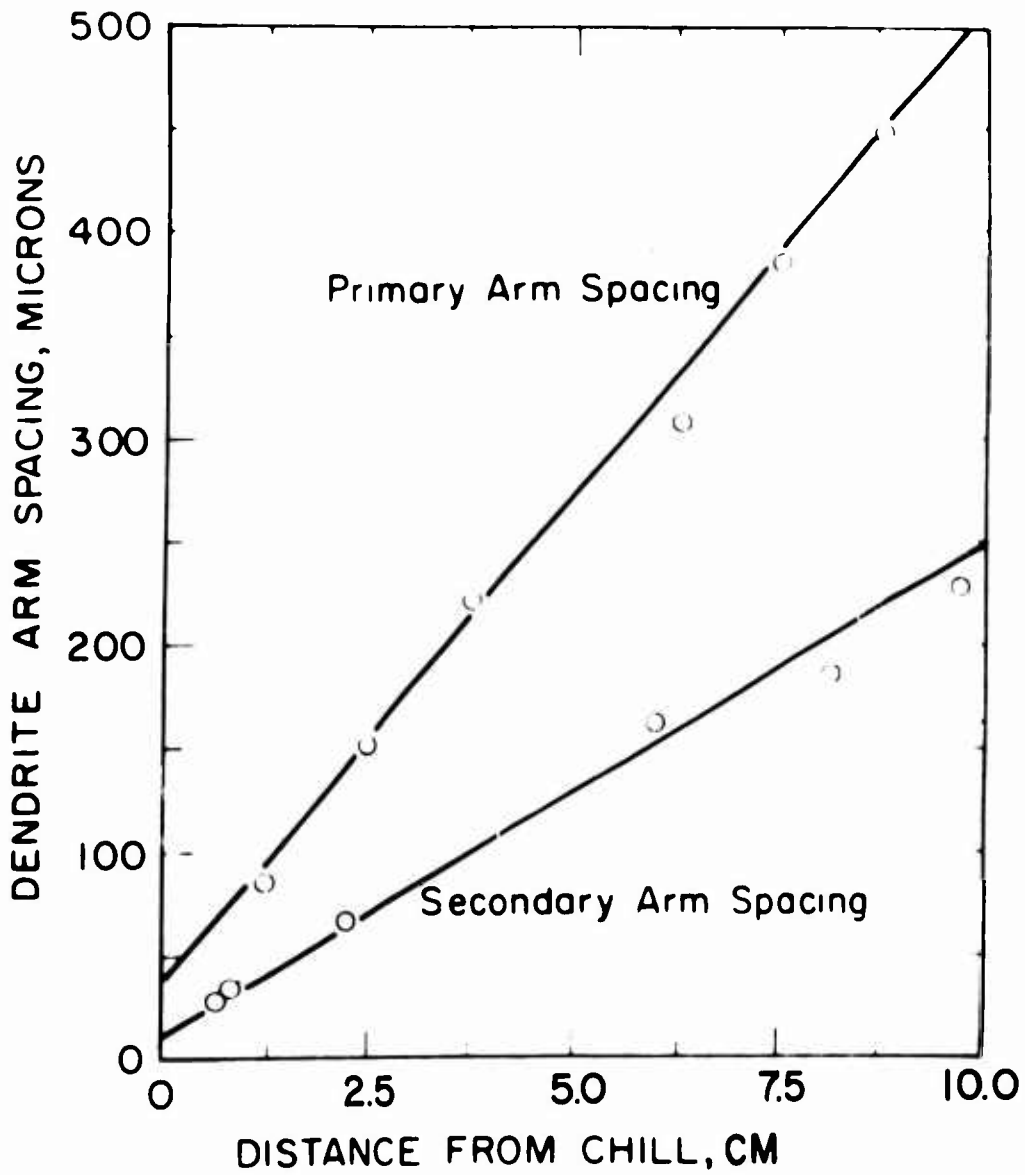

Figure 17: Dendrite arm spacing in 52100 unidirectional ingot[15].

For the columnar samples, the normalized intensities were converted to compositions by the use of a calibration curve based on homogenized standards all with approximately 1 per cent carbon. Analyses were carried out using an A.R.L. microprobe with a "take-off" angle of 52.5°. The results of these microprobe analyses are given in Table IV. Maxima and minima only were determined for these samples.

For the equiaxed small ingots, maxima and minima were determined in similar manner, except that X-ray intensities were converted to weight per cent chromium using the procedure outlined in Appendix F. In addition, three of the specimens (ingots d, e, and f) were scanned with long paths of random orientation, to obtain directly the form of the overall final solute distribution; i.e., chromium concentration, C_{Si} versus fraction solid, f_S'*. This is done following a procedure identical to that for determining amount of second phase by lineal analysis; in this case the amount of "second phase" is the volume fraction solid, f_S', with a composition of C_{Si} and greater. It is determined simply from the results of a probe scan, as shown schematically in Figure 18, as:

$$f_S' = \frac{\ell_1 + \ell_2 + \ell_3 + \ldots}{L} \qquad (10)$$

The three specimens scanned to determine f_S', (d, e, and f) were scanned at 40, 80, and 80 microns per minute, respectively. Each specimen was scanned a total of 5000 microns. Statistics of lineal

---

* This procedure was first suggested by Dr. Paul J. Ahearn and employed in his doctoral thesis, "Solute Redistribution in the Dendritic Solidification of a Tin Alloy", Department of Metallurgy, M.I.T., February, 1966.

TABLE IV

Microsegregation of Chromium in AUSTU 52100
Unidirectional Ingot*

Distance from Chill, Inches	Minimum % Cr, C°_{m}	Maximum % Cr, C°_{M}	Segregation Ratio $S = C^{\circ}_{m}/C^{\circ}_{M}$
1/2	1.2	4.6	4.0
2	1.2	4.8	4.1
3-1/2	1.0	4.3	4.3
5	1.0	4.2	4.0

* Segregation data obtained under an earlier research program and reported previously[15].

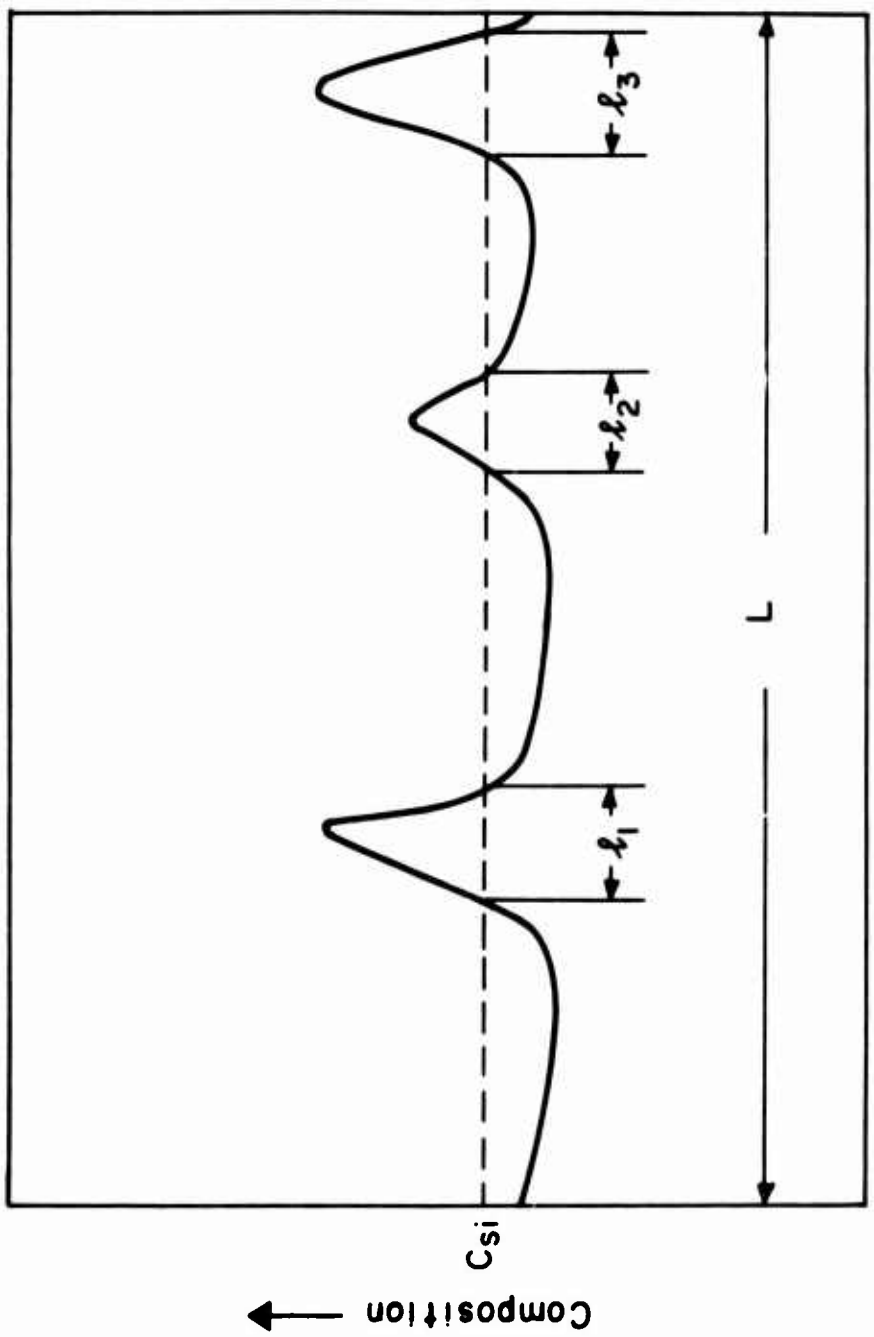

Figure 18: Schematic microprobe analysis to determine volume fraction of material with a composition of $C^{\bullet}_{S1}$ and greater.

analysis as given by Hilliard and Cahn[20] were applied to these experimental conditions to indicate probable erros.

B. Results

1. Microsegregation in Unidirectionally Solidified AISI 52100 (Iron-1.5 Per Cent Chromium-1.0 Per Cent Carbon).

Table IV summarizes the results of microprobe data for AISI 52100 alloy at four different distances from the chill. Minimum and maximum values of composition, and segregation ratio, do not change appreciably with distance from the chill (and hence with cooling rate). Minimum values are essentially those predicted by theory given in Part I (Figure 7) while maximum values are somewhat less, presumably because of some diffusion in the solid down to steep concentration gradients present near the end of solidification.

An estimate of extent of diffusion of alloy elements in the solid during solidification can be made from the factor, α_i, where[16]:

$$\alpha_i = \frac{a \bar{D}_{Si} t_f}{d^2} \tag{11}$$

where: a = constant (4 or 8 depending on whether df_s/dt is assumed a linear or parabolic function of time)

$\bar{D}S_i$ = mean diffusion coefficient during solidification in the solid

t_f = solidification time interval

d = dendrite arm spacing

For $\alpha_i << 1$, diffusion in the solid during solidification is negligible, and for $\alpha_1 >> 1$, diffusion is complete.

As example of application of equation (11), consider the unidirectional ingot, 6.5 cm. from the chill. Here, $d = 160 \times 10^{-4}$ cm., (secondary dendrite arm spacing, Figure 17). Local solidification time, θ_f, is 860 seconds (determined from Figure 15 assuming liquidus and solidus temperature as given by Figure 10). Now take the diffusion coefficients of carbon[21] and chromium[22] as:

$$D_C = 0.12 \exp \left[- \frac{16,100}{T} \right] \tag{12a}$$

$$D_{Cr} = 2.35 \times 10^{-5} \exp \left[- \frac{17,300}{T} \right] \tag{12b}$$

Using these values at a temperature we expect the alloy to be approximately 50 per cent solid (1420°C, Figure 10), $\alpha_C \approx 120$, and $\alpha_{Cr} \approx .01$. Hence, we consider that, as the model examined in most detail in Part I assumed, diffusion of carbon is essentially complete during solidification. We expect the diffusion of chromium to be small but as experiment seems to indicate, not negligible.

Of course, some of the reduction of the maxima in solute concentrations observed could be due to diffusion in the solid after, as well as during, solidification. In this case, it can be readily shown that the extent of diffusion depends on the parameter

$$(\alpha_i)_{Cooling} = \int_0^t \frac{4D_S t}{d^2} \, dt \tag{13}$$

and when $(\alpha_i)_{Cooling}$ is much less than 1 diffusion during cooling is small; when $(\alpha_i)_{Cooling}$ is much less than α_i, this diffusion is small

compared with that occurring during solidification. The quantity (α_1) cooling was calculated for chromium for each thermocouple location in the unidirectional ingot (Figure 14) and in each case was approximately 10^{-3}. Hence, it is concluded that diffusion in the solid during cooling may be neglected for this alloy.

2. Effect of Carbon.

(a) Segregation Ratio.

Segregation ratios for the iron-carbon-chromium containing approximately 1.5 per cent chromium are shown in Figures 19 and 20. The segregation ratios shown in Figure 19 are based on the maximum concentration of the carbide in ledeburite when present divided by minimum measured compositions. In Figure 20, the maximum concentration is the average of the ledeburite phases. Also shown in Figures 19 and 20 are (1) data from low alloy steels given in Table 1[9], (2) data for iron-carbon-1.5 per cent chromium alloys of Melford and Doherty[14], and (3) a point for an iron-1.5 per cent chromium alloy containing 0 per cent carbon obtained in this work.

The alloys of Figures 19 and 20 may be classified into three groups:

1. Up to approximately 0.5 per cent carbon, initially ferrite solidifies.
2. From 0.5 per cent to approximately 1.5 per cent carbon, only austenite forms during the solidification, and
3. When more than 1.5 per cent carbon is present, the alloys solidify as austenite with ledeburite forming as the liquid

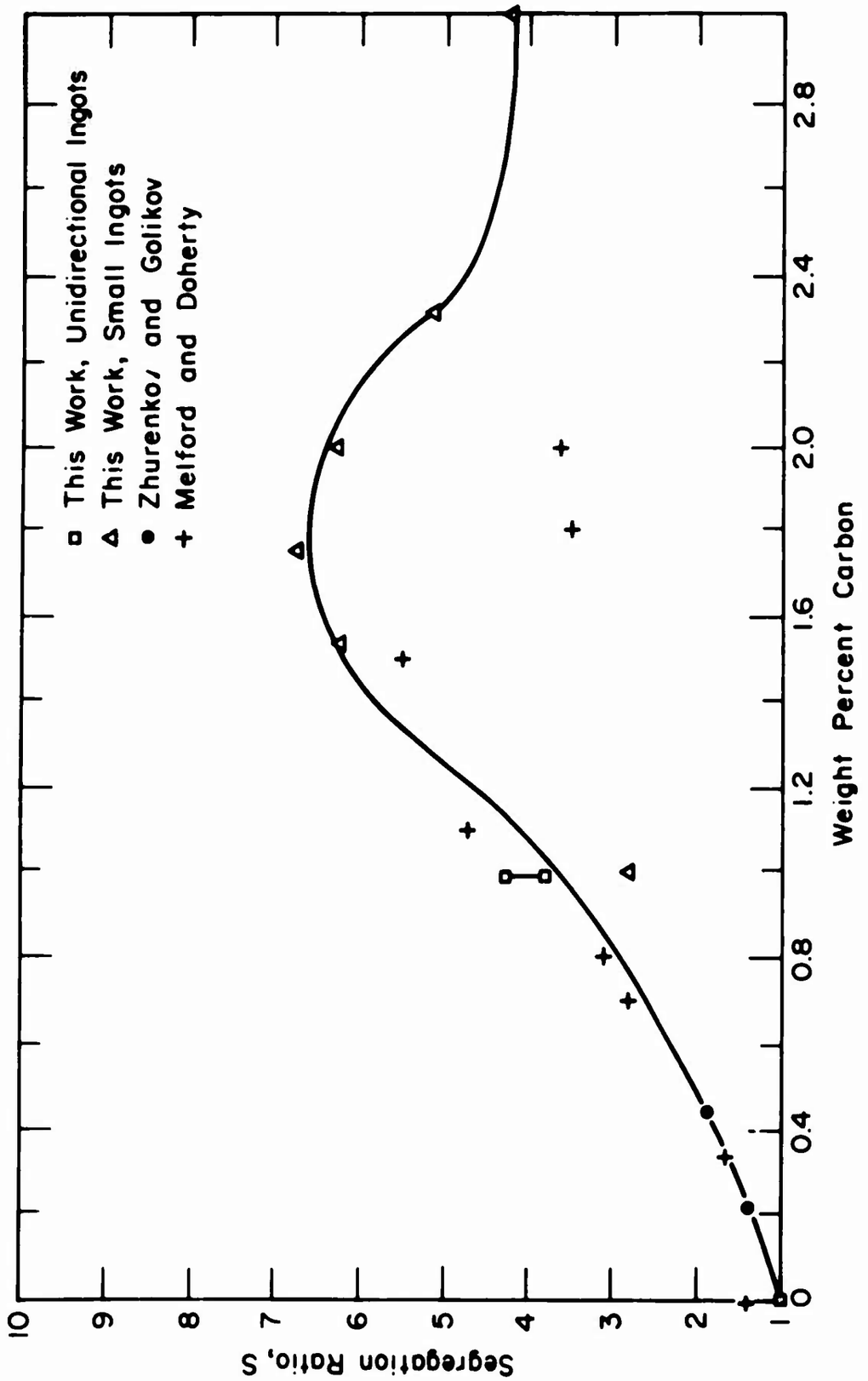

Figure 19: Segregation ratio of chromium versus carbon content for steels containing approximately 1.5 per cent chromium. From this work, Zhurenkov and Golikov[9], and Melford and Doherty[14].

Where eutectic was present in ingots cast in this study, C_{max} (for calculation of S) was taken as the maximum composition of the carbide within the eutectic.

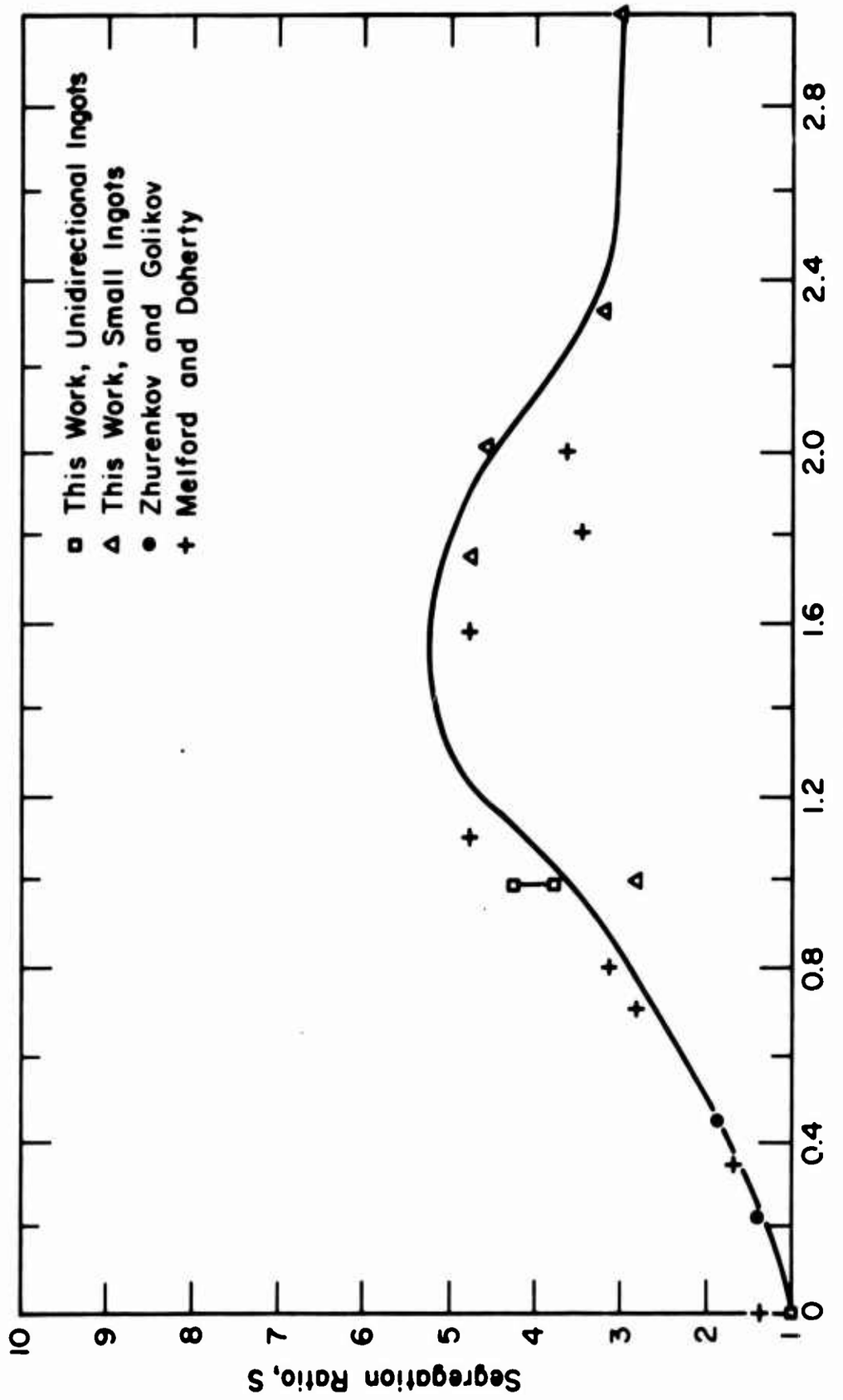

Figure 20: Segregation ratio versus weight per cent carbon. Identical to Figure 19 except that where eutectic was present in ingot cast in this study (black triangles), C_{max} (for calculation of S) was taken as the average composition of the eutectic.

becomes enriched enough in carbon that the ledeburite-liquid eutectic valley is reached.

Note the segregation ratio increases as carbon increases until ledeburite forming alloys are reached where the segregation index decreases as carbon increases still more.

In the small castings, as in the unidirectional ingot discussed above, reasonable assumptions are complete diffusion of carbon and small diffusion of chromium since, using the data of Table III, and the curves of Figure 10 to calculate α_i at approximately 50 per cent solid for all alloys, $\alpha_C \approx 100$ and $\alpha_{Cr} \approx .01$.

(b) Concentration Profiles.

Experimental profiles for the three alloys examined (using the lineal analysis technique described above) are given in Figures 21 through 23. These are compared with the theoretical curves calculated earlier and presented in Figure 9. Note the generally close agreement of experiment with theory; it is expected that deviations are primarily due to (1) presence of limited diffusion of chromium during solidification, and (2) errors in phase diagram determination. Figure 24 summarizes the experimental and theoretical results of segregation ratio, S, versus weight per cent carbon.

The composition deviation index, σ^m, described earlier, was calculated from the experimental curves of Figures 21 through 23. Results are shown in Figure 25, and compared with the theoretical curve presented earlier in Figure 13. Agreement between experiment and theory is

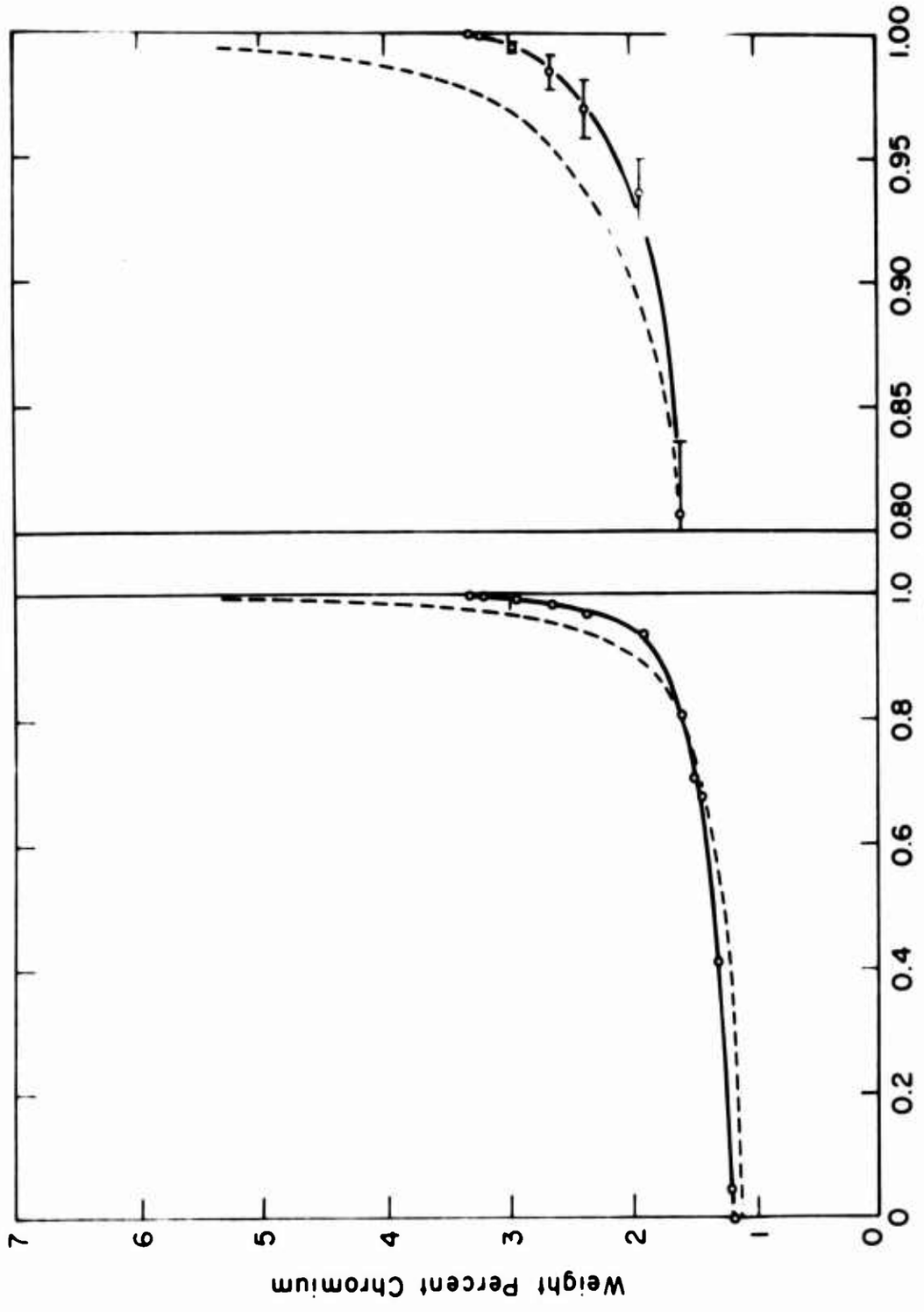

Figure 21: Concentration profile for iron-1.0 per cent carbon alloy. Solid curves are experimental and dashed curves are theoretical. Statistical errors are indicated in the expanded portion for the last .20 volume fraction.

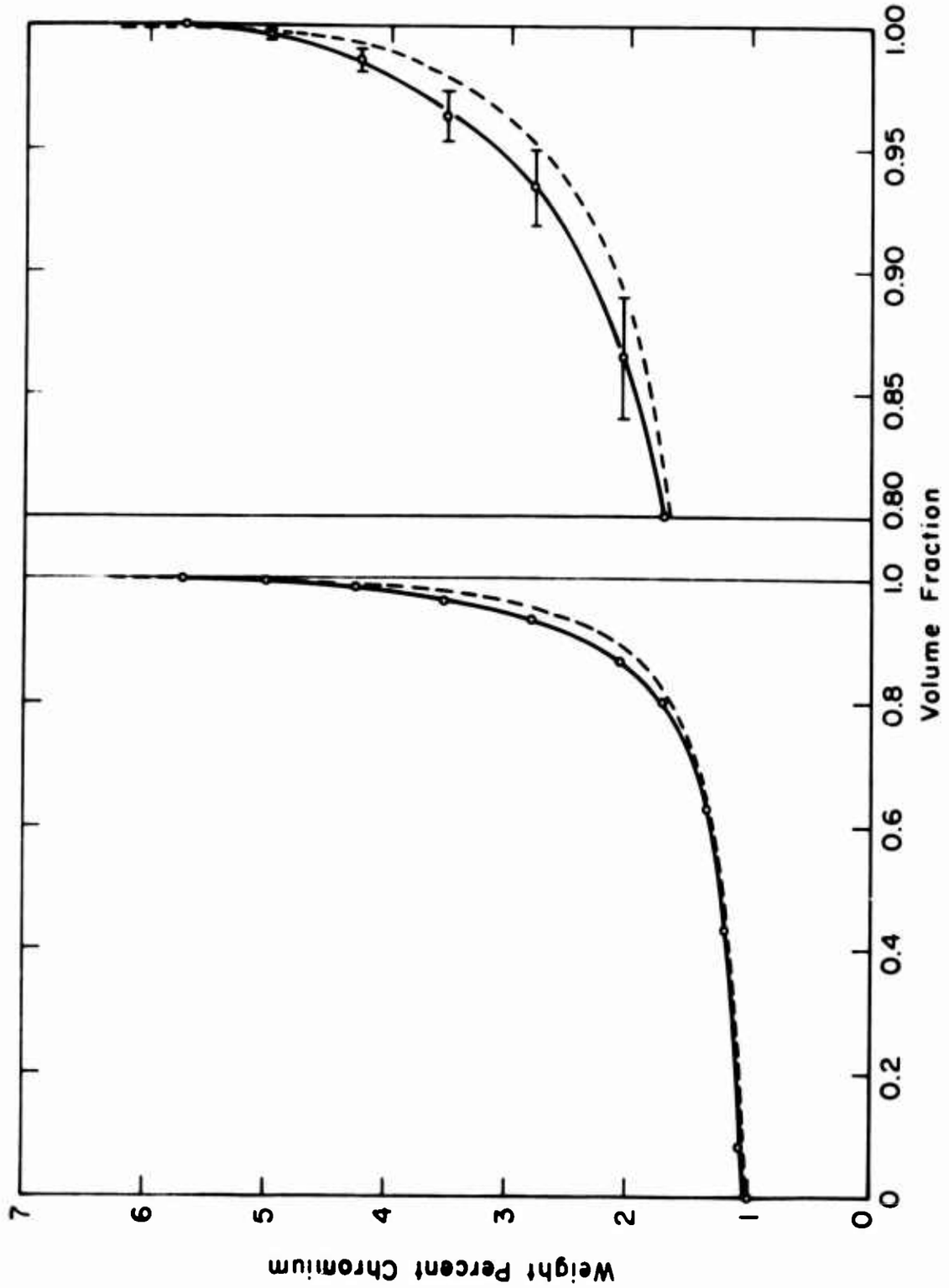

Figure 22: Concentration profile for iron-1.5 per cent carbon alloy. Solid curves are experimental and dashed curves are theoretical. Statistical errors are indicated in the expanded portion for the last .20 volume fraction.

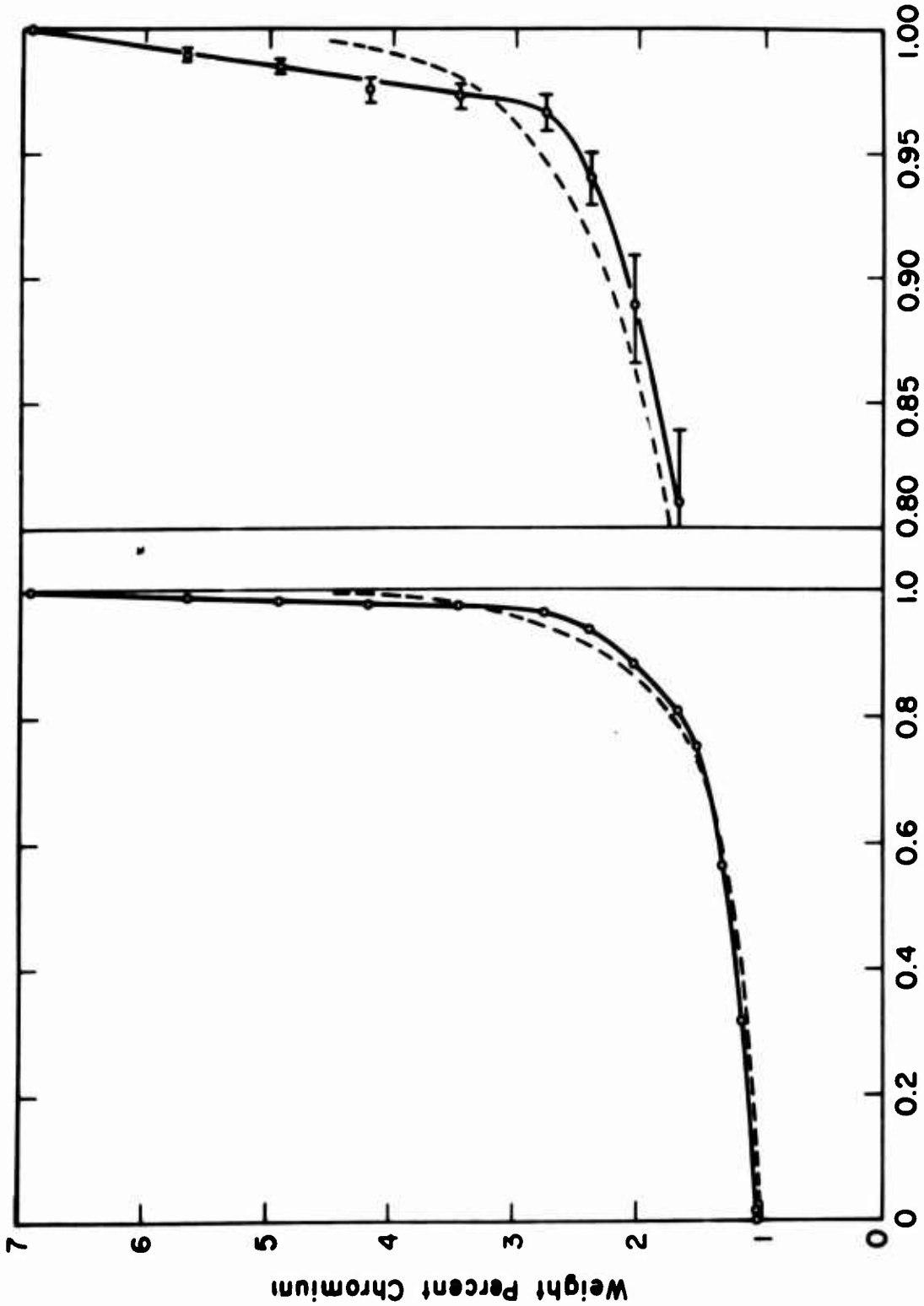

Figure 23: Concentration profile for iron-1.75 per cent carbon alloy. Solid curves are experimental and dashed curves are theoretical. Statistical errors are indicated in the expanded portion for the last .20 volume fraction.

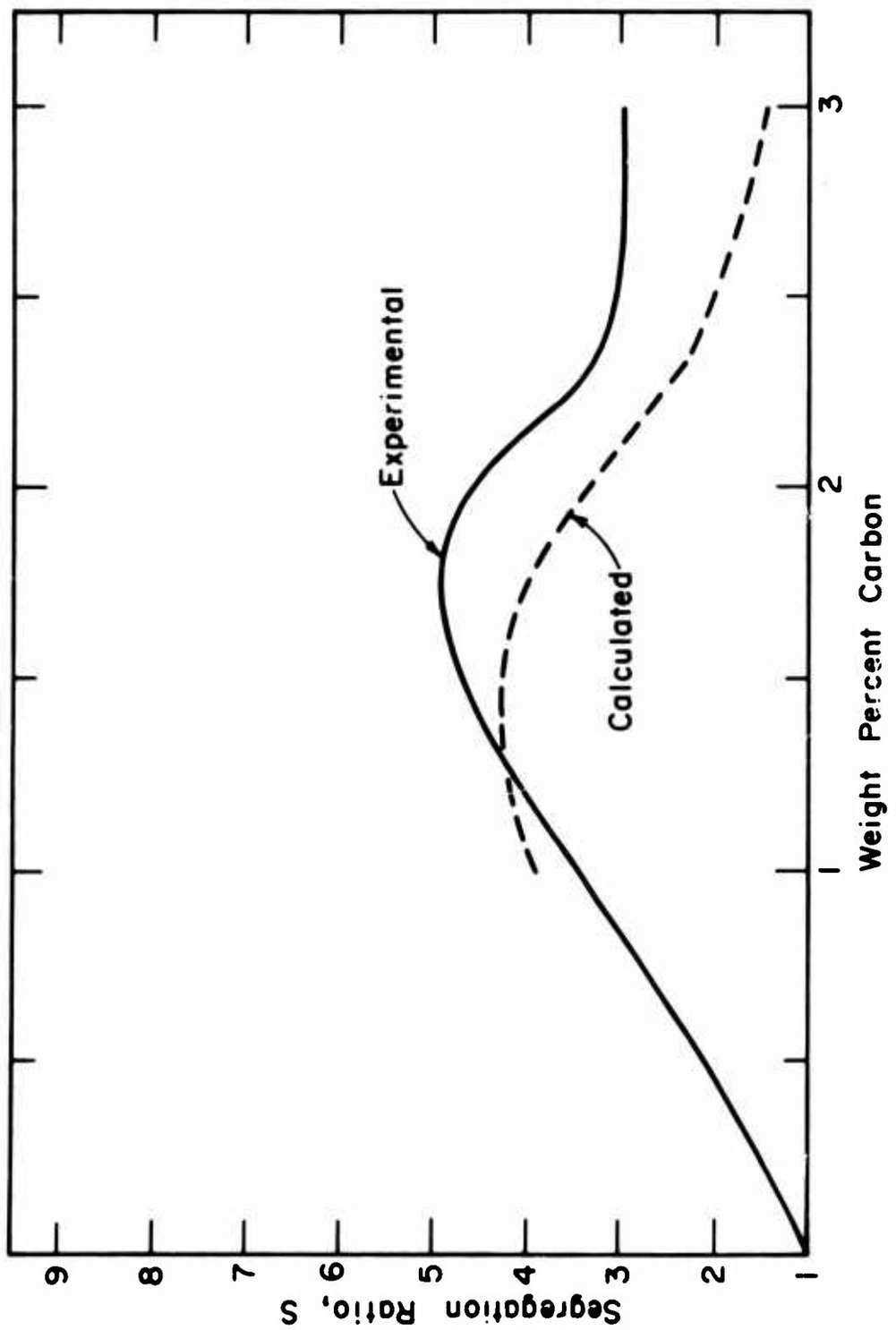

Figure 24: Comparison of calculated and experimental segregation ratio for iron-1.5 per cent chromium alloys. Curves are taken from Figure 11 and Figure 20.

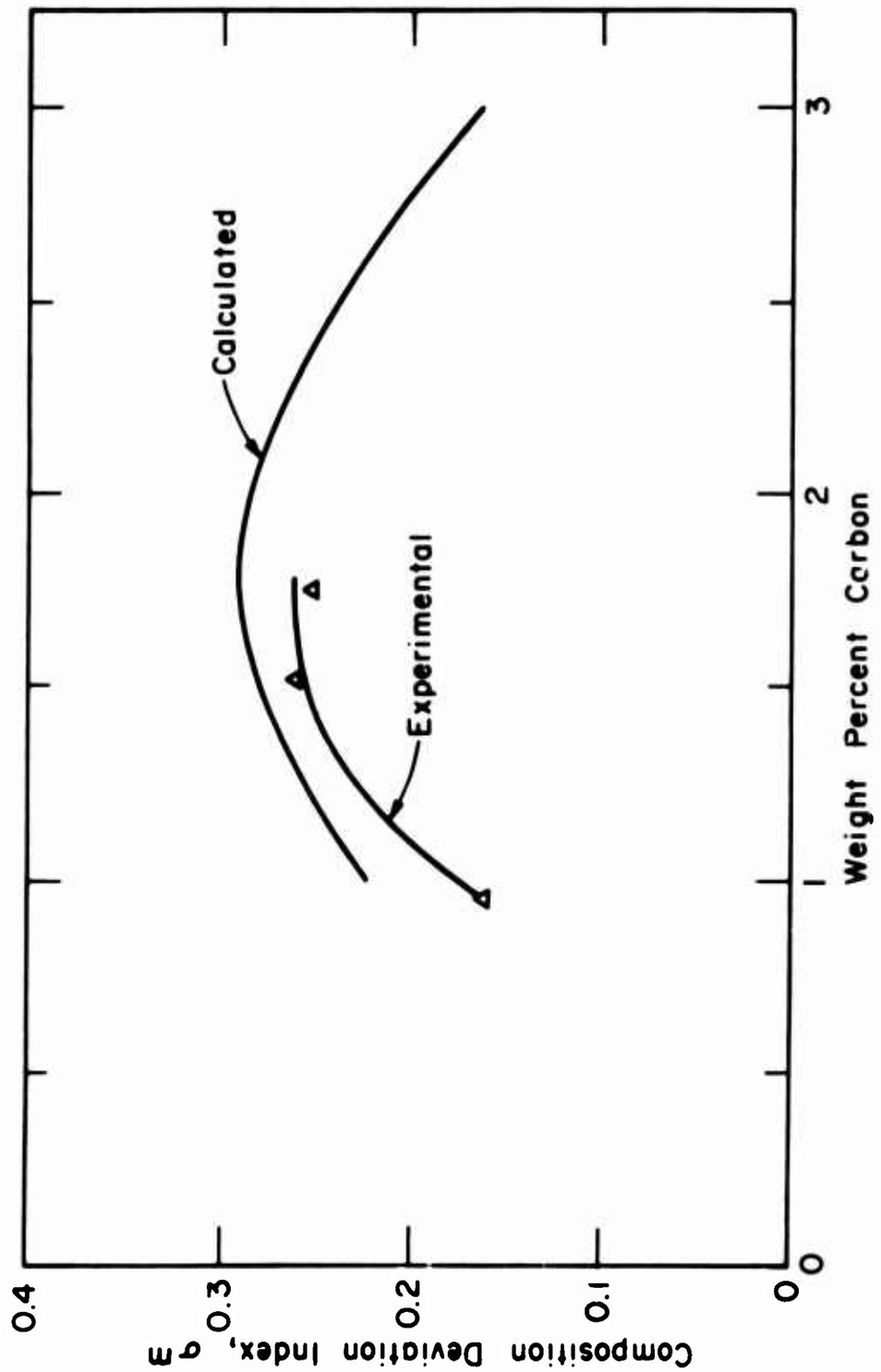

Figure 25: Comparison of calculated and experimental composition deviation indicies from iron-1.5 per cent chromium alloys. Calculated curve is from Figure 13.

excellent. The experimental curve is completely below the theoretical as to be expected if some diffusion took place in the solid during solidification.

One further discrepancy between theory and experiment should be mentioned. Alloys studied herein which contained greater than about 1.5 per cent carbon were found to form some ledeburite at the end of solidification. However, theory (e.g., Figures 9, 10, and 12) indicates that about 2.1 per cent carbon should be required to form ledeburite. This descrepancy is probably related to the assumption made in calculations that the activity coefficient of carbon in the solid is independent of chromium content. The assumption appears to be excellent for low carbon alloys but to introduce significant error for carbon contents of 1.5 per cent or greater. Introduction of a chromium's effect on carbon's activity coefficient would result in lower predicted carbon levels for ledeburite formation, in agreement with experiment[23].

II. SUMMARY AND CONCLUSIONS

1. An analytical and experimental study has been made of solute redistribution in dendritic solidification of ternary iron-carbon-chromium alloys. Three possible cases of solidification were considered; all assumed uniform concentrations of carbon and chromium in the interdendritic liquid, and equilibrium at the solid-liquid interface. Case 1 assumed complete diffusion of both carbon and chromium in the solid; Case 2 assumed no diffusion of either carbon or chromium in the solid; Case 3 solidification assumed no diffusion of chromium and complete diffusion of carbon in the solid.

2. Estimates of the extent of diffusion for carbon and chromium showed Case 3 to be the best of the three models for iron-1.5 per cent chromium with carbon contents between 0.96 per cent and 3.00 per cent.

3. Microprobe analyses were carried out to determine "Segregation Ratio", S, of chromium, and data from the literature were compiled which include segregation ratios of common alloying elements in medium carbon, low alloy steel.

4. An alternate measure of microsegregation in the "Segregation Ratio" was introduced. This parameter, σ^m, is termed "Composition Deviation Index" and is obtained by simple calculation from results of statistically long, random microprobe scans.

5. Advantages of describing microsegregation by σ^m rather than S include:

   (a) σ^m is readily measured experimentally, and for many alloys (e.g., solid solutions) it is expected that measurements of σ^m will be more reliable than those of S.

   (b) σ^m depends on all values of the concentration and not merely the minimum and maximum.

   (c) For certain alloys (e.g., complete solid solutions) small amounts of diffusion in the solid may change S markedly, with relatively little effect on σ^m.

   (d) σ^m allows comparison of single phased and eutectic forming alloys, and

   (e) σ^m is a parameter that can be introduced into formulations of homogenization kinetics.

6. The "solidification curves" (fraction solid as a function of temperature) for iron-1.5 per cent chromium alloys containing carbon between 0.96 and 3.00 per cent have been calculations. Calculations for these alloys indicate that for carbon contents greater than about 2.1 per cent carbon, ledeburite will form at the end of solidification. Experimental results show that ledeburite forms in those alloys containing about 1.5 per cent carbon and greater.

7. The concentration profiles (chromium composition versus volume fraction of material) were calculated for three alloys of 1.5 per

cent carbon and compared directly with concentration profiles determined by the use of statistically long microprobe scans. Estimates of the extent of diffusion in the solid, as well as comparison of the theoretical and measured concentration profiles, indicate that limited diffusion of chromium in the solid occurs during solidification.

8. Segregation ratios of chromium in iron-1.5 per cent chromium alloys were measured for six alloys containing 0.96 per cent to 3.00 per cent carbon. Measurements of other investigators were also used. The segregation ratio for chromium was found to increase from unity (i.e., no microsegregation) at zero per cent carbon to about 4.5 to 1.5 per cent carbon; with higher concentrations of carbon the segregation ratio decreased to about 3 for three per cent carbon. Theoretically derived segregation ratios between 0.96 and 3.00 per cent carbon showed that the same general dependence of carbon on the segregation ratio; however, the theoretical values were lower except at one per cent carbon.

9. The composition deviation index, σ^m, was calculated from six iron-1.5 per cent chromium alloys containing 0.96 per cent to 3.00 per cent carbon based on the respective theoretical concentration profiles. The σ^m was also calculated for the three experimental concentration profiles with carbon contents of 0.96, 1.54, and 1.75 per cent carbon, respectively. Theoretical values of σ^m increased from 0.22 at 0.96 per cent carbon to .35 at 1.75 per cent carbon and

then decreased to .16 at 3.00 per cent carbon. The three experimental values were somewhat lower (15 to 30 per cent lower) because of limited diffusion of chromium in the solid.

10. Fundamental to the study of microsegregation is knowledge of the equilibria between liquid and solid. For this reason the study of solidification was preceded by the determination of the austenite-liquidus equilibria for the iron-carbon-chromium system. Results of this study include:

    (a) The gamma-liquidus surface was determined for iron-carbon-chromium alloys containing up to twenty per cent chromium.
    (b) An experimental method was devised to measure the solid-liquid equilibria partition ratio in a ternary system. The method should be applicable to measure the equilibria of any element in multi-component systems that can be measured with a microprobe analyzer. Specifically, the partition ratio was measured for chromium in iron-carbon-chromium alloys between austenite and liquid iron.
    (c) Using data from the literature concerning the thermodynamics of the iron-carbon-chromium system, and the chromium equilibrium measurements between austenite and liquid, the activities of carbon, chromium, and iron were determined as functions of composition and temperature for both liquid and austenite.

(d) The austenite solidus surface was determined based on the thermodynamic study. A presentation for ternary systems was devised to represent two-phase equilibria other than the customary manner of presenting a series of isotherms with tie lines.

BIBLIOGRAPHY

1. "Investigation of Solidification of High Strength Steel Castings", M.I.T., Interim Report, Contract No. DA-19-020-ORD-5443(X), Army Materials Research Agency, October 1963.

2. R. V. Barone, H. D. Brody, M. C. Flemings, "Investigation of Solidification of High-Strength Steel Castings", M.I.T., Interim Report, Contract No. DA-19-020-ORD-5443(X), Army Materials Research Agency, 30 September 1964.

3. T. Z. Kattamis, M. C. Flemings, "Dendrite Morphology, Microsegregation and Homogenization of Low Alloy Steels", Trans. A.I.M.E., V. 233, 1965, pp. 992-999.

4. F. C. Quigley, P. J. Ahearn, "Homogenization of Steel Castings at 2500°F", Trans. A.F.S., V. 72, 1964, pp. 813-817.

5. T. B. Smith, J. S. Thomas, R. Goodall, "Banding in a 1-1/2% Nickel-Chromium-Molybdenum Steel", J.I.S.I., V. 209, 1963, p. 602.

6. J. Philibert, H. Bizouard, "Quelques Nouvelles Applications de la Microsonde Electronique de Castaing et leur Importance Practique", Memoires Scientifiques de la Revue de Metallurgie, V. 46, 1959, p. 187.

7. C. Crussard, A. Kohn, C. de Beaulieu, J. Philibert, "Etude de la Segregation de l'As et du Cu Parla Technique Autoradiographique et Examen Quantitatif a la Microsconde de Castaing", Rev. Met., V. 56, 1959, p. 395.

8. W. Steven, D. R. Thorneycroft, "Variations of Transformation Characteristics Within Samples of an Alloy Steel", J.I.S.I., V. 187, 1957, p. 15.

9. P. M. Zhurenkov, I. N. Golikov, "Dendritic Liquation of Alloyed Elements in Structural Steels", Metal Sci. Heat Treat Metals, No. 5-6, 1964, p. 293.

10. P. J. Ahearn, F. C. Quigley, "Mass Effect and Microsegregation in a High-Strength Steel Casting", Modern Castings, V. 47, 1964, p. 435.

11. C. de Beaulieu, J. Philibert, "Etude Quantitative de l'heterogeneite Dendritique dans les Alliages de Fer", Comptes Rendus, V. 246, 1958, p. 3615.

12. D. A. Colling, P. J. Ahearn, M. C. Flemings, "Effect of Solidification Variables on Mechanical Properties of Cast Steel", Trans. A.F.S., V. 70, 1962, p. 1083.

13. J. Philibert, E. Weinryb, M. Ancey, "A Quantitative Study of Dendritic Segregation in Iron-Base Alloys with the Electron Probe Microanalyzer", Metallurgia, November 1965, p. 203.

14. R. O. Melford, D. A. Doherty, "A Study of Solidification and Microsegration in Killed Steel Ingots with Particular Reference to 1% C, 1.5% Cr Steel", Tube Investments Research Laboratories, Technical Report No. 201, January 1966.

15. D. R. Poirier, R. F. Polich, M. C. Flemings, "Development of Superior Steels for Precision Gyro Spin Bearings", M.I.T., Contract No. AF 33(615)-1030, Wright-Patterson Air Force Base, Ohio, 1964.

16. H. D. Brody, M. C. Flemings, "Solute Redistribution in Dendritic Solidification", Trans. A.I.M.E., V. 236, 1966, p. 615.

17. T. F. Bower, H. D. Brody, M. C. Flemings, "Measurements of Solute Redistribution in Dendritic Solidification", Trans. A.I.M.E., V. 236, 1966, p. 624.

18. M. C. Flemings, "Microsegregation in Castings and Ingots", Hoyt Memorial Lecture of American Foundrymen's Society, Atlantic City, New Jersey, presented May 1964.

19. A. B. Michael and M. B. Bever, "Solidification of Aluminum-Rich Aluminum-Copper Alloys", Trans. A.I.M.E., V. 200, 1954, p. 47.

20. J. E. Hilliard, J. W. Cahn, "An Evaluation of Procedures in Quantitative Metallography for Volume-Fraction Analysis", Trans. A.I.M.E., V. 221, 1961, p. 344.

21. C. Wells, R. F. Mehl, "Rate of Diffusion of Carbon in Austenite in Plain Carbon, in Nickel and in Manganese Steels", Trans. A.I.M.E., V. 140, 1940, p. 279.

22. N. L. Peterson, "Diffusion in Refractory Metals", WADD Technical Report 60-793 (AMR-1107), 1960, p. 117.

23. D. R. Poirier, "Microsegregation in Ternary Iron-Carbon-Chromium Alloys", Sc.D. Thesis, M.I.T., 1966.

24. C. Austin, "Alloys in the Ternary System Fe-Cr-C", J.I.S.I., V. 108, 1923, p. 235.

25. A. B. Kinzel, W. Crafts, The Alloys of Iron and Chromium, McGraw-Hill, New York, 1937, p. 65.

26. N. R. Griffing, W. D. Forgeng, G. W. Healy, "C-Cr-Fe Liquidus Surface", Trans. A.I.M.E., V. 224, 1962, p. 148.

27. M. G. Benz, J. F. Elliott, "The Austenite Solidus and Revised Iron-Carbon Diagram", Trans. A.I.M.E., V. 221, p. 323.

28. F. Adcock, "The Chromium-Iron Constitutional Phase Diagram", J.I.S.I., V. 125, 1931, p. 99.

29. A. Rist, J. Chipman, "Activity of Carbon in Liquid Iron-Carbon Solutions", The Physical Chemistry of Steelmaking, Technology Press and John Wiley, New York, 1958, p. 3.

30. F. D. Richardson, W. E. Dennis, "Thermodynamic Study of Dilute Solutions of Carbon in Molten Iron", Trans. Faraday Soc., V. 49, 1953, p. 171.

31. R. P. Smith, "Equilibrium of Iron-Carbon Alloys with Mixtures of $CO-CO_2$ and CH_4-H_2", J.A.C.S., V. 68, 1946, p. 1163.

32. H. Schenck, H. Kaiser, "Untersuchungen uber die Aktivitat des Kohlenstoffs in kristallisierten binaren und ternaren Eisen-Kohlenstoff-Legierungen", Archiv. fur das Eisenhuttenwesen, V. 31, 1960, p. 227.

33. E. Scheil, T. Schmidt, J. Wunning, "Ermittlung der Gleichgewichte von Kohlenoxyd-Kohlensaure-Gemischen mit dem γ-Mischkristall, mit Zementit und mit Graphit", Archiv. fur das Eisenhuttenwesen, V. 32, 1961, p. 1.

34. K. Bundgardt, H. Preisendanz, G. Lehnert, "Einfluss von Chrom auf den Aktivitatsverlauf von Kohlenstoff im System Eisen-Chrom-Kohlenstoff bei 1000°C", Archiv fur das Eisenhuttenwesen, V. 35, 1964, p. 1.

35. J. S. Kirkaldy, G. R. Purdy, "The Thermodynamics of Dilute Ternary Austenite Solutions", Canadian J. of Physics, V. 40, 1962, p. 202.

36. T. Fuwa, J. Chipman, "Activity of Carbon in Liquid-Iron Alloys", Trans. A.I.M.E., V. 215, 1959, p 708.

37. F. D. Richardson, W. E. Dennis, "Effect of Chromium on the Thermodynamic Activity of Carbon in Liquid Iron", J.I.S.I., V. 175, 1953, p. 257.

38. K. Goto, S. Ban-ya, S. Matoba, "Activity of Carbon and Oxygen in Molten Iron-Nickel and Iron-Chromium Alloys", Tetsu to Hagana, V. 49, 1963, p. 138.

39. M. Ohtani, "On the Activities of Cr and C in Molten Fe-Cr-C Alloys", Tetsu to Hagane, V. 42, 1956, p. 1095.

40. S. Ban-ya, S. Matoba, "The Effect of Si, Cr and Mn on the Equilibrium of Carbon and Oxygen in Molten Iron Saturated with Carbon (II)", Technology Reports, Tohoku University, V. 22, 1957, p. 97.

41. J. S. Kirkaldy, R. J. Brigham, "The Interaction Parameter for Solutions of Carbon and Chromium in Austenite at 1000°C, Trans. A.I.M.E., V. 227, 1963, p. 538.

42. L. C. Brown, J. S. Kirkaldy, "Carbon Diffusion in Dilute Ternary Austenites", Trans. A.I.M.E., V. 230, 1964, p. 223.

43. C. Wagner, Thermodynamics of Alloys, Addison-Wesley, Reading, Massachusetts, 1952, p. 18.

44. Y. Jeannin, C. Mannerskantz, F. D. Richardson, "Activities in Iron-Chromium Alloys", Trans. A.I.M.E., V. 227, 1963, p. 300.

45. O, Kubaschewski, G. Heymer, Acta Met., V. 8, 1960, p. 416.

46. T. O. Ziebold, R. E. Ogilvie, "An Empirical Method for Electron Microanalysis", Anal. Chem., V. 36, 1964, p. 322.

APPENDIX A

LIQUID-AUSTENITE EQUILIBRIA FOR THE IRON-CARBON-CHROMIUM SYSTEM

A. Liquidus Determinations

In order to supplement and check the data available in the literature[24-26] on the gamma liquidus surface, the liquidus temperatures for eleven alloys were determined by a cooling curve technique. In the preparation of the alloys 1/4 inch and 1/8 inch diameter bars manufactured from vacuum melted electrolytic iron were charged with high purity graphite of low ash residue and chromium of 99.35 per cent purity.

The iron, chromium, and graphite were charged (80 - 100 grams total) into an alumina crucible and melted under vacuum in a Balzer's induction furnace. A schematic diagram of the experimental set-up is shown in Figures A1 and A2. After meltdown helium was introduced to a pressure of 30 cm. mercury. A preliminary cooling curve was then made to approximate the liquidus temperature, and then the cooling curve was made at a rate (20 - 30°C per minute) where thermocouple lag was less than 1°C. The analyses of these heats and the respective liquidus temperatures are given in Table A1.

The vertical sections through the iron-carbon-chromium system, showing the freezing temperatures, are presented in Figures A3 - A7. The liquidus for null chromium is that presented by Benz and Elliott[27]. The other vertical sections are composed of data from Adcock[28], Austin[24], Tofaute et al as reported by Kinzel and Craft[25], and Table A1. From these vertical sections the gamma liquidus surface was constructed, Figure 2.

The positions of the eutectic valleys and the gamma-delta joint are from Figures A3 - A7 and approximately correspond to Griffing et al[26]. The dip in some of the isotherms at approximately 16 per cent chromium is real although not indicated by Griffing et al[26].

B. Solidus Determinations

Two similar techniques were employed for the determination of the solid chromium concentration in equilibrium with liquid iron-carbon-chromium alloys using the apparatus depicted in Figure A8. The first method involved the insertion of a pure iron-bar into the melt held at a constant temperature above its liquidus. An interface, with the equilibrium partition of chromium, can be established at any position without the collapse of the liquid column by containing the iron rod within an alumina tube and applying a vacuum to its free end, as depicted in Figure A8. At the end of a run the alumina tube with its contents was withdrawn from the melt; the liquid remaining in the bottom of the tube solidified dendritically fast. Subsequent sectioning and metallographic preparation showed the interface, and the samples were micro-analyzed to determine the concentration of chromium in the solid in equilibrium with the liquid alloys. The liquid concentration was determined by chemically analyzing the remaining solidified ingot.

The second method employed the same apparatus with the exception that no iron rod was immersed. Instead, the alloy was cooled to some temperature between its liquidus and solidus. The temperature of the solid-liquid ingot was held constant for a period of time and then cooled by shutting off the power and immersing an iron rod, 1/4 inch diameter.

The ingots cooled at a rate of approximately 1/2°C per second, while completing solidification, and then 3°C per second down to 800°C.

All alloys were made by charging the vacuum melted electrolytic iron, metallic chromium, and low ash graphite in alumina crucibles and melting under a helium atmosphere. Before entering the system, the helium was passed through anhydrous calcium sulfate and then titanium chips heated to 700°C. The temperature control was maintained by means of a tungsten-3 rhenium/tungsten-25 rhenium thermocouple connected to a control system utilizing a null detector. Four heats were run for each of the two methods described and the temperature of all the heats were held at $\pm$ 1/2°C of the set point.

Macrostructures obtained from both methods are shown in Figures A9a and A9b. In Figure A9b, a "solid-liquid" ingot, the solid was not uniformly distributed but, rather, was concentrated all in the top due to radiation heat loss. The solid of interest which was in equilibrium with the liquid is therefore that right next to the liquid. Also, material could easily be removed from the ingots for chemical analyses representing just the liquid, itself.

A brief summary of these heats is presented in Table AII along with compositions of chromium in the solid in equilibrium determined by microprobe analyses. The relative intensities of chromium were converted to weight per cent by utilizing the procedure outlined in Appendix F.

With these experiments one could determine the chromium partition between liquid and solid for entire gamma liquidus surface; however, the

equilibrium carbon concentrations can not be determined. A thermodynamic analysis of the iron-carbon-chromium system is then evident in order to reduce the experimental work to a practical limit.

The solidus surface presented in Figure 3 was developed by such an analysis. The treatment relies upon the activity data of carbon in iron-carbon austenite, iron-carbon liquid, and the effect of chromium on the activity of carbon on both phases, as well as the thermodynamics of the iron-chromium system. Using this data, the results of the austenite-liquid chromium equilibria, and applying Gibbs-Duhem relations for ternary systems, the activities of all three components is analytically described. The following sections give this thermodynamic analysis leading to the construction of the solidus surface.

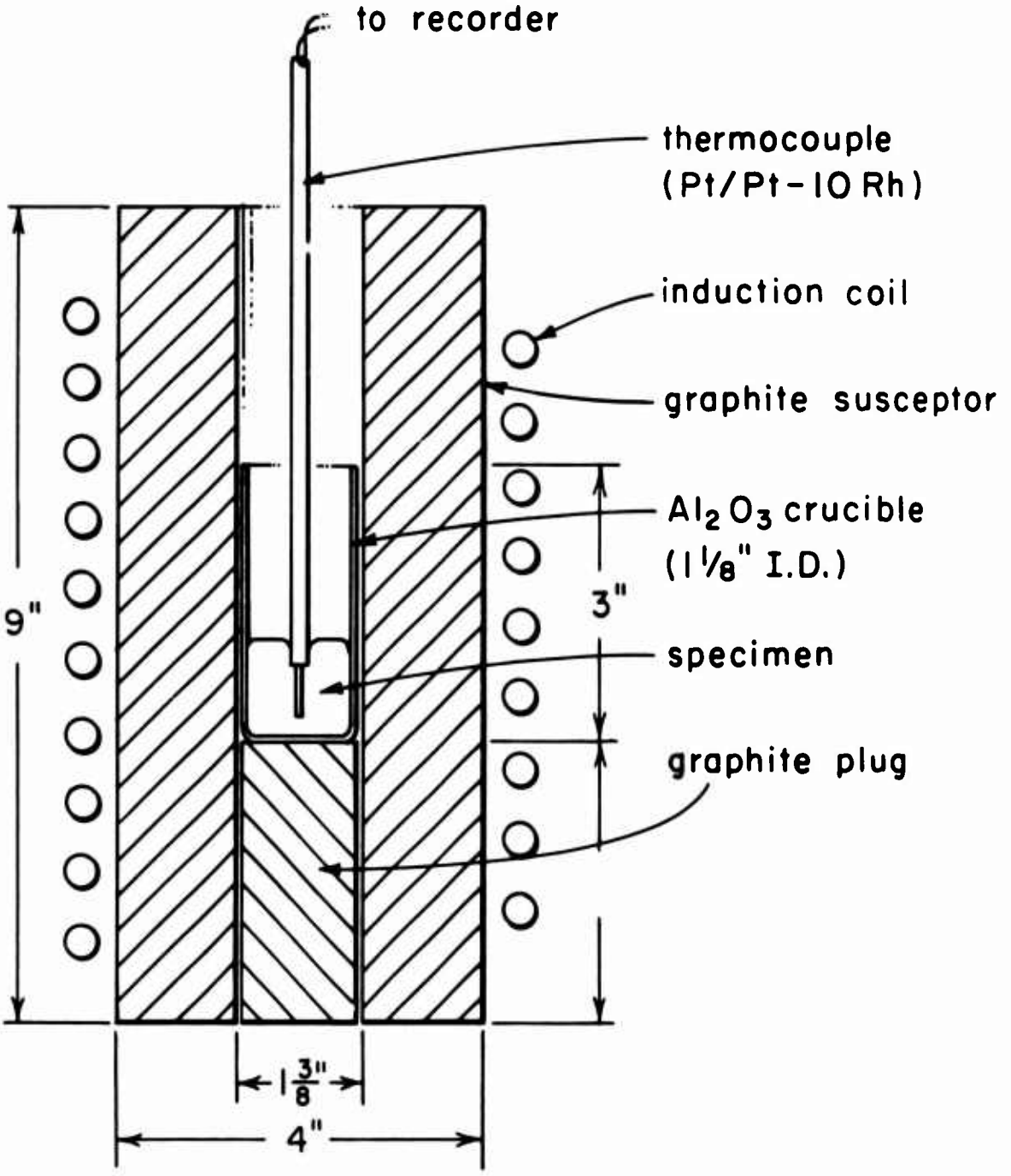

Figure A1: Assembly used for cooling curves of small melts.

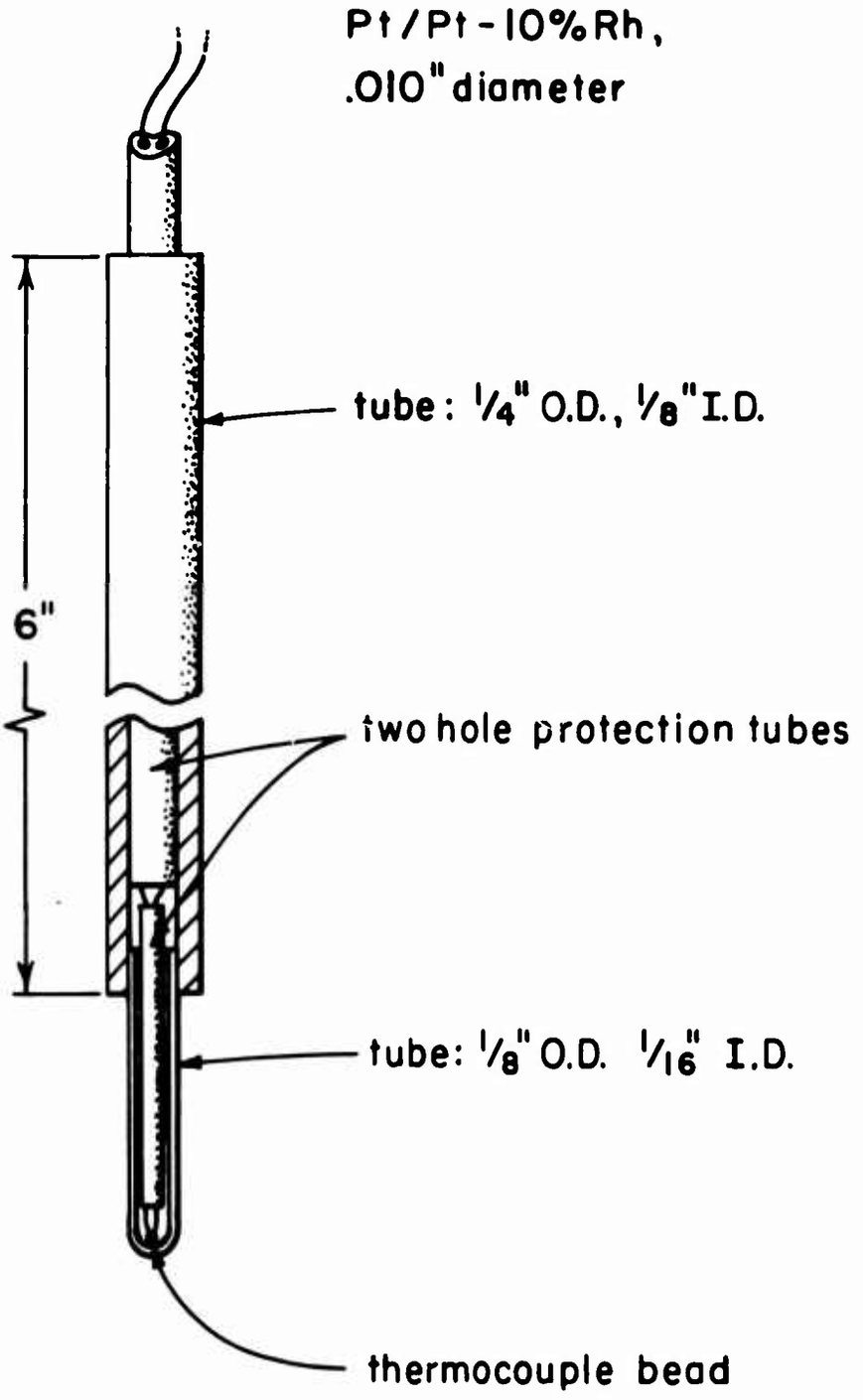

Figure A2: Thermocouple assembly for liquidus temperature measurements.

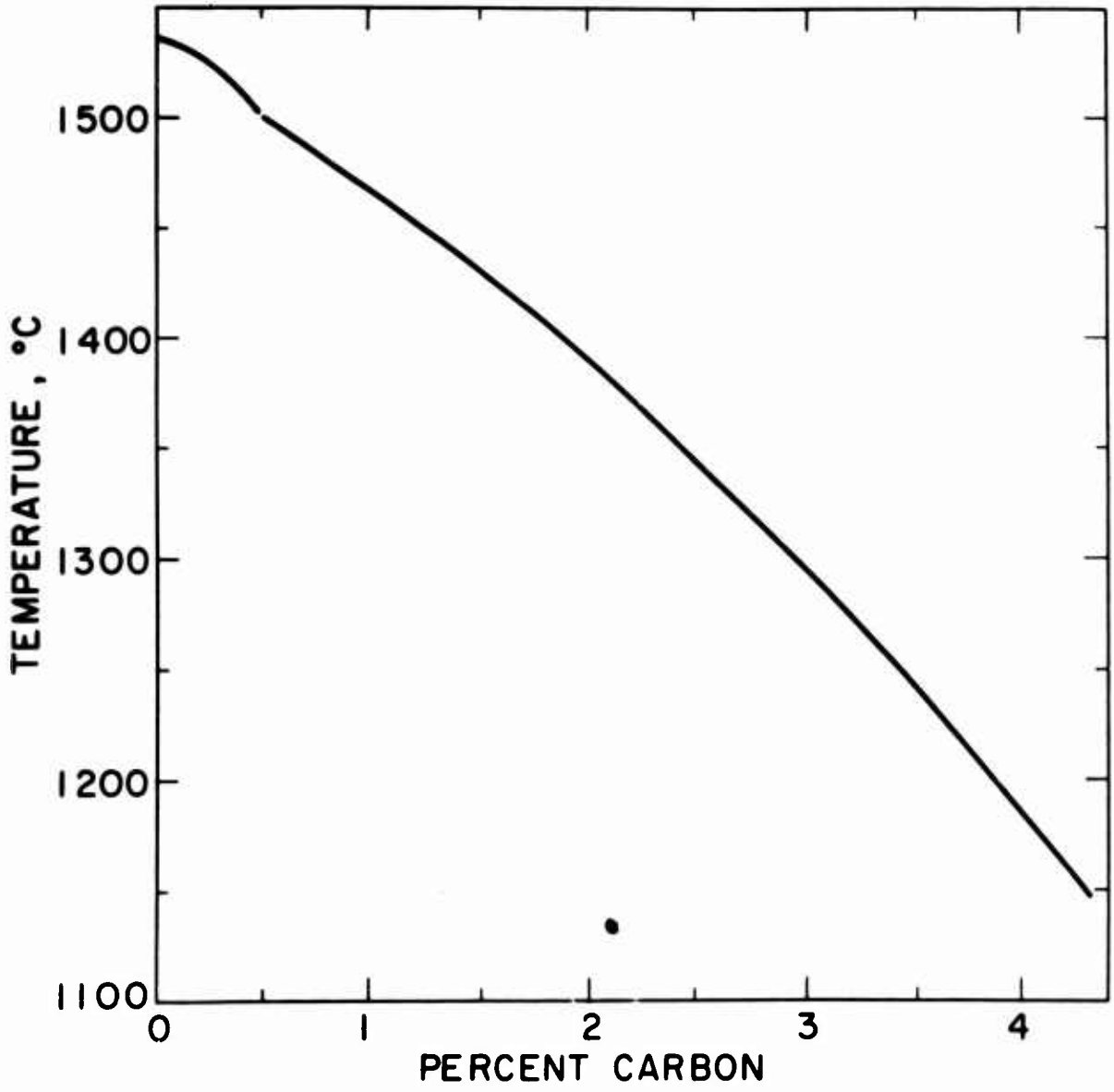

Figure A3: The liquidus at zero per cent chromium[27].

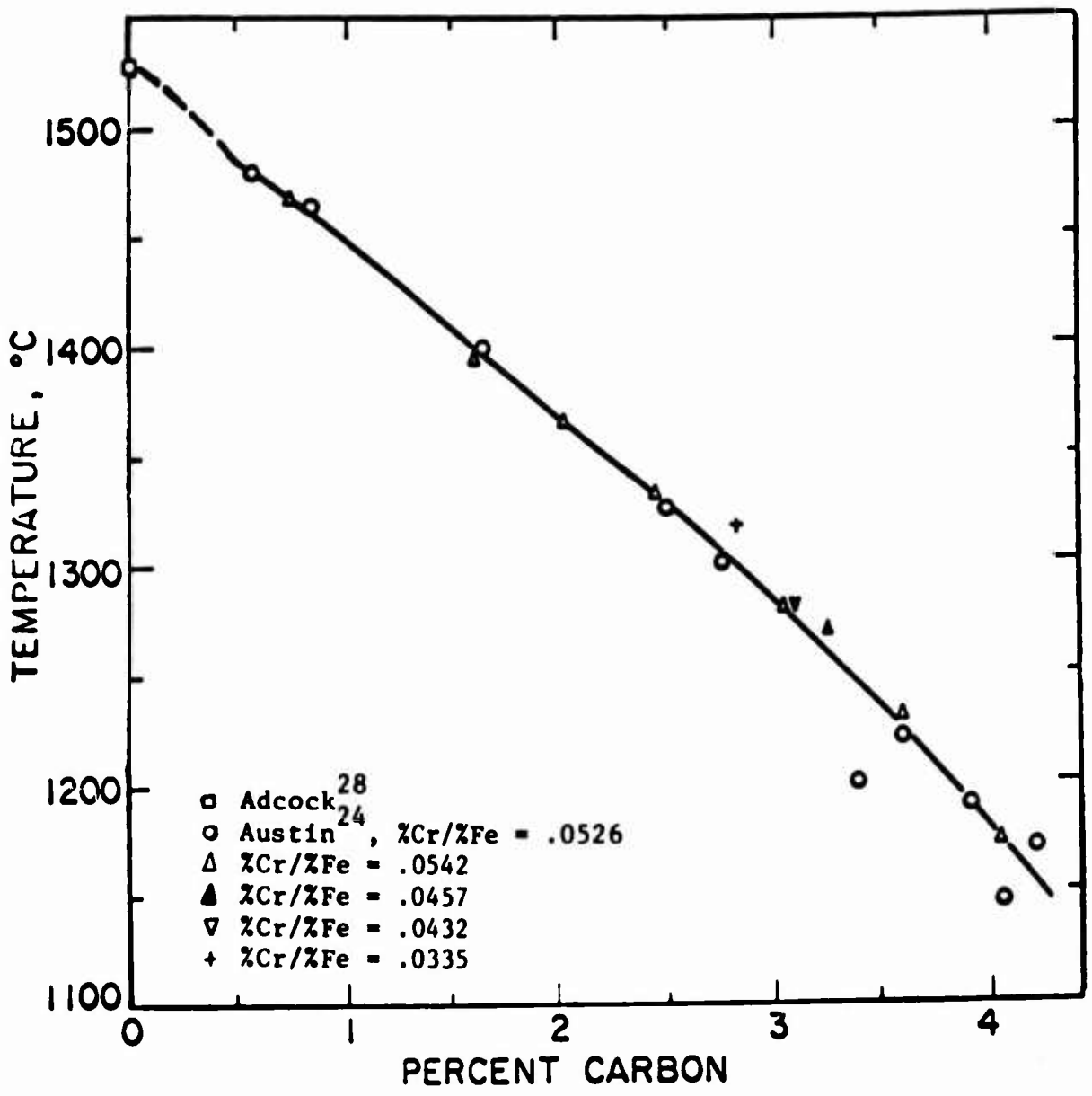

Figure A4: The liquidus at a chromium-iron ratio of .053.

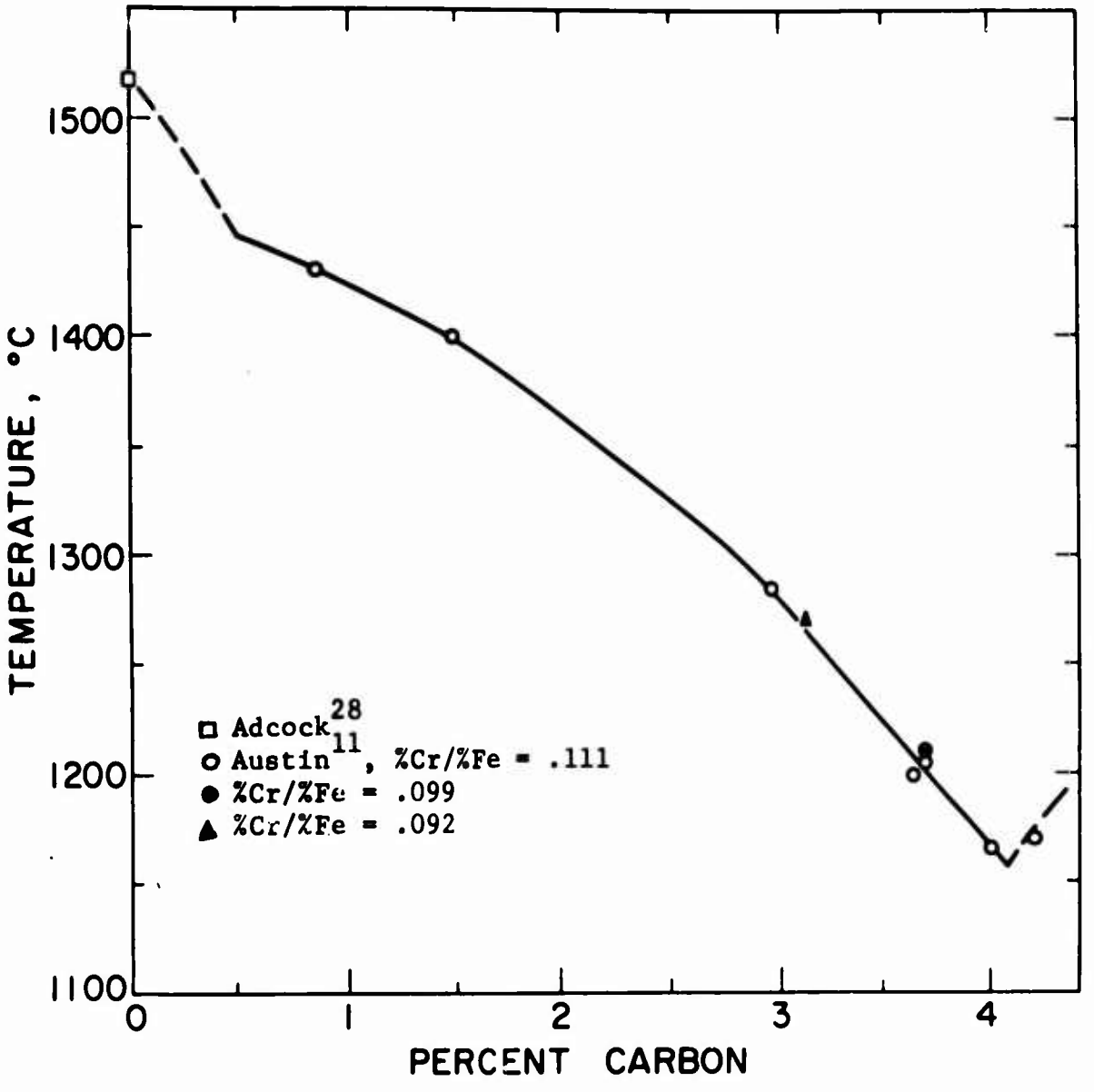

Figure A5: The liquidus at a chromium-iron ratio of .111.

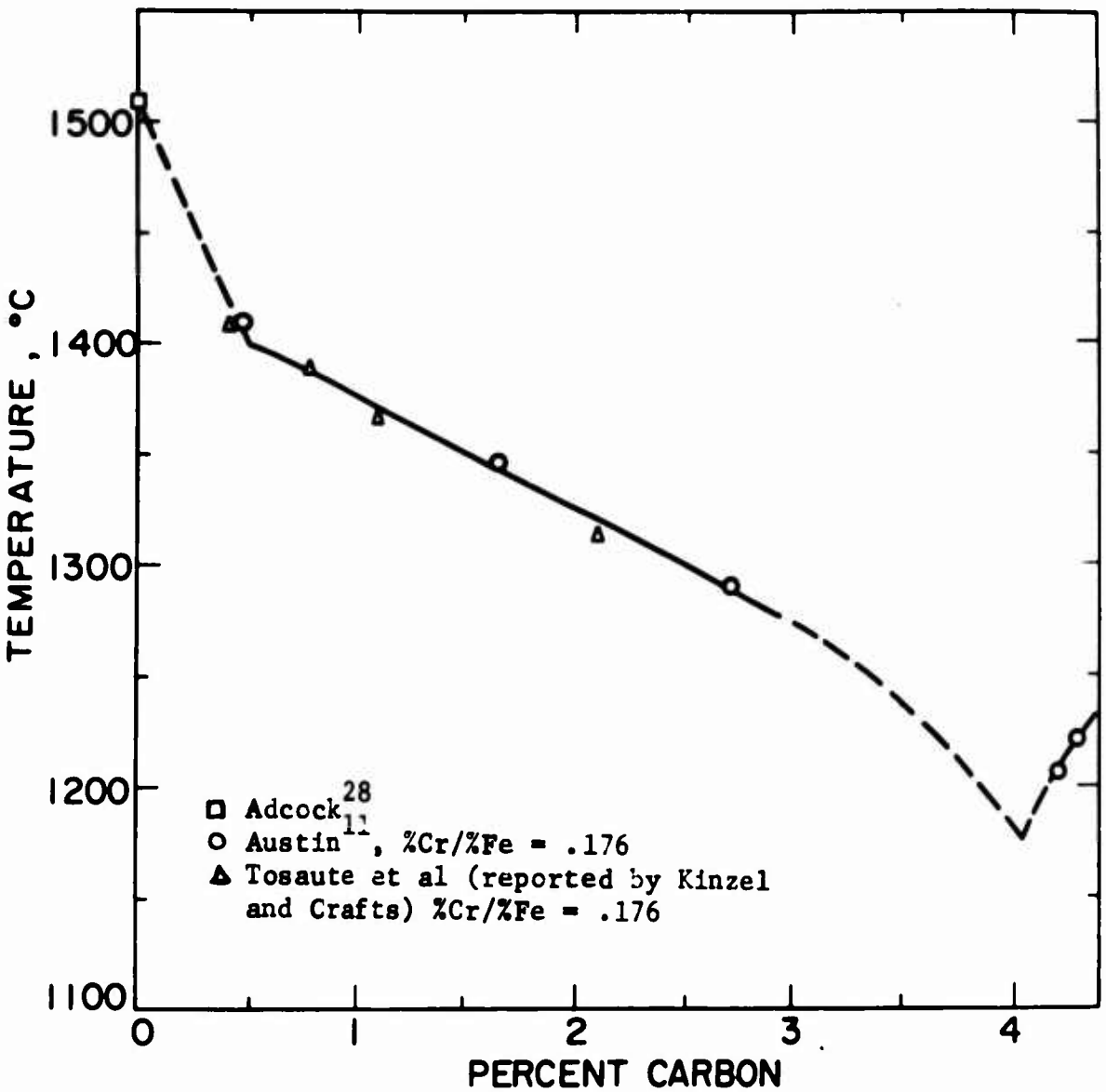

Figure A6: The liquidus at a chromium-iron ratio of .176.

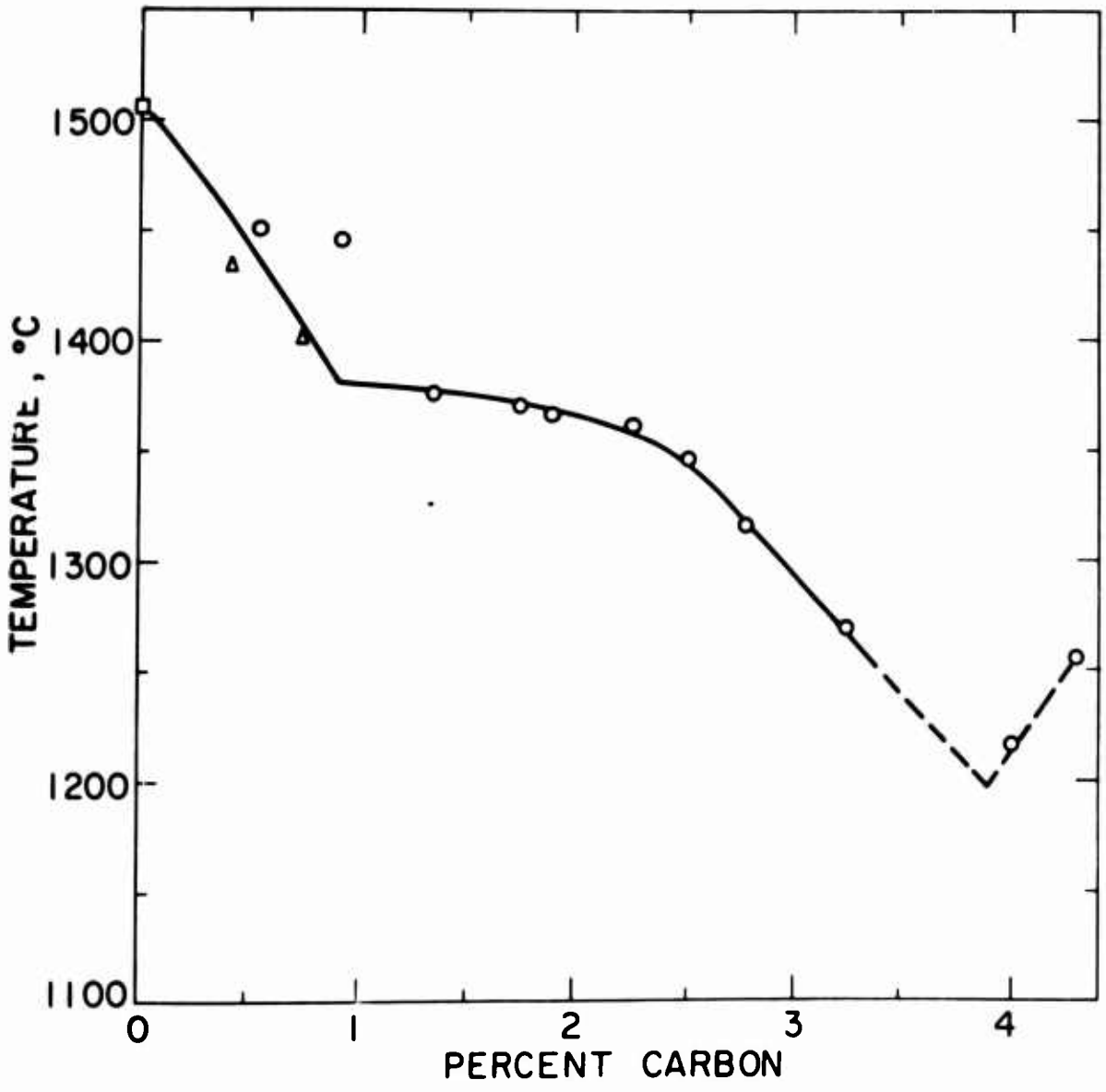

Figure A7: The liquidus at a chromium-iron ratio of .250.

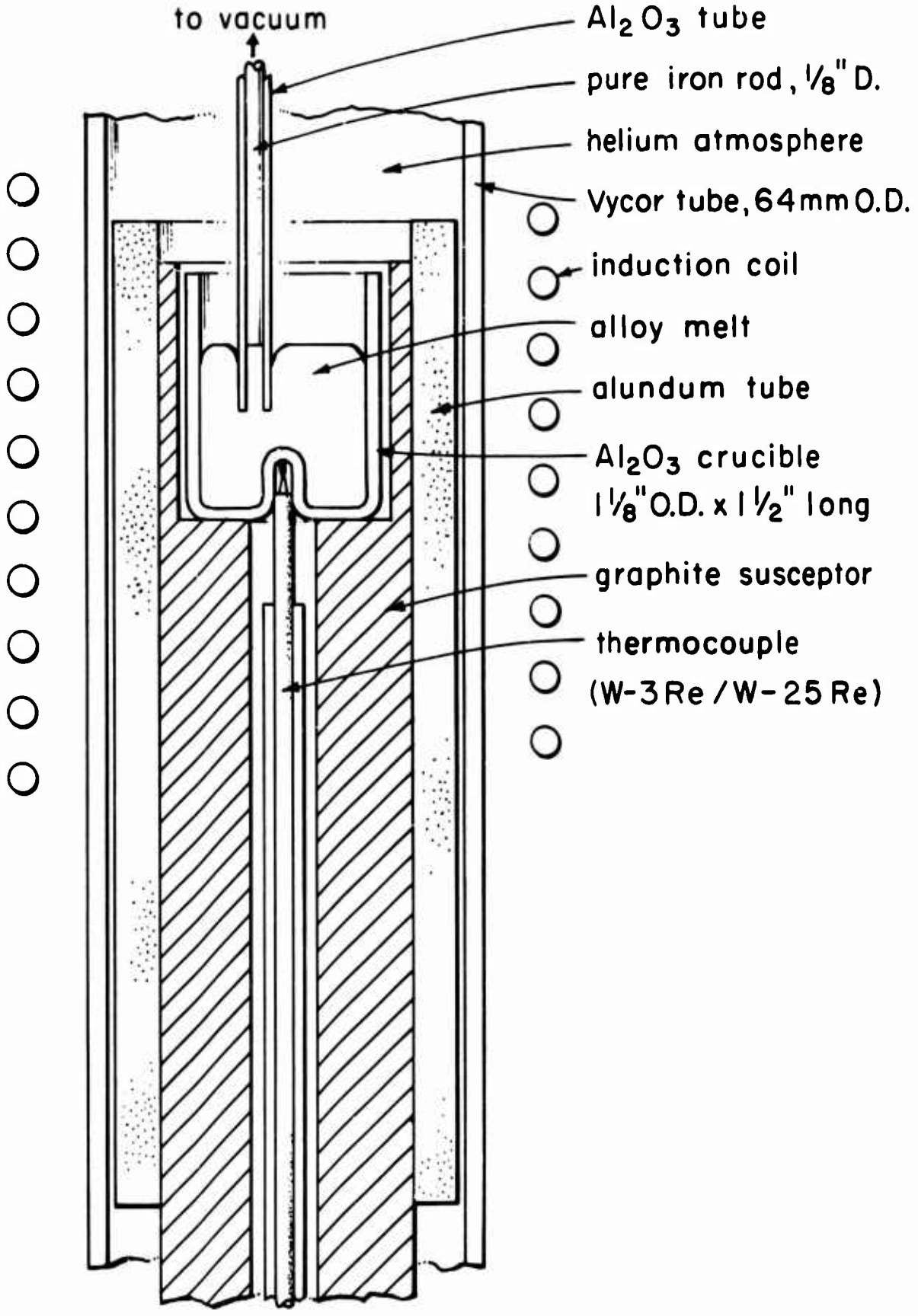

Figure A8: Schematic diagram of apparatus used for austenite-liquid equilibria of chromium.

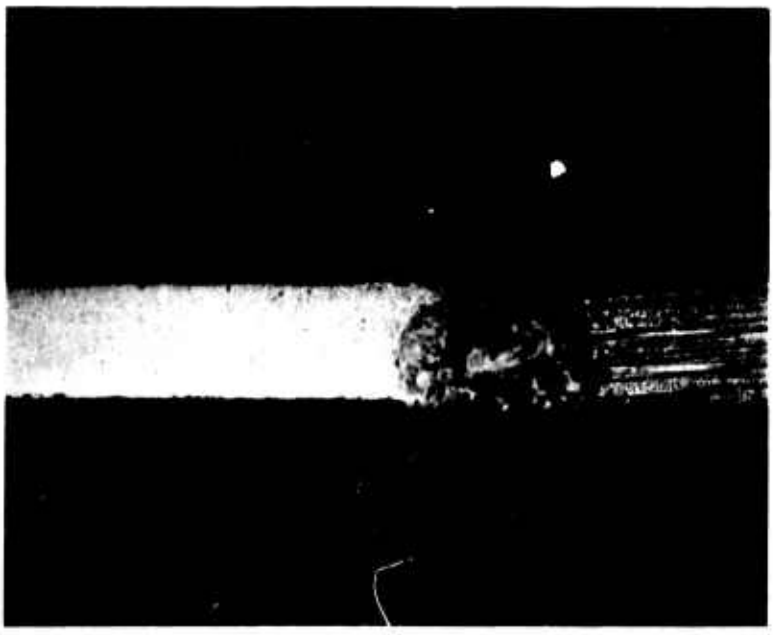

(a)

(b)

Figure A9: Macrophotographs of austenite-liquid chromium equilibria specimens.

(a) heat number 8, 4X.
(b) heat number 12, 4X.

TABLE AI

ANALYSES OF HEATS FOR LIQUIDUS TEMPERATURES

Heat	% C	% Cr	% Cr/% Fe	Liquidus Temperature, °C
1	3.26	4.23	.0457	1270
2	3.08	4.01	.0432	1280
3	2.82	3.15	.0335	1318
4	3.13	8.16	.0920	1270
5a	.75	5.09	.0541	1468
b	1.62	5.02	.0538	1396
c	2.02	5.08	.0547	1366
d	2.45	4.87	.0525	1331
e	3.05	5.01	.0545	1279
f	3.61	4.96	.0542	1230
g	4.03	4.91	.0539	1174
			.0542 Avg.	

TABLE AII

AUSTENITE-LIQUID EQUILIBRIA OF CHROMIUM IN Fe-C-Cr ALLOYS

Heat Number	Time of Run, Hrs.	Set-Point Temperature, °C	Liquid Composition % C	Liquid Composition % Cr	Solid Composition % Cr
Interface Heats					
6	3	1430	1.64	1.85	1.37
7	2	1412	2.08	2.52	1.68
8	2-3/4	1340	2.46	3.02	2.19
9	3	1300	2.86	4.25	3.50
Solid-Liquid Heats					
10	2-3/4	1270	3.26	4.23	2.54
11	3/4	1450	1.25	1.60	.99
12	2-1/2	1270	3.13	8.16	5.74
13	3	1320	2.62	4.32	3.08

APPENDIX B

ACTIVITY OF CARBON IN AUSTENITIC AND LIQUID IRON-CARBON SOLUTIONS

A. Introduction

1. Liquid Solutions.

The activity of carbon in iron-carbon liquid solutions has been given by Rist and Chipman[29] based on their own data and on work of Richardson and Dennis[30]. The activity coefficient in their analysis was assumed to obey the relation:

$$\log \gamma_1 = \alpha(1 - X_1^2) + I \qquad \text{(B1)}$$

where γ_1 = activity coefficient of carbon

X_1 = atom fraction of carbon

I = factor depending on choice of standard state

and,

$$\alpha = -\frac{4350}{T}\ [1 + .0004\ (T - 1770)] \qquad \text{(B2)}$$

The standard state chosen for this analysis is graphite. Thus

$$I = -\ \alpha(1 - X_1^\circ)^2 - \log X_1^\circ \qquad \text{(B3)}$$

where X_1° = saturation atom fraction of carbon in binary liquid iron-carbon solutions

From Elliott and Benz's[27] review of the iron-carbon phase diagram:

$$X_1^\circ = 0.0462 + 8.785 \times 10^{-5}\ T \qquad \text{(B4)}$$

2. Austenite Solutions.

Figure B1 shows the activity of carbon in iron-carbon austenite, as determined by Smith[31], Schenck and Kaiser[32], Scheil et al[33], and Bungardt et al[34]. It is the purpose of the following argument to describe the activity of carbon in austenite as a function of carbon concentration and temperature including temperatures above which data of Figure B1 apply, by use of the accurate austenite-liquid phase equilibria of Elliott and Benz[27].

B. Thermodynamic Model for Austenite

Kirkaldy and Purdy[35] have presented a model based on nearest-neighbor interactions with regular behavior for austenite. With this model the activity of carbon in austenite can be given by:

$$RT\ln\left[\frac{a_1}{X_1}(1 - 2X_1)\right] = A_0 + A_1\left(\frac{X_1}{1 - X_1}\right) \qquad (B5)$$

where a_1 = activity of carbon

A_0, A_1 = coefficients that are functions of temperature and assumed independent of composition

The functional relationship between the activity of carbon and the concentration of carbon, as indicated by equation (B5), fits the data very well. An example is shown in Figure B2 where the data of Smith[31] at 1000°C have been plotted and the "least-squares" line drawn. All the data of the various investigators likewise follow the form of equation (B5). However, when the "least-squares" lines are compared for all four

investigators at 1000°C (Figure B3) obvious differences arise. Such differences between the various sets of data are not nearly so evident when Figure B1 is referred to.

Due to the fact that the data plotted in Figure B3 show wide variations in A_0 and A_1 (the same is true at 800°C) and that the activity of carbon has not been measured enough at 900, 1100, and 1200°C, the temperature dependence of A_0 and A_1 cannot be ascertained with reliability solely from the data of Figure B1. However, the gamma solidus for the iron-carbon-system has been accurately determined by Elliott and Benz[27]. Their data (per cent carbon versus temperature for gamma solidus), in conjunction with the known activity of carbon in the liquid gives several carbon activities at temperatures ranging from 1153°C (gamma-graphite-liquid eutectic) to 1499°C (gamma-delta-liquid peritectic). These higher temperature data, along with the data of Figure B1, are combined to yield the temperature dependence of the activity.

From chemical thermodynamics we write:

$$\left[\frac{\partial \ln \gamma_1}{\partial \left(\frac{1}{T}\right)}\right]_{X_1} = \frac{H_1^M}{R} \qquad \text{(B6)}$$

where H_1^M = relative heat of mixing for carbon

γ_1 = activity coefficient of carbon ($\gamma_1 = \frac{a_1}{X_L}$)

The relative heat of mixing will be assumed independent of temperature but is a function of carbon concentration. This requires that A_0 and A_1 be linear with temperature.

$$A_0 = H + bT \qquad \text{(B7)}$$

and

$$A_1 = G + cT \qquad \text{(B8)}$$

The four constants (H, G, b and c) are evaluated to best fit the data to Figure B1 along with the data taken from the gamma solidus in the following manner. Substituting equations (B7) and (B8) into equation (B5) yields:

$$R\ln\left[\frac{a_1}{X_1}(1 - 2X_1)\right] = \frac{1}{T}\left[H + G\left(\frac{X_1}{1 - X_1}\right)\right] + \left[b + c\left(\frac{X_1}{1 - X_1}\right)\right] \qquad \text{(B9)}$$

Thus for a fixed carbon concentration, a plot of $R\ln\left[\frac{a_1}{X_1}(1 - 2X_1)\right]$ versus $\frac{1}{T}$ should yield a straight line. Ten compositions along the entire gamma solidus were selected. The activities for these compositions were calculated from Rist and Chipman's[29] relation (equations B1 - B3) applied to the compositions of the liquid in equilibrium with the respective austenite compositions. From the thermodynamic model plots (such as Figure B2) the values of the left side of equation (B9) were taken at the carbon concentrations in question, i.e., $X_1/(1 - X_1)$. The plots were then made for each composition and the "least-squares" line drawn. Figure B4 shows two extremes of the compositions chosen. The agreement of the low temperature data with the points calculated from the phase diagram point shown for $(X_1/1 - X_1)$ equal to 0.1002 was the largest encountered for all ten plots.

From these ten plots values of $R\ln\left[\frac{a_1}{X_1}(1 - 2X)\right]$ were taken and plotted versus $X_1/(1 - X_1)$ at constant reciprocal temperatures. These plots are also straight lines:

$$R\ln\left[\frac{a_1}{X_1}(1 - 2X_1)\right] = \left(\frac{H}{T} + b\right) + \left(\frac{G}{T} + c\right)\left(\frac{X_1}{1 - X_1}\right) \quad \text{(B10)}$$

whose intercepts $\left(\frac{H}{T} + b\right)$ and slopes $(G/T + c)$ are shown in Figures B5 yielding these results:

$H = 10{,}550$ cal/mole

$G = -5{,}125$ cal/mole

$b = -4.106$ cal/mole-deg

$c = 15.967$ cal/mole-deg

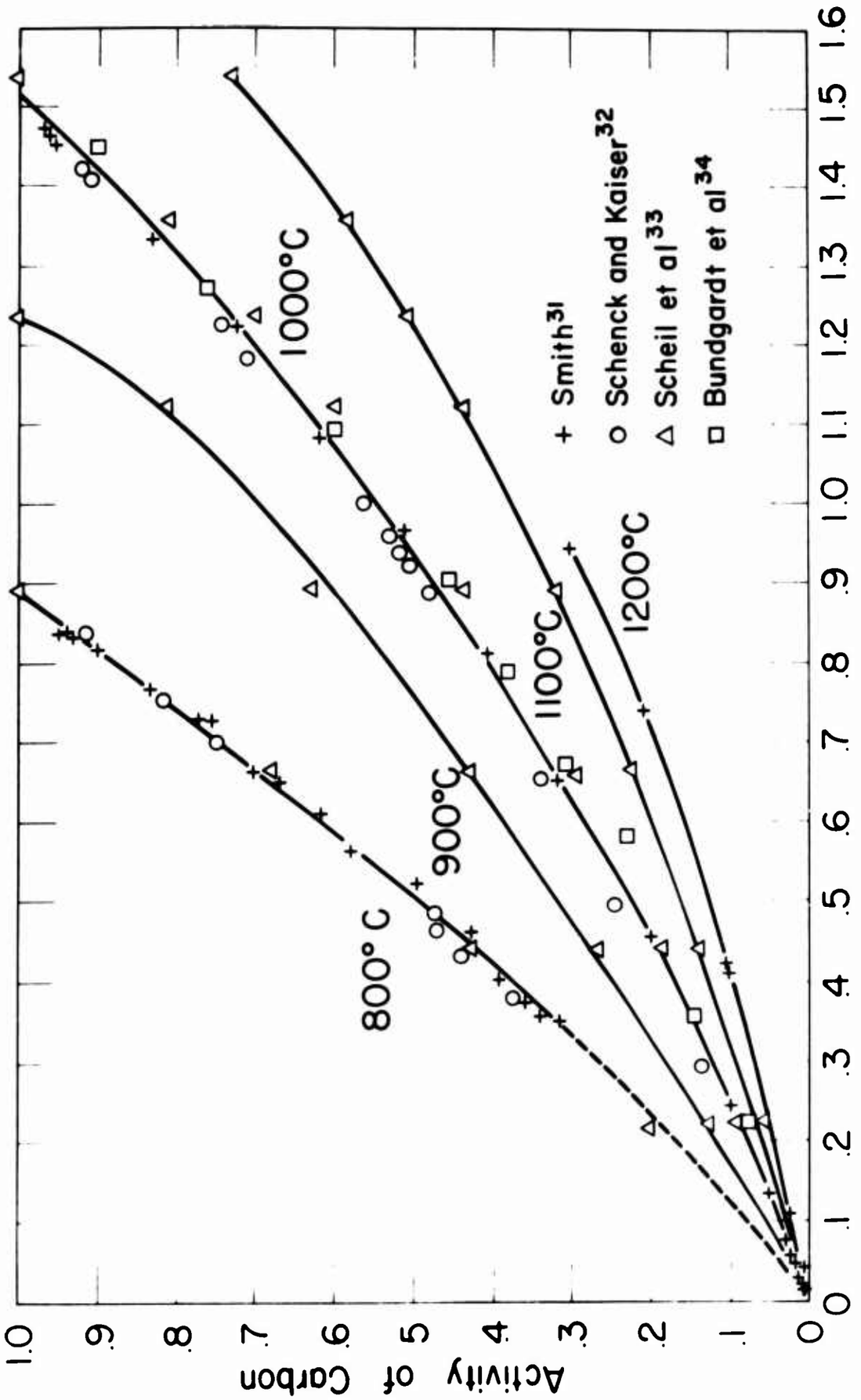

Figure B1: The activity of carbon in austenite as determined by various investigators.

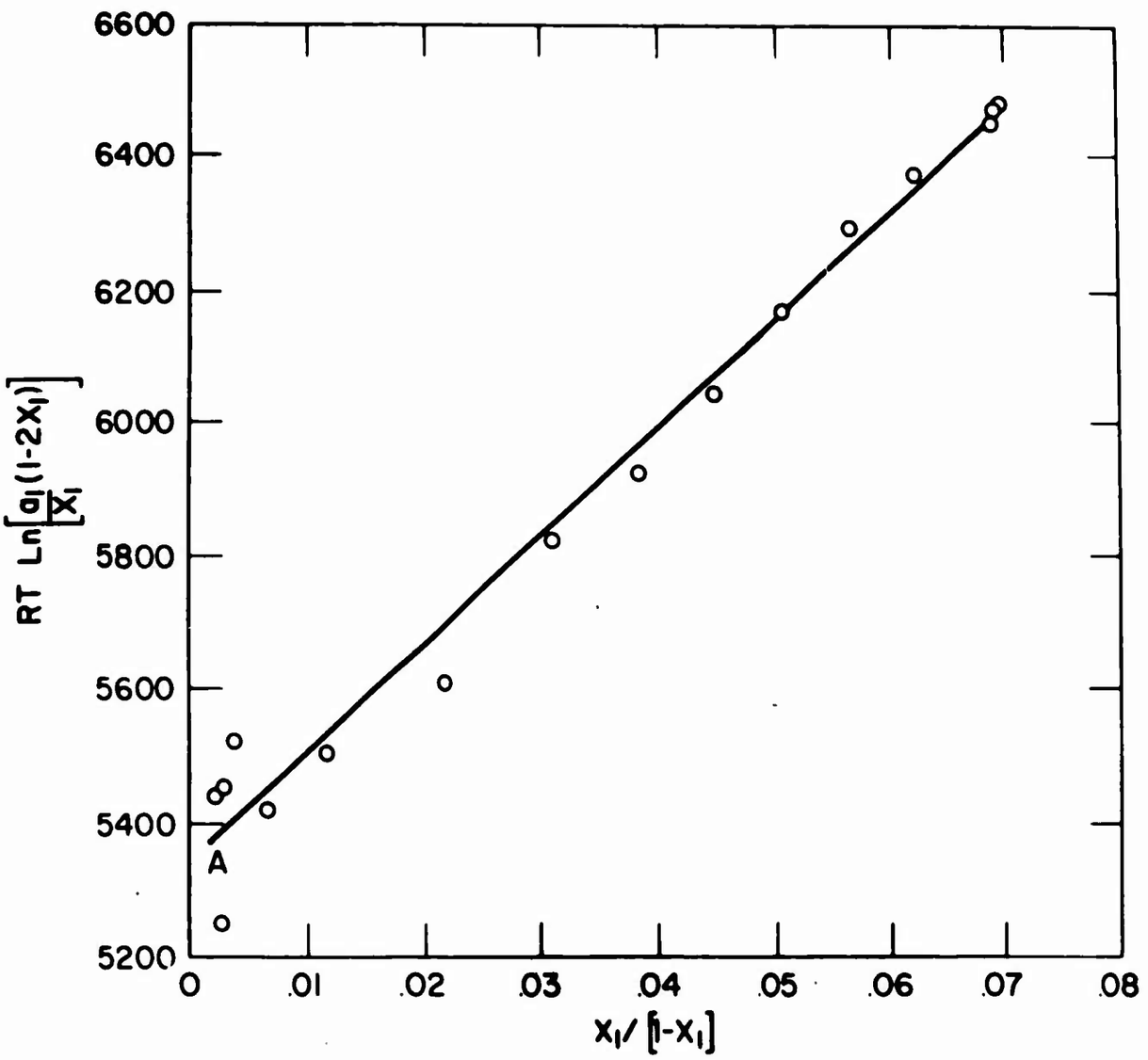

Figure B2: Application of the thermodynamic model. Data from Smith[31] at 1000°C.

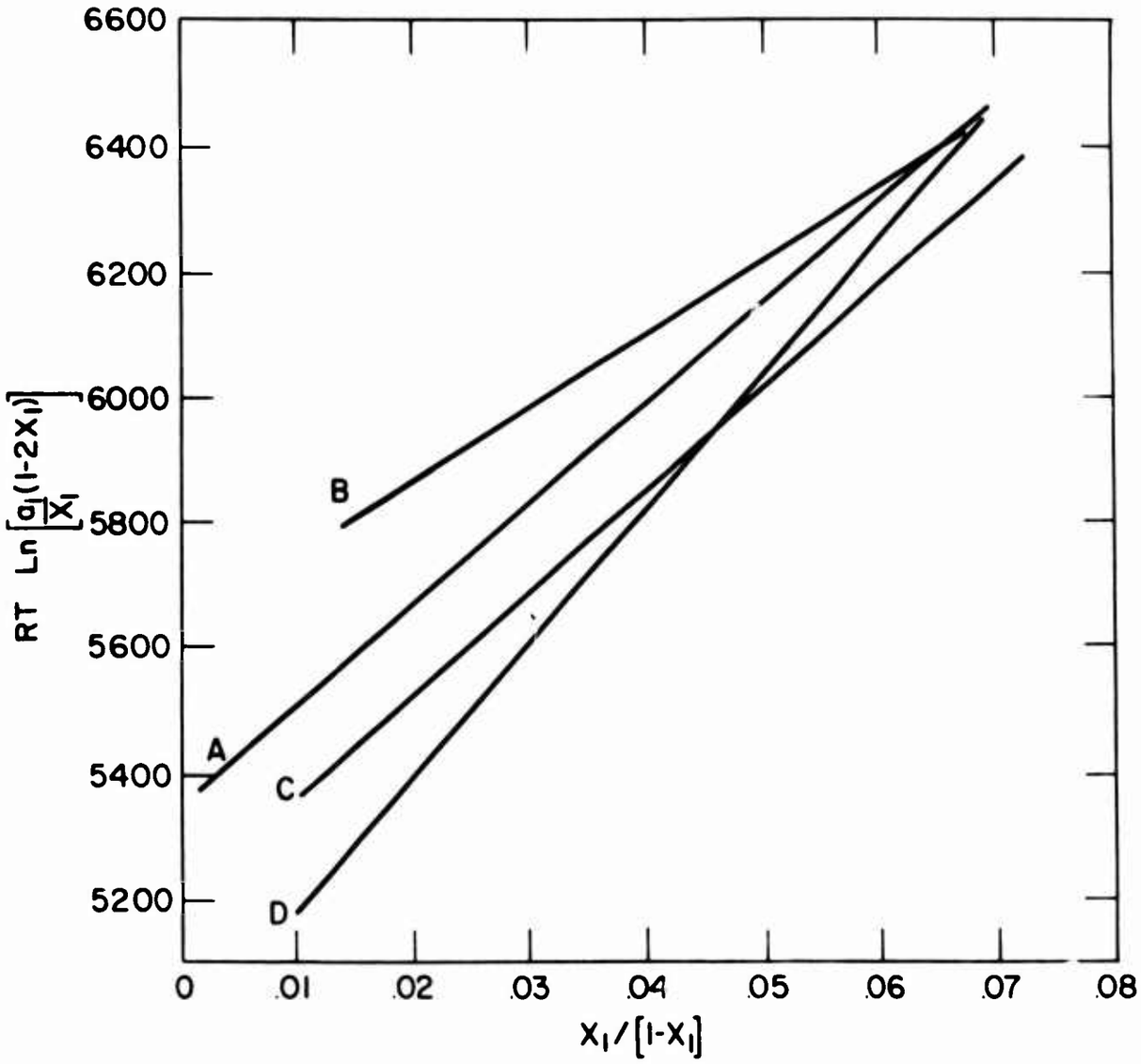

Figure B3: The activity of carbon as depicted by the thermodynamic model applied at 1000°C.

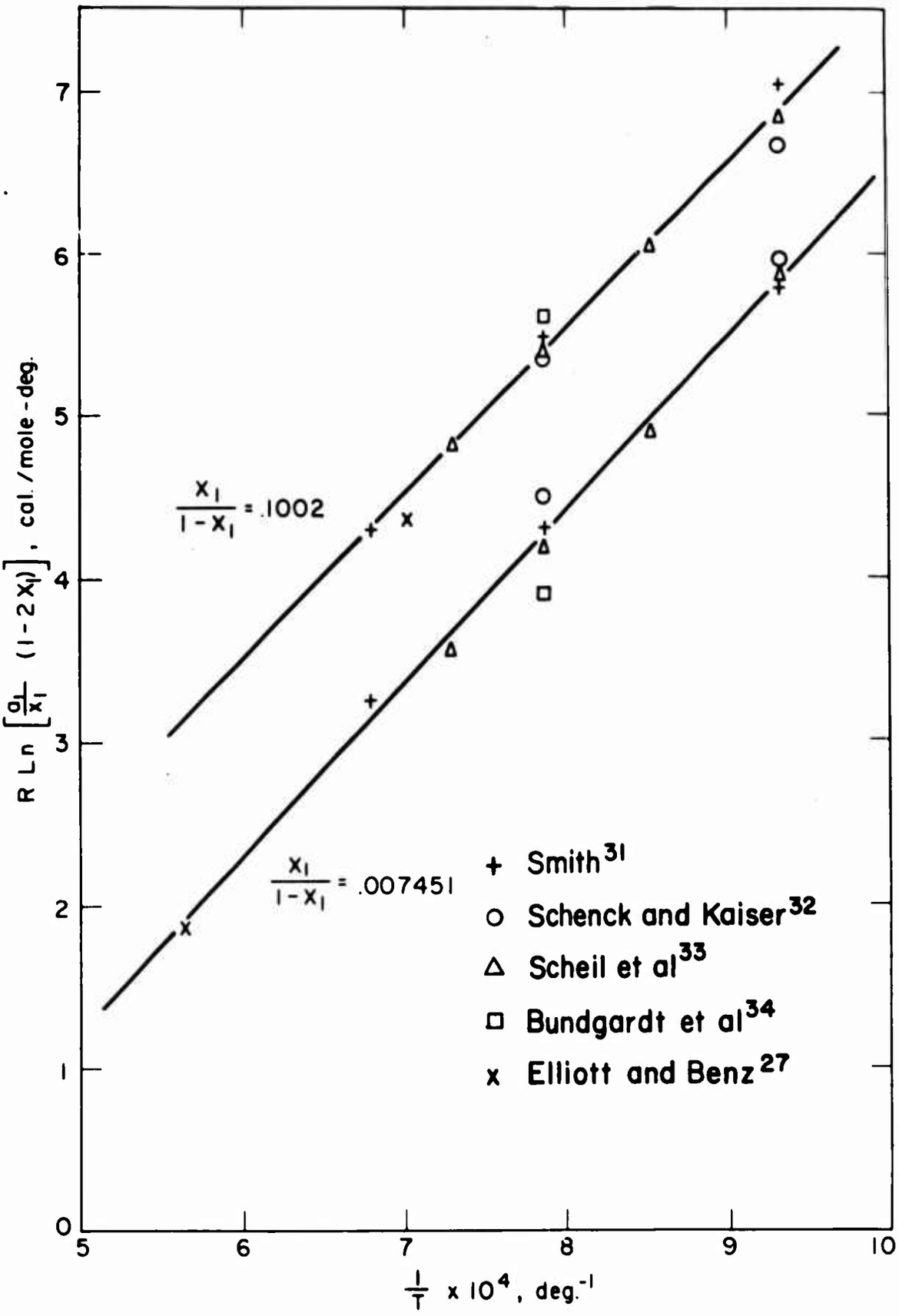

Figure B4: Temperature dependence of the activity of carbon for two concentrations.

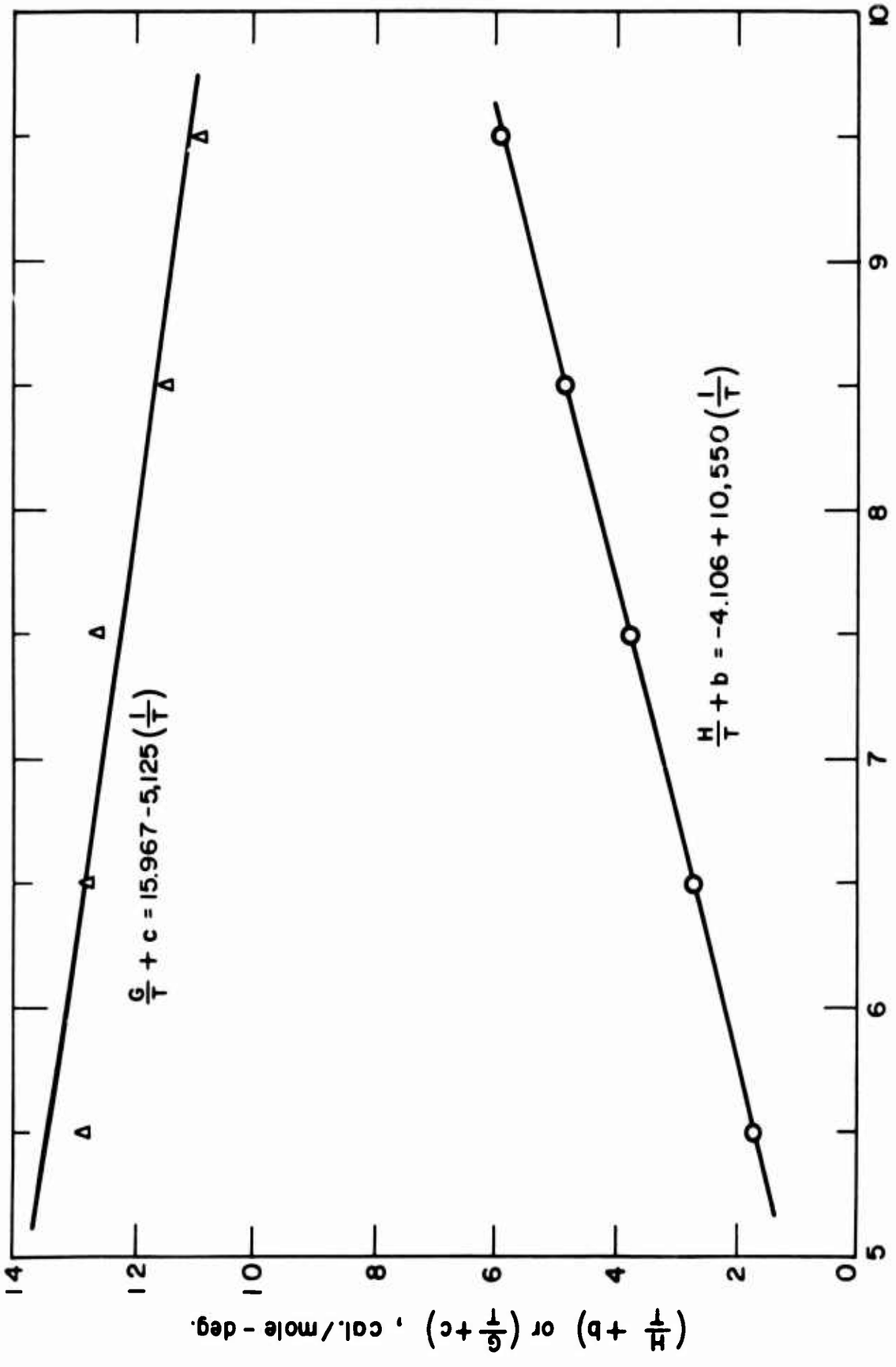

Figure B5: Determination of the four constants H, G, b and c.

APPENDIX C

ACTIVITY OF CARBON IN LIQUID-IRON-CARBON CHROMIUM SOLUTIONS

A. Introduction

The activity of carbon in iron-carbon-chromium liquid solutions has been measured by Richardson and Dennis[37], Fuwa and Chipman[36] and Goto et al[38]. Fuwa and Chipman[36] have presented their data along with data of Richardson and Dennis[37] and utilized an interaction parameter. However, the interaction parameter is only valid for dilute solutions of carbon because, as they indicated, the same interaction parameter does not apply to more concentrated solutions of carbon (i.e., the effect of chromium on the saturation of graphite in liquid iron). Ohtani[39] has attempted to account for the effect of carbon concentration on the interaction parameter; however even his analysis does not apply to the saturation data. Also, the effect of temperature on interaction parameters must be taken into account. Therefore, in any process where the concentration of carbon and/or the temperature changes over wide ranges (such as solidification), the use of an interaction parameter is not adequate to know the activity of carbon.

B. Empirical Relation for the Activity of Carbon

The purpose of the following argument is to make use of the existing data on the effect of chromium on the activity of carbon in liquid iron solutions in such a way that the activity can be described as a function of both composition and temperature. The method is an extension of Rist

and Chipman's[29] analysis for the binary iron-carbon solutions. As in Rist and Chipman's analysis, the activity coefficient is assumed to obey the relation:

$$\log \gamma_1 = \alpha_t (1 - X_1)^2 + I_t \qquad (C1)$$

where, for the ternary solution α_t is a factor dependent on temperature and chromium concentration, and

$$I_t = -\alpha_t (1 - X_{1S})^2 - \log X_{1S} \qquad (C2)$$

where: X_{1S} = saturation atom fraction of carbon which depends on temperature and chromium concentration.

The saturation of carbon in iron melts containing chromium was determined from the data of Ban-Ya and Matoba[40] (1400°C to 1600°C) and Griffing et al[26] (1600°C to 1800°C). These data are presented in Figure C1 and by least-square analysis are found to obey the relation:

$$X_{1S} = X_1^o + 0.2552\, X_2 \qquad (C3)$$

where: X_1^o = saturation of graphite in iron-carbon binary melts

X_2 = mole fraction of chromium.

C. Application of the Empirical Relation for the Experimental Data

The data of Richardson and Dennis[37] (chromium contents up to 25 per cent) are used exclusively to determine the factor α_t in equation (C1). Fuwa and Chipman's[36] data are not used because they are limited to only one activity and have wide scatter while the data of Goto et al[38] yield

somewhat lower activities than Richardson and Dennis. Also, the measurements of Richardson and Dennis were made at three temperatures while those of the other workers are only at one temperature. Figure C2 shows the data of Richardson and Dennis[37] at 1660°C where equation (C1) is assumed to hold for a constant ratio of X_2/X_3 using saturation points computed from equation (3). Similar plots were made at 1560°C and 1760°C and all slopes, α_t, were determined by least-square analysis. The effect of chromium on the activity of carbon is then shown in Figure C3, where

$$T\,(\alpha_t - \alpha) = -4880\,\left(\frac{X_2}{X_3}\right) \qquad (C4)$$

With these results we summarize this section:

The activity of coefficient carbon in iron-carbon-chromium melts is given by:

$$\log \gamma_1 = \alpha_t(1 - X_1)^2 + I_t \qquad (C1)$$

$$\alpha_t = -\frac{4880}{T}\left(\frac{X_2}{X_3}\right) - \frac{4350}{T}\,[1 + .0004(T - 1770)] \qquad (C4)$$

$$I_t = -\alpha_t(1 - X_{1S})^2 - \log X_{1S} \qquad (C2)$$

$$X_{1S} = 0.0462 + 8.785 \times 10^{-5}T + 0.2552\,X_2 \qquad (C3)$$

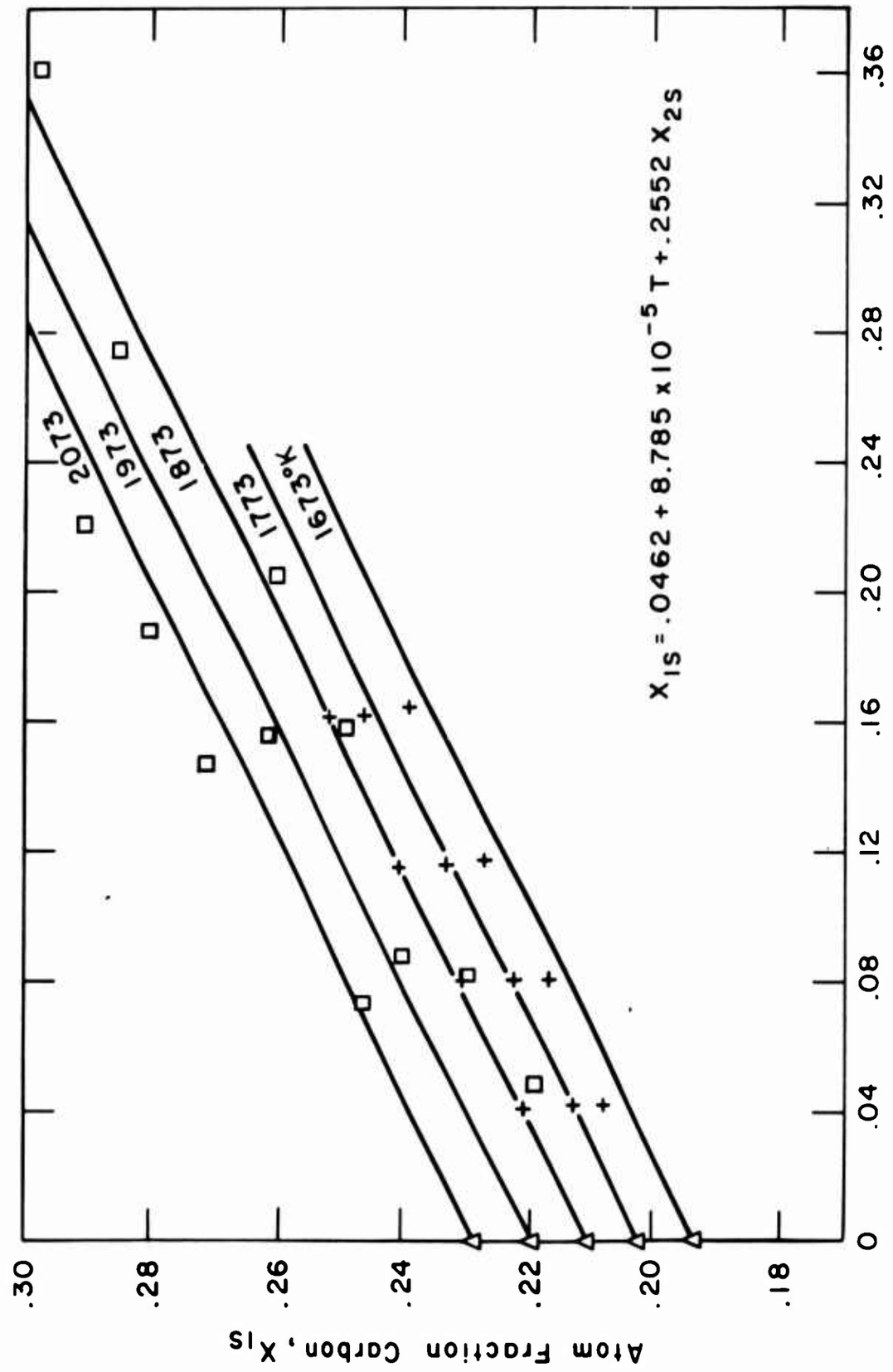

Figure C1: Effect of chromium on the saturation of graphite in liquid iron.
+ Ban-ya and Matoba[40] □ Griffing et al[26] Δ Benz and Elliott[27]

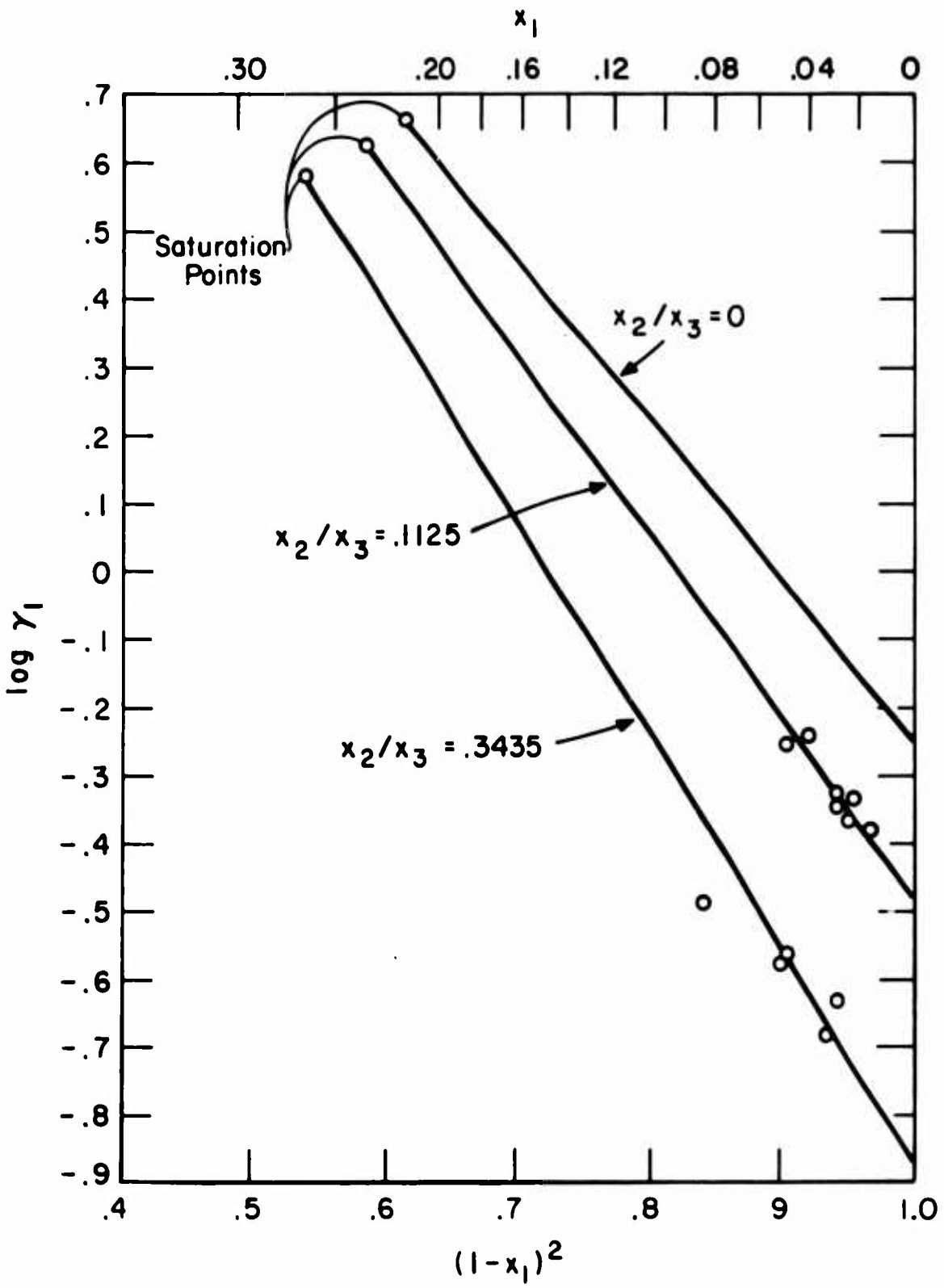

Figure C2: Activity coefficient of carbon in liquid iron at 1660°C for different chromium concentrations. Saturation points from equation (C3) and remaining points from Richardson and Dennis[37].

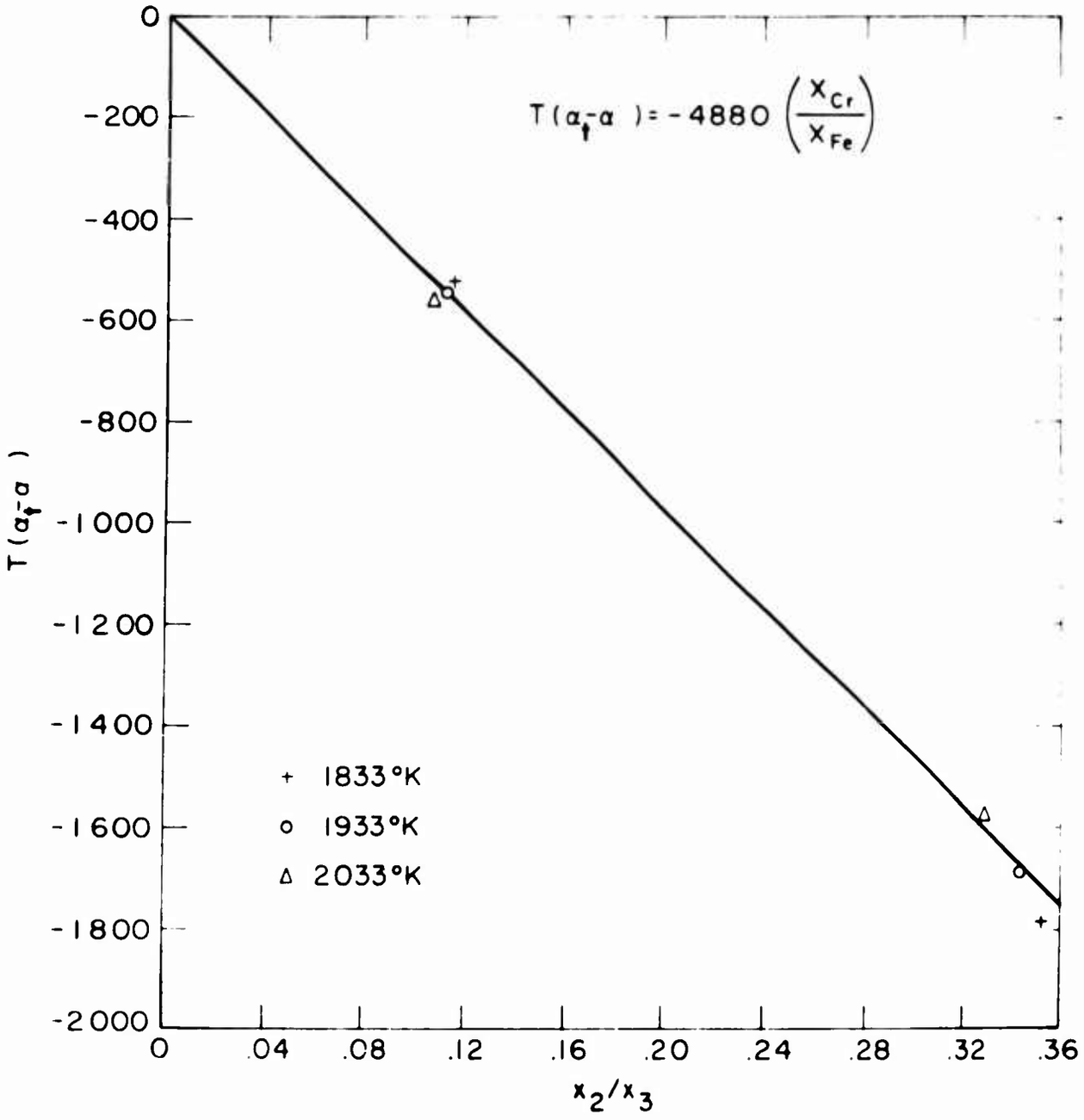

Figure C3: Effect of chromium on the parameter, α_t, in liquid iron-carbon-chromium alloys.

APPENDIX D

ACTIVITY OF CARBON, CHROMIUM, AND IRON IN AUSTENITIC AND LIQUID SOLUTIONS

A. Introduction

The quasi-chemical model as described and used for the activity of carbon in binary iron-carbon austenite is also utilized herein. Extending this analysis for a ternary austenite yields:

$$RT\ln\left[\frac{a_1}{X_1}(1 - 2X_1)\right] = A_0 + A_1\left(\frac{X_1}{1 - X_1}\right) + A_2\left(\frac{X_2}{1 - X_1}\right) \qquad (D1)$$

Just as A_0 and A_1 were shown to be linear functions of temperature in Appendix B, A_2 is also a linear function of temperature and is likewise assumed to be independent of composition.

One purpose of this section is to determine A_2, and then the effect of chromium on the activity of carbon in austenite can be described. The available data in the literature are limited to a small temperature range, 950° to 1050°C. To supplement this the data of the literature, experimentally measured chromium distributions between liquid alloys and austenite are used to evaluate A_2 at higher temperatures.

B. Data from Literature for the Activity of Carbon in Iron-Carbon-Chromium Austenite

The activity of carbon in iron-carbon-chromium austenite has been measured by Kirkaldy and Brigham[41] (1000°C), Schenck and Kaiser[32] (950, 1000, and 1050°C), and Bundgardt et al[34] (1000°C). All these investigators measured the activity by the use of CO-CO_2 or CH_4-H_2

gas mixtures. In addition Kirkaldy and Brown[42] have made measurements at 1050°C by a "transient equilibrium" method.

For the determinations involving the use of gas mixtures the data for each investigator were reduced in a manner such that $A_2(X_2/1-X_1)$ could be calculated using equation (D1). The values of A_0 and A_1 chosen were those determined from the binary system for the particular investigator, i.e., Bundgardt et al's data were referred to their own particular carbon activities in binary austenite; the same was true for Schenck et al. Kirkaldy and Brigham's data referred to Smith's activity of carbon in binary austenite because they reported using the same experimental method. The different binary reference levels for the various investigators were used in order to isolate the effect of chromium, alone, that they measured.

C. Evaluation of the Experimental Distributions Between Liquid Alloys and Austenite

The experiments used to determine the chromium distribution between the liquid alloys and austenite yielded the temperature, composition of both carbon and chromium in the liquid, but only the composition of chromium in the solid. Thus, the activity of carbon in the liquid is known, but when equation (C1) is applied to the solid to satisfy the requirement that the activity of carbon in both phases must be equal, two unknowns (X_1 and X_2) arise. The values of A_2 derived from the data in the literature are limited to a small temperature range and cannot be extrapolated to the higher temperatures so that a means is developed to independently evaluate this parameter at higher temperatures. This

is accomplished by dealing with the activity of iron and/or chromium in addition to carbon in both phases.

1. Activities in Ternary Systems.

Following a discussion of Wagner[43], the Gibbs-Duhem relation applied to ternary solutions yields

$$F^E = (1 - X_1)[F^E (X_1 = 0) + \int_0^{X_1} \frac{F_1^E}{(1 - X_1)^2} dX_1]_{X_2/X_3,T} \quad \text{(D2)}$$

where: F^E = integral excess molar free energy

F_1^E = partial excess molar free energy of carbon

Since,

$$F_1^E = RT \ln \frac{a_1}{X_1} = RT \ln \gamma_1 \quad \text{(D3)}$$

and supposing the integral excess molar free energy is known for the binary iron-chromium solutions, equation (D2) enables the calculation of F^E for the ternary solutions. From F^E the activity of iron and chromium can then be determined as:

$$RT \ln \gamma_2 = F_2^E = F^E + (1 - X_2)\left(\frac{\partial F^E}{\partial X_2}\right)_{X_1/X_3} \quad \text{and,} \quad \text{(D4)}$$

$$RT \ln \gamma_3 = F_3^E = F^E + (1 - X_3)\left(\frac{\partial F^E}{\partial X_3}\right)_{X_1/X_2} \quad \text{(D5)}$$

2. Application of Gibbs-Duhem Relation to the Liquid.

Referring to the relations for the activity of carbon in liquid iron-carbon-chromium solutions, (equations C1 - C4) we write:

$$F^E = (1 - X_1)[F^E(X_1 = 0) + 4.576T \int_0^{X_1} \frac{\alpha_t(1 - X_1)^2 + I_t}{(1 - X_1)^2} dX_1]_{X_2/X_3,T} \quad (D6)$$

At a constant X_2/X_3,T both α_t and I_t are constants. Also, the integral excess molar free energy (F^E) for liquid iron-chromium solutions is zero because iron and chromium form ideal solutions[39]. Performing the integration, equation (D6) becomes:

$$F^E = 4.576T\ [\alpha_t X_1(1 - X_1) + I_t X_1] \quad (D7)$$

Referring to equation (D4) F_2^E can be found if $(\partial F^E/\partial X_2)_{X_1/X_3}$ is established. When X_1/X_3 is held constant, the differentiation of equation (D7) is tedious because α_t and I_t vary. For this reason only the results of this operation are presented.

$$F_2^E = RT \ln \gamma_2 = F^E + (1 - X_2)\left(\frac{\partial F^E}{\partial X_2}\right)_{X_1/X_3} \quad (D4)$$

where,

$$\left(\frac{\partial F^E}{\partial X_2}\right)_{X_1/X_3} = 4.576T\{-[A]\frac{X_1}{X_1+X_3} + [B]\left(\frac{\partial \alpha_t}{\partial X_2}\right)_{X_1/X_3} + [C]\left(\frac{\partial X_{1S}}{\partial X_2}\right)_{X_1/X_3}\} \quad (D8)$$

$$[A] = \alpha_t[(1 - 2X_1) - (1 - X_{1S})^2] + \log \frac{1}{X_{1S}} \quad \text{(D9)}$$

$$[B] = X_1[(1 - X_1) - (1 - X_{1S})^2] \quad \text{(D10)}$$

$$[C] = X_1[2\alpha_t(1 - X_{1S}) - \frac{1}{2.303X_{1S}}] \quad \text{(D11)}$$

$$\left(\frac{\partial \alpha_t}{\partial X_2}\right)_{X_1/X_3} = \frac{-4880}{T} \left(\frac{1}{X_3}\right)\left[\frac{1}{X_3 + X_1}\right] \quad \text{(D12)}$$

$$\left(\frac{\partial X_{1S}}{\partial X_2}\right)_{X_1/X_3} = .2552\left(\frac{1 - X_1^o}{1.2552X_2 + X_3}\right)\left[1 - \left(\frac{X_2}{1.2552X_2 + X_3}\right)\left(\frac{.2552X_3 + 1.2552X_1}{X_3 + X_1}\right)\right]$$

..... (D13)

To evaluate the partial excess molar free energy for iron, the following expression is used:

$$F^E = X_1F_1^E + X_2F_2^E + X_3F_3^E \quad \text{(D14)}$$

3. Application of Gibbs-Duhem Relation to the Solid.

Referring to equation (D1), the partial excess molar free energy for carbon in austenite can be written as

$$F_1^E = A_0 + A_1\left(\frac{X_1}{1 - X_1}\right) + A_2\left(\frac{X_2}{1 - X_1}\right) - RT \ln (1 - 2X_1) \quad \text{(D15)}$$

The binary system for austenitic iron-chromium alloy is assumed to be regular so that

$$F^E(X_1 = 0) = \Omega X_2^b X_3^b \quad \text{(D16)}$$

where: X_2^b, X_3^b represent binary concentrations.

The activities in iron-chromium austenitic alloys have been measured by Jeannin et al[44] at 1200°C and Kubaschewski and Heymer[45] at 1341 to 1370°C. Since the present argument concerns only austenite, the activity of iron was treated in order to determine Ω for equation (D16). For a regular solution of iron and chromium

$$RT \ln \gamma_3 = \Omega X_2^2 \tag{D17}$$

According to the number of determinations of the respective investigators, a mean value was established.

$$\Omega = 2490 \text{ cal/mole}$$

This value of Ω is good for $0 \leq X_2 \leq 0.092$.

Performing the operations indicated by equations (D2), (D4), and (D5) and noting that

$$X_2^b X_3^b = \frac{X_2 X_3}{(1 - X_1)^2} \tag{D18}$$

the excess free energies are developed

$$F^E = (1 - X_1)\{\Omega\frac{X_2 X_3}{(1-X_1)^2} + A_0 \left(\frac{X_1}{1-X_1}\right) + A_1 \left[\frac{X_1^2}{2(1-X_1)^2}\right] + A_2 \left[\frac{X_1 X_2}{(1-X_1)^2}\right]$$

$$-RT \left[\frac{\ln(1-2X_1)}{(1 - X_1)} + 2\ln \left(\frac{1-X_1}{1-2X_1}\right) \right]\} \tag{D19}$$

$$F_2^E = \frac{\Omega X_3^2}{(1-X_1)^2} - \left[\frac{X_1^2}{2(1-X_1)^2}\right] A_1 + \frac{X_1 X_3}{(1-X_1)^2} A_2 + RT \ln \left[\frac{(1-2X_1)}{(1-X_1)^2}\right] \qquad (D20)$$

$$F_3^E = \frac{\Omega X_2^2}{(1-X_1)^2} - \left[\frac{X_1^2}{2(1-X_1)^2}\right] A_1 - \frac{X_1 X_2}{(1-X_1)^2} A_2 + RT \ln \left[\frac{(1-2X_1)}{(1-X_1)^2}\right] \qquad (D21)$$

As a check, equations (D15), (D19), (D20), and (D21) satisfy

$$F^E = X_1 F_1^E + X_2 F_2^E + X_3 F_3^E \qquad (D22)$$

4. Calculation of the Effect of Chromium from the Solid-Liquid Equilibria.

The activities of carbon, iron and chromium can all be calculated for the liquid alloys using equations developed herein. The activity of carbon in the solid is then known since the standard state (pure graphite) is the same for both phases. By changing the standard state from pure liquid to pure gamma iron for the activity of iron in the liquid, the activity of iron in the solid is calculated. Equation (D1) is rearranged to read

$$A_2 X_2 = RT(1 - X_1) \ln\left[\frac{a_1}{X_1}(1 - 2X_1)\right] - A_0(1 - X_1) - A_1 X_1 \qquad (D23)$$

Since the per cent chromium was measured in the solid, the mole fraction of carbon is fixed for a given per cent carbon. Thus successive trials were made by varying the per cent carbon and a set of corresponding values of X_1, X_2 and A_2 were generated.

These values are then substituted into equation (D21) to determine the activity of iron apart from its calculated activity in the liquid phase. Thus a plot of the activity of iron versus per cent carbon can be made. An example of such a plot is shown in Figure D1. The curve displays a minimum and because only one solution is physically possible, the minimum is the solution. These minimums never exactly correspond with the activity of iron as calculated for the liquid but all were within $\pm$ 1 per cent error, as shown in Table DI.

The value of A_2 that corresponds to the minimums was also calculated. However, as Figure D1 shows, A_2 is extremely sensitive to the concentration of carbon. For this reason the plot of A_2 versus temperature, Figure D2, includes limits that correspond to $\pm$ 2.5 per cent error in the carbon concentration found at the minimums. When least square analysis is applied to this high temperature, as well as the low temperature data, an expression for A_2 is finally developed.

$$A_2 = 82.64T - 135,000 \qquad (D24)$$

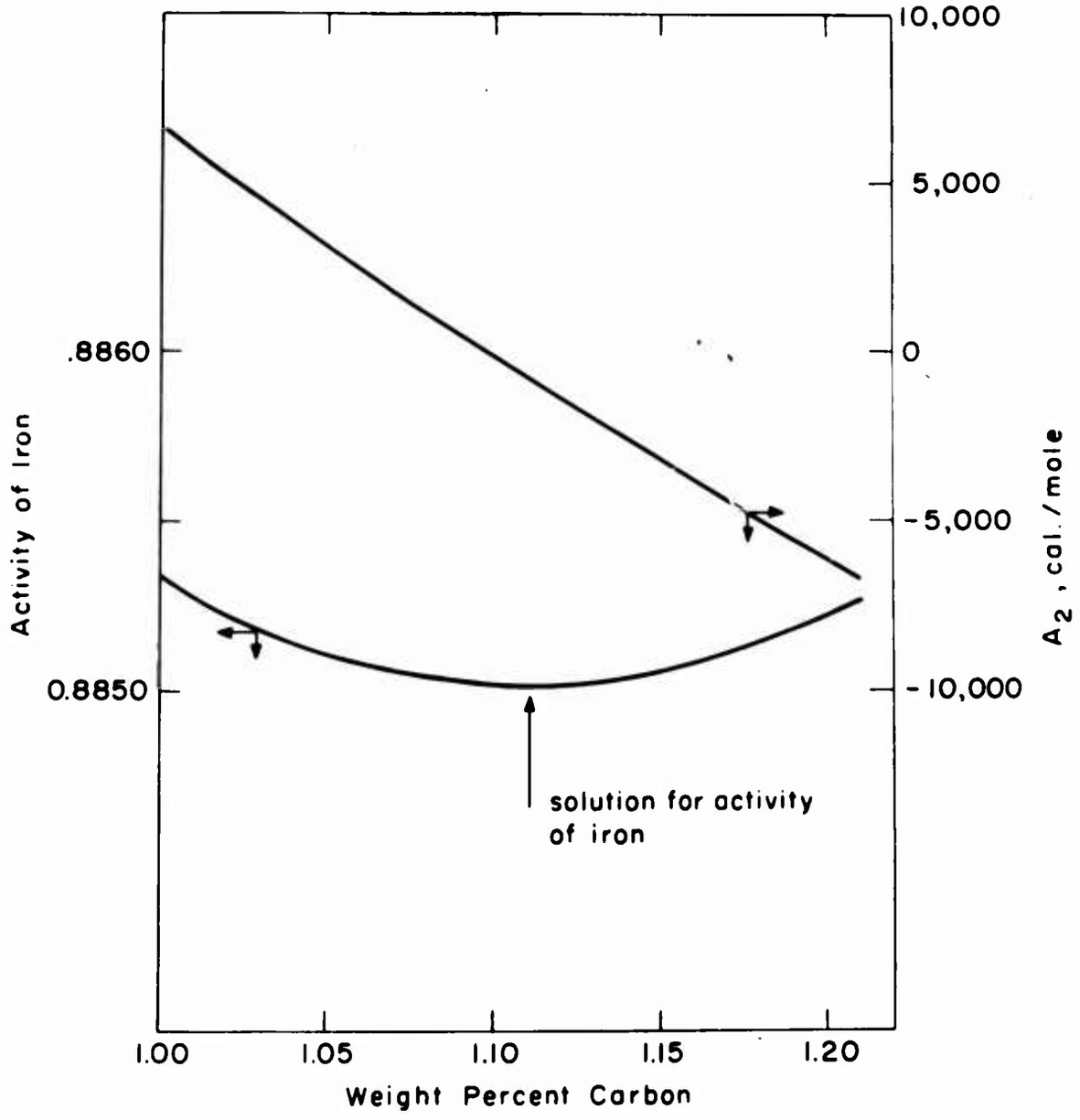

Figure D1: A calculation for the activity of iron in austenite and the corresponding A_2 value. Heat 11, Table AII is chosen as the example.

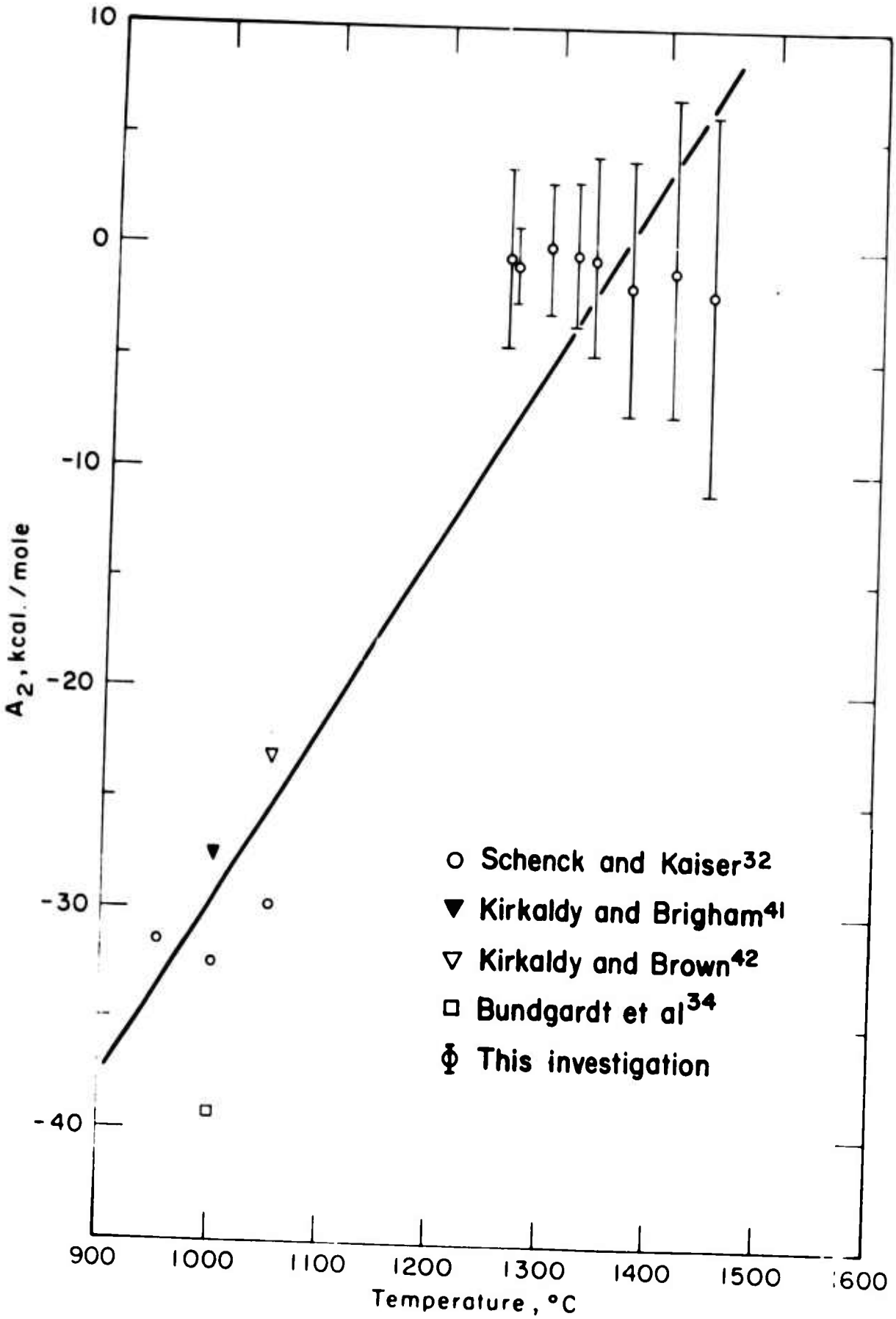

Figure D2: The parameter, A_2, versus temperature.

TABLE DI

COMPARISON OF IRON ACTIVITIES CALCULATED
FOR THE LIQUID AND FOR THE SOLID

Equilibrium Temperature, °C	Activity of Iron* Calculated for Solid	Activity of Iron* Calculated for Liquid
1444	.9688	.9678
1265	.8850	.8944
1318	.9164	.9237
1336	.9271	.9339
1370	.9422	.9492
2159	.9017	.9012
1295	.9051	.9163
1410	.9560	.9599

* Standard State is pure gamma iron.

APPENDIX E

CONSTRUCTION OF SOLIDUS SURFACE

In principle if the activities of all three components can be described for two phases, then the equilibrium between the two phases can be completely described. However, since the liquidus is known, it is only necessary to consider the activity of two components. Carbon is an obvious choice for one of the components; if iron is chosen as the second component difficulties arise so that a means is developed to use chromium as the standard state.

Referring to Figure D1, the activity of iron is seen to be hardly sensitive to the concentration of carbon; because the activity of iron is only known to within .01 (Table DI), the weight per cent of chromium could only be known to about $\pm$ 1 per cent (absolute, not a relative value).

To avoid the difficulty of working with the activity of iron, a relation was developed to express the change of state from chromium from the liquid to the hypothetical standard state of pure austenitic chromium. Using the eight experimental chromium equilibria determinations and accepting the activities for carbon and chromium calculated in the liquid equations (D15) and (D20) are solved simultaneously for the concentration of carbon, X_1, and the activity of chromium in austenite, a_2. The carbon concentrations derived in this manner were within the limits specified for the determination of A_2 in Figure D2. The ratio of chromium activities for the austenite relative to the liquid is plotted in Figure E1

which yields the following relation for the change of standard state for chromium:

$$\log \frac{a_2^{\gamma}}{a_2^{\ell}} = \frac{2411}{T} - 1.076 \qquad \text{(E1)}$$

With this equation the solidus surface can now be constructed by requiring that the activity of carbon and chromium in both phases be equal when based on the same standard state. Equation (D1) is compared with the analogous equation for the change of standard state between δ-chromium and liquid-chromium in Figure E1. The curve involving γ-chromium is higher than δ-chromium as it should be because δ-chromium is the stable phase.

The solidus derived in this manner is presented in Figure 3. In Figure E2 the concentrations of chromium in the solid in equilibrium with the experimental liquid compositions of Table AII are compared with the concentrations derived from the solidus. The probable error, based on deviations from the line of perfect correlation, is $\pm$ 0.171 per cent chromium.

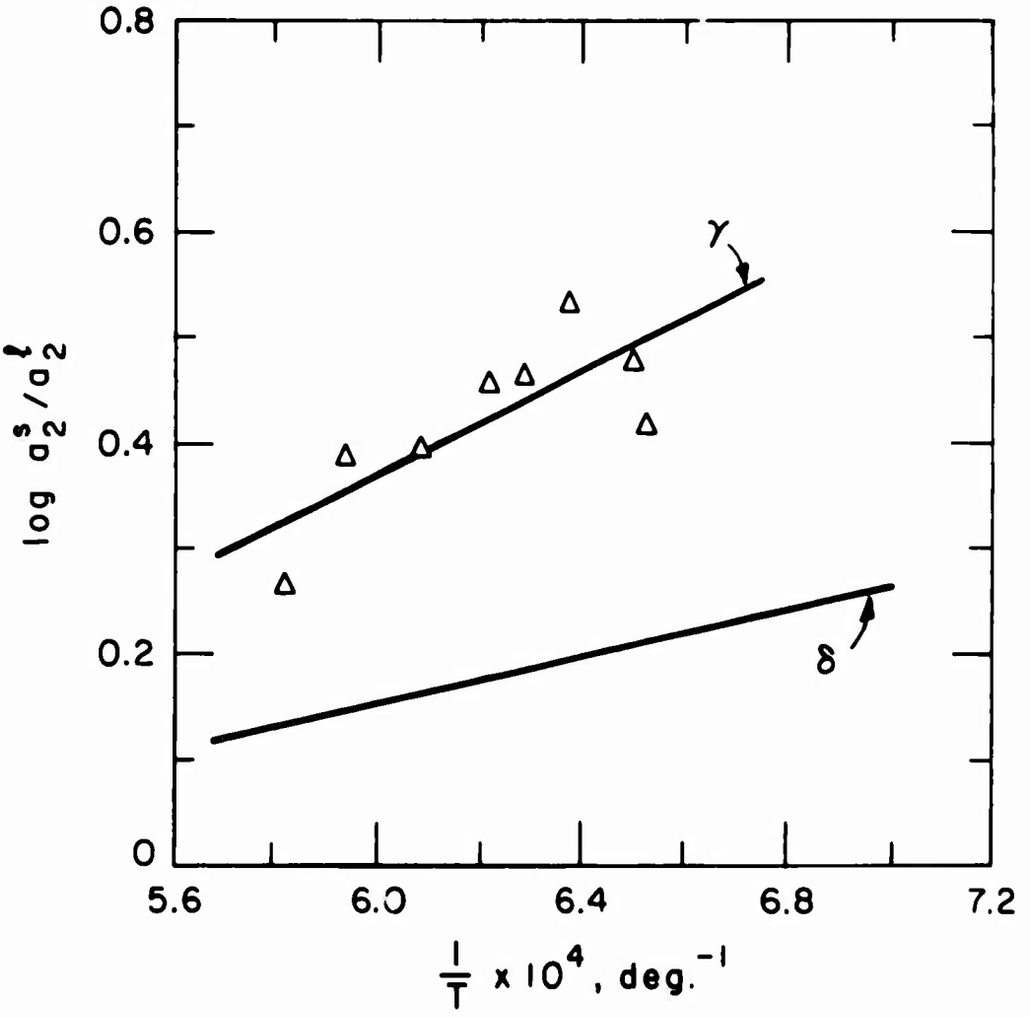

Figure E1: Change of standard state for chromium between pure liquid chromium and the hypothetical pure γ-chromium and comparison with the change of standard state involving δ-chromium.

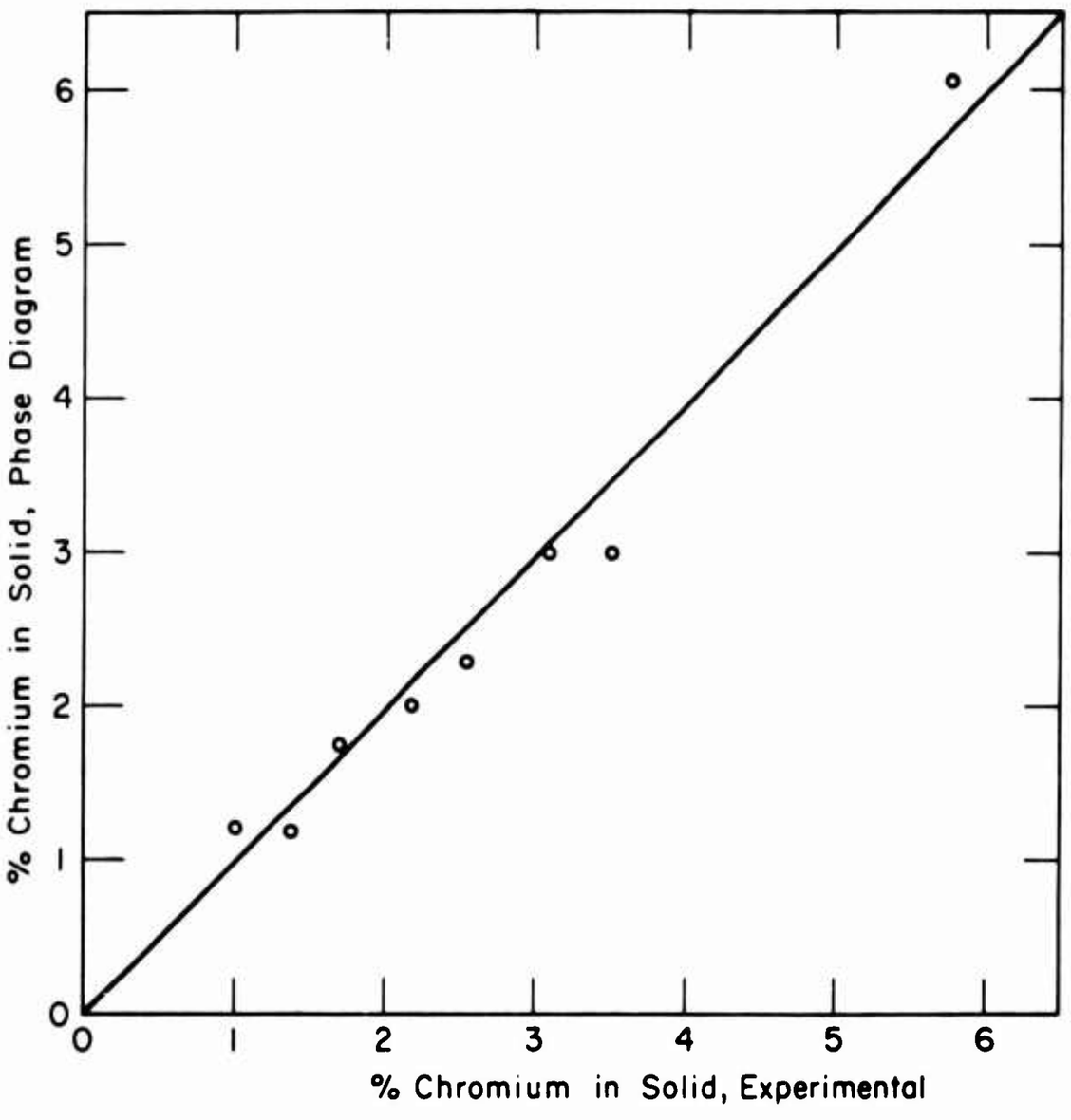

Figure E2: Comparison of experimental chromium concentrations in austenite with those from the derived phase diagram.

APPENDIX F

CONVERSION OF X-RAY INTENSITIES TO WEIGHT PER CENT CHROMIUM

Empirical relations developed by Ogilvie and Ziebold[46] for ternary systems were utilized. For the iron-carbon-chromium system their empirical relations can be expressed simply as:

$$\frac{C_2}{K_2} = C_3(a_{23} - 1) + 1 \qquad \text{(F1)}$$

and

$$\frac{C_3}{K_3} = C_2(a_{32} - 1) + 1 \qquad \text{(F2)}$$

where: C_2 = composition of chromium, weight fraction

C_3 = composition of iron, weight fraction

K_2 = normalized intensity of chromium

K_3 = normalized intensity of iron

a_{23}, a_{32} = constants determined by the use of standards

Equations (F1) and (F2) can be realized because carbon atoms do not flouresce either iron or chromium atoms, nor absorb chromium or iron characteristic radiation.

To determine the parameters a_{23} and a_{32}, the average intensity ratios of non-homogeneous specimens were determined by scanning in a random manner for approximately 400 seconds while collecting detector counts. Using equation (F1), the composition of chromium can be calculated if the concentration of carbon is known. If the concentration of carbon is not known then both the intensities of chromium and iron are recorded and equations (F1) and (F2) are solved simultaneously for C_2.